AEDC-TR-70-44

Copy 8

AERODYNAMIC HOLOGRAPHY

J. D. Trolinger and J. E. O'Hare

ARO, Inc.

August 1970

ARNOLD ENGINEERING DEVELOPMENT CENTER
AIR FORCE SYSTEMS COMMAND
ARNOLD AIR FORCE STATION, TENNESSEE

NOTICES

When U. S. Government drawings specifications, or other data are used for any purpose other than a definitely related Government procurement operation, the Government thereby incurs no responsibility nor any obligation whatsoever, and the fact that the Government may have formulated, furnished, or in any way supplied the said drawings, specifications, or other data, is not to be regarded by implication or otherwise, or in any manner licensing the holder or any other person or corporation, or conveying any rights or permission to manufacture, use, or sell any patented invention that may in any way be related thereto.

Qualified users may obtain copies of this report from the Defense Documentation Center.

References to named commercial products in this report are not to he considered in any sense as an endorsement of the product by the United States Air Force or the Government.

AERODYNAMIC HOLOGRAPHY

J. D. Trolinger and J. E. O'Hare
ARO, Inc.

FOREWORD

The work reported herein was done at the request of the Arnold Engineering Development Center (AEDC), Air Force Systems Command (AFSC), under Program Elements 64719F and 62201F, Project 4344.

The results of research presented were obtained by ARO, Inc. (a subsidiary of Sverdrup & Parcel and Associates, Inc.), contract operator of AEDC, AFSC, Arnold Air Force Station, Tennessee, under Contract F40600-71-C-0002. The research was conducted from July 1967 to July 1969 under ARO Project No. BC5016, and the manuscript was submitted for publication on January 15, 1970.

The authors acknowledge W. L. Templeton, von Kármán Gas Dynamics Facility, and R. E. Whitlock, Office of the Managing Director, who assisted with the experimental work throughout the program, and K. R. Kneile, Central Computer Operations, who performed the computer analysis and wrote Appendix III. Portions of the work in Fraunhofer holography were based on masters theses by W. M. Farmer and R. A. Belz, who were University of Tennessee Space Institute research assistants assigned to ARO, Inc.

This technical report has been reviewed and is approved.

David G. Francis
First Lieutenant, USAF
Research and Development Division
Directorate of Plans and Technology

Harry L. Maynard
Colonel, USAF
Director of Plans and Technology

ABSTRACT

A summary of the work in holography at AEDC is presented. The work includes basic and applied research with emphasis on the applications of holography to aerodynamic testing.

CONTENTS

APPENDIXES

I. ILLUSTRATIONS

Figure

NOMENCLATURE

A_i	Real amplitude of the $i^{\underline{th}}$ wave
C_j	Expansion coefficient
D	Particle diameter
F	General fractional fringe shift
f(x)	Functional dependence on x
I	Intensity
K	A constant
k	Wave number (equal $2\pi/\lambda$)
k'	Boltzmann's constant
M	Magnification

N	Far field number
n	Index of refraction
p	Fractional fringe shift for a special case
r_n	Radius of the model nose
T	Transmission coefficient
U	Complex amplitude
U'	Reconstructed complex amplitude
U_i	Modulated complex amplitude of the $i^{\underline{th}}$ wave
U_i^*	Complex conjugate of U_i
U_r	Reference complex amplitude
U_t	Transmitted complex amplitude
x_i, y_i, z_i	Image coordinates
x_o, y_o, z_o	Reference wave coordinates
x_p, y_p, z_p	Reconstruction wave coordinates
α	Angle between wave vector and x-axis
λ_i	Wavelength of the $i^{\underline{th}}$ wave
ρ	Gas density
ϕ_o	Constant phase shift
$\phi(y)$	One-dimensional phase shift

SECTION I
INTRODUCTION

1.1 PURPOSE

The purpose of this report is to present the results to date of a continuing effort in the research and development of holographic techniques for application at the Arnold Engineering Development Center (AEDC) and other Air Force facilities which have supported the projects. The applications reported are of a wide variety, illustrating the broad potential utility of holography in aerodynamic facilities. Included are particle field analysis, velocimetry, three-dimensional field recording, a multitude of flow visualization techniques, and several types of interferometry. Much of the work reported is original with ARO, Inc. perssonel; however, information and techniques generated by other laboratories are also included where necessary to make the report complete.

1.2 HISTORY AND SUMMARY OF AEDC PROGRAMS IN HOLOGRAPHY

The techniques of the simplest types of holography were first disclosed by Dennis Gabor (Ref. 1) in 1947, nearly ten years before lasers were conceived and sixteen years before the first laser was successfully operated. Combining the highly coherent illumination of the laser with a generalization of the concepts of holography in 1963 (Ref. 2) made it a potentially useful scientific tool. Even so, it was not until 1965 when pulsed laser holography (Ref. 3) became practical and more application concepts were discovered that the aerodynamicist could seriously consider practical application. Many ideas concerning the application of holography appeared in the literature during those years; however, in most cases the quality of the experimental results confined the work to research laboratories. Required photographic emulsions were too insensitive; available pulsed lasers were unreliable and not sufficiently coherent; holographic systems required specialists even for poor results. Nevertheless, a few highly specialized applications did become feasible from an operational standpoint before 1965. The first of these was Fraunhofer holography of particle fields, perhaps the simplest and least demanding of all holography techniques (Ref. 4).

During the latter part of 1966, the technical staff of Experimental Research (TS/ER) began surveying the possible uses of holography at AEDC. Partially supported by the Flight Dynamics Laboratory, Wright-Patterson Air Force Base, experimental and theoretical studies

were initiated in the application of Fraunhofer holography to study the properties and motion of particle fields in gaseous and liquid flows. One application under serious consideration was that of local velocity determination of fluids through determination of velocity of small seeding elements placed in the fluid. A capability was established covering a broad range of holographic methods, experimental and theoretical. Conventional particle field holography was extended through multiple exposure techniques to allow time-motion studies (Refs. 5 through 8). Studies were continued to define the ultimate practical limits in measurement obtainable. These studies produced a number of optical filtering techniques which improved the data and expanded the range of utility.

During this period more suitable recording materials, better pulsed lasers, and more advanced holography techniques became available, making off-axis pulsed holography potentially more practical for application as an aerodynamic tool. By 1968 the more powerful off-axis holography which had been primarily limited to high stability tables (at AEDC) was extended to pulsed lasers, eliminating stringent stability requirements which had severely limited the applications. Because of experience at AEDC with pulsed laser in-line holography and CW off-axis holography, the incorporation of pulsed laser off-axis holography in the overall capability was quickly achieved. By early 1968 the TS/ER had achieved a state-of-the-art understanding, both experimental and theoretical, in most of the types of holography which appeared potentially applicable at AEDC; however, the work was still confined to laboratory research.

At this point, an extremely critical second stage in the applications development became apparent. In most cases, the feasibility of an application of holography can be deduced to a fair degree with knowledge gained in the research laboratory. The holography problems per se can therein be solved. The integration of such methods with AEDC facility wind tunnels and cells is, however, a new problem in itself. To accomplish this, one must force the method to work under conditions which usually are characterized by adverse environments and larger scale. Any such systems must be more reliable, must be automated to some extent, and often must be programmed for remote control.

Clearly, these problems are best understood by support groups working directly with everyday facility operations. At this point a few such groups became actively involved in the holographic instrumentation program. In August 1968, the Instrument Branch of the Aerodynamics Division of the von Kármán Gas Dynamics Facility (VKF-AD/I), working

jointly with TS/ER, planned the first AEDC application of holographic flow visualization systems in wind tunnel studies. The first installation of a pilot system was accomplished in Hypersonic Wind Tunnel (D). Results were highly marginal, but, as had been expected, the critical problems remaining were uncovered by these tests. VKF-AD/I concentrated on those problems related to the VKF application until the more critical ones were solved (Refs. 9 through 11).

In January 1969, a refined holographic flow visualization system (HFVS) was installed in Hypersonic Wind Tunnel (B). The system performed well, providing all of the types of data which had been expected (Ref. 11). This constituted (to the authors' knowledge) the first HFVS of its size ever to be employed on an operating wind tunnel. A number of new techniques and devices were engineered during this development program. Detailed discussion of these techniques is presented in subsequent chapters. Some of the more notable include new alignment concepts, the invention of holographic color schlieren methods (Ref. 12), and establishment of stored beam holographic interferometry for large-scale flow studies. A considerable amount of development still remains for the establishment of HFVS of reliability and utility comparable to conventional tools which have evolved from many years of development.

Concurrent with the above studies, a program was established in the Rocket Test Facility, T-Cells Division for the application of small particle holography to the study of rocket exhausts. The joint effort resulted in the development of a refined portable holocamera which operated successfully in the adverse environment of the rocket test cells (Ref. 13). These studies showed that holograms could be made reliably through an extremely intense rocket exhaust with little loss in image quality.

Until April 1969, holographic data acquisition in an actual user test as an integral part of the test was still untried. At that time, VKF-AD/I was faced with a visualization problem which could not be solved with conventional means. The techniques of in-line Fraunhofer holography were ideally suited to the problem. Subsequently, these methods were employed and provided the user with data which could apparently not have been otherwise obtained.

During 1968-69 it became apparent that many other age-old problem areas could be attacked holographically. Studies are presently underway along two lines: (1) basic theoretical and experimental analysis of the physics and technology of holography and optical information processing, and (2) the engineering problems of applied holography.

The vast amounts of information storage ordinarily associated with holographic systems had uncovered a new requirement for better analysis and interpretation of holographic data. Since the methods of coherent optical information processing seemed to offer a potential solution to the problem, studies of such possibilities were initiated by TS/ER during 1969. The results of the preliminary investigations are reported separately (Ref. 14).

1.3 ORGANIZATION OF THE REPORT

Sections II and III are a summary of the theoretical and experimental methods of holography in general. These are the foundations for subsequent chapters. They are largely a collection of facts resulting from a detailed study of work which was completed in other laboratories and repeated in the AEDC research labs, although some of the facts and interpretations arose from experience during the latter. Those with a working knowledge of holography will not find it necessary to read these sections. Section IV reports details of development programs in applied holography which have resulted in significant achievements at AEDC. Section V discusses some of the shortcomings of the methods at present and the studies which have been initiated to eliminate such shortcomings. Also, areas which appear promising have been included as future areas of study.

SECTION II
INTRODUCTION TO HOLOGRAPHY

2.1 QUALITATIVE DESCRIPTION OF THE HOLOGRAPHIC PROCESS

When any instrument (e.g., the eye or a camera) is used to visually observe an object or object field, the observation is carried out through a series of operations upon an electromagnetic (light) wave which reaches the viewing instrument after passing through or reflecting from the field of view. It is the detection, modulation, and subsequent interpretation of the information carried by the electromagnetic field which results in one's "seeing" the object field. If, in some manner, the same electromagnetic wave could be synthesized without the presence of an object field, an observer of the synthesized wave could in no way distinguish the genuine observation with the synthesized one. Information-wise, they would be equivalent. Holography provides such a method for synthesizing any desired wave form. This can be done through one of two

holographic processes. On the one hand, if a wave exists in space, its entire information content can be recorded through holography, allowing the same wave to be synthesized at a later time. On the other hand, any wave of known information content can, in principle, be synthesized by a computer-generated hologram, even if the wave has never existed.

A hologram is a recording which has been coded in such a way that it can convert a predetermined complex wave (sonic or electromagnetic) from one form to a second completely different, predetermined form. The coding is usually accomplished by using two waves, of which one is an information-free wave, while the other is an information-rich wave. The types of holograms under discussion here are optical holograms made on photographic film. When properly illuminated, the film can convert the illuminating wave into a wave which forms a truly three-dimensional image of any object field. A hologram can be made by combining at the film a reproducible reference light beam with a beam which has passed through or reflected from the object field (Fig. 1a, Appendix I). Both beams must arise from a coherent source (e.g., a laser) which allows them to interfere and produce a fringe pattern which the film records. The fringe pattern acting much like an interference grating (when re-illuminated by the reference beam) then reproduces the object beam as it would appear if it had continued on past the film during the initial recording (Fig. 1b). Consequently, by looking into this wave, the object field appears to be sitting behind the hologram. Viewing an object field image by holographic reconstruction is optically equivalent to viewing the actual object field through a window of which the dimensions are the same as those of the hologram.

Any of the holograms mentioned can, in principle, be generated by computer. This process is discussed in a separate report (Ref. 14).

The importance of holography stems from the fact that it provides a means for freezing electromagnetic waves (from an information point of view) so that any such wave can be studied at length at any convenient time. From an optical standpoint, this is equivalent to being able to return later to any point in space time and dwell there for as long as is required to extract desired information from the wave.

2.2 BASIC HOLOGRAM EQUATIONS

2.2.1 Simplified Theory of Holography

It is possible to derive a few simple and fairly general expressions which form the basic foundation for all holographic techniques. These

will show that first it is possible to store in a two-dimensional recording both phase and amplitude information, and second, that any desired wave can be stored and synthesized later.

Consider a simple EM wave which is represented by the complex amplitude function U and which is modulated by a field of interest. After modulation the wave U is changed to a wave U_1 (Fig. 2a). Now it is desired to store U_1 for later synthesis. This can be done by mixing U_1 with a reproducible second wave, U_r (a reference wave), and exposing a photographic plate with the combination. The total amplitude, U_t, is

$$U_t = U_1 + U_r \tag{1}$$

The time averaged intensity of an EM wave of the type under consideration is proportional to

$$I = U_t U_t^* = |U_r|^2 + |U_1|^2 + U_1 U_r^* + U_1^* U_r \tag{2}$$

A photographic emulsion responds to this intensity so that the developed plate can be characterized by an amplitude transmission coefficient, T.

$$T = f(I) = 1 - KI + K^1 I^2 + \ldots . \tag{3}$$

Considering for the moment only the first two terms in Eq. (3),

$$T = 1 - K\,(|U_r|^2 + |U_1|^2 + U_r U_1^* + U_r^* U_1) \tag{4}$$

Now it can be shown that the hologram represented by Eq. (4) can be used to synthesize the informative wave U_1. If the developed plate is illuminated by a wave U_r, the transmitted wave U' is given by

$$U' = U_r T \tag{5}$$

Using Eqs. (4) and (5), the transmitted wave is seen to be

$$U' = (1 - K|U_r|^2 - K|U_1|^2)\,U_r - KU_r U_r U_1^* - K|U_r|^2\,U_1 \tag{6}$$

Here can be seen the reason for the necessity of a reproducible reference beam. The first term is simply a spatially modulated form of the illuminating wave U_r. The third term represents a wave U_1 with a real amplification factor $K|U_r|^2$. This is the synthesized wave which was sought, the so-called reconstructed virtual wavefront. Its position

relative to the wave U_r is the same as during the formation of the hologram (Fig. 2b). It can be shown that the second term is a wave exactly like the third with the exception that it has a displaced origin.

Notice that in Eq. (1) no assumption about the direction of the wave U_r was made. When the wave U_r strikes the plate at the same angle as the object wave, U_1, the hologram is said to be in line. When an angle exists between U_r and U_1, the hologram is called off axis or sideband. If the waves U_r and U_1 lie at an angle during hologram formation, then, according to Eq. (5), they are likewise separated during reconstruction; and this allows for easier observation of U_1. In the in-line method, the reference light is often that which passed undisturbed around the object and mixes in-line with the light scattered by the object. During reconstruction for this case, Eq. (6) shows that the three waves fall on top of each other. In-line holograms are the simplest to form and for small objects (i. e., in the far field of the hologram) the easiest to work with. However, when the hologram of interest is in the near field of the object, interference between the three terms in Eq. (5) tend to degrade the quality of the images. Furthermore, the reference light must be of an easily reproducible form and cannot, therefore, pass through an object field which distorts it. As a result, nearly all holograms of large objects and of phase objects employ sideband techniques to record the hologram.

2.2.2 Useful Relationships

The derivation in Section 2. 2. 1 is useful for understanding the holographic process; but to be of more practical utility, the equations of holography must be generalized to account for the fact that a different wavelength and wave form must often be used for the reconstruction. The expressions given are derived in Ref. 15, and the derivations will not be repeated here. Most of the derivations of hologram relations are highly simplified if the object and reference waves are plane or spherical. Such a derivation can be considered to be general if the recording process is linear. Linearity in this case means that having the results for a general point object allows one to infer results for a three-dimensional object by a linear superposition of many points, each point lying somewhere on the three-dimensional object. Although the process is, in fact, rarely ever exactly linear, the simplicity of such an argument and the practical value of its application justify the approximation. Except where noted, a linear holographic process will be assumed. Effects of nonlinearities are analyzed in Ref. 16.

Consider the geometry of Figs. 2a and b. Assume that a hologram is formed with radiation of wavelength λ_1. When an object point lies

at $x_o y_o z_o$ with the reference beam originating at point $x_r y_r z_r$, a hologram is formed in the x, y plane. If the hologram is then illuminated by a reconstruction beam of wavelength λ_2 which is located at $x_p y_p z_p$, the reconstructed images, two points of light, will be at the following points.

$$z_i = \left(\frac{1}{z_p} \pm \frac{\lambda_2}{\lambda_1 |z_r|} \mp \frac{\lambda_2}{\lambda_1 |z_o|}\right)^{-1} \tag{7a}$$

$$x_i = \pm \frac{\lambda_2}{\lambda_1} \frac{z_i}{|z_o|} x_o \pm \frac{\lambda_2}{\lambda_1} \frac{z_i}{|z_r|} x_r - \frac{z_i}{|z_p|} x_p \tag{7b}$$

$$y_i = \pm \frac{\lambda_2}{\lambda_1} \frac{z_i}{|z_o|} y_o \pm \frac{\lambda_2}{\lambda_1} \frac{z_i}{|z_r|} y_r - \frac{z_i}{z_p} y_p \tag{7c}$$

where the upper sign corresponds to one of the reconstructed images while the lower sign corresponds to the other. It is important to notice that the reconstructed image is magnified when the position and wavelength of the reconstruction reference wave are different from those of the formation reference wave. Magnification, M, can be determined from Eqs. (7a), (7b), and (7c).

$$M = \frac{\Delta x_i}{\Delta x_o} = \frac{\lambda_2}{\lambda_1} \frac{|z_i|}{|z_o|} = \left| \left(1 - \frac{z_o}{|z_r|} \pm \frac{\lambda_1}{\lambda_2} \frac{|z_o|}{z_p}\right)^{-1} \right| \tag{8}$$

These equations are applicable for all of the holograms which will be considered here. Most dynamic holography is performed by pulsed ruby laser illumination ($\lambda = 0.6943\ \mu$). It is convenient to reconstruct these with CW helium neon ($\lambda = 0.6328\ \mu$). Figure 3 is a plot of magnification as a function of $z_o z_r$ for various values of $z_o z_p$ for $\lambda_2/\lambda_1 = 0.6328/0.6943$.

2.3 CLASSIFICATION OF HOLOGRAMS

While there are many geometries for forming optical holograms, these are basically the same; a reference beam is mixed with an object beam at a photographic plate. The wide variety of possibilities does, however, lead to formation of certain holograms which have properties unique to a given class.

By altering the form of the object or reference wave forms and by altering the relative positions of the object and reference wavefronts,

holograms with markedly different properties can be produced. An attempt will be made to define the most important of these by describing the special conditions under which they occur. Unfortunately, many synonymous terms have arisen in the classification, and an investigator must be familiar with all of them.

1. In-line (Gabor) Hologram - The object and reference waves are approximately collinear.
2. Off-axis (Sideband) (Leith-Upatnieks) Hologram - The object and reference waves are incident upon the recording plane with an appreciable angle between them.
3. Fraunhofer Hologram - The Fraunhofer diffraction field of the object is the object wave.
4. Fresnel Hologram - The Fresnel diffraction field is the object wave.
5. Fourier-Transform Hologram - The recording is made not of the object itself but of a spatial frequency spectrum of the object (i. e., of the object Fourier transform). One procedure for accomplishing this is by introducing a lens between the object and the hologram such that the object and hologram are in the front and back focal plane of the lens, respectively. The reconstructed wave must, in general, be passed through a second lens for viewing the image of the object.
6. Image Hologram - The "object" wave emerges from or proceeds toward an image of the object field during recording (i. e., it is a hologram of an image of an object as opposed to a hologram of an object).
7. Reflected Illumination Hologram - The object wave is one which has reflected from an object field.
8. Transillumination (Shadow) Hologram - The object wave has passed through the object field as opposed to reflected from it. The term shadow hologram, while widely used, is not, in general, a correct one since it implies that the object field is characterized by some opacity. Many object fields observable by transillumination holography are pure phase objects and cast no shadow whatever.
9. Reflection Hologram - The object and reference waves are introduced from the opposite sides of the recording plane. The reconstructed image is viewed by reflecting

light from the viewer's side of the hologram. White light can be used for the reconstruction in certain instances. This is one of the few types of holograms which rely upon the thickness of the recording emulsion to obtain the desired effect.

10. Multiplexed Hologram - More than one recording is made on the same hologram with the reference beam angle to the film normal being changed for each separate recording.

Other types of holograms exhibit different properties according to the type of recording medium.

11. Amplitude (Thin Emulsion) Hologram - The hologram relies upon diffraction by amplitude modulation of the reconstruction wave.

12. Phase (Dielectric) Hologram - The hologram relies upon refraction by phase modulation of the reconstruction wave. This can be achieved through a number of processes, many of which are still under intensive development by other laboratories. The most promising feature of phase holograms is their efficiencies which, in principle, can approach 100 percent. The most common types are:

    a. Bleached Holograms - The silver in the developed photographic emulsion is "bleached" by replacing it with a transparent compound whose index of refraction differs from that of the emulsion. Appendix I gives the most common processing formula.

    b. Relief Hologram - The silver in the developed hologram is completely removed causing the emulsion to "cave in", resulting in a relief pattern which refracts light.

    c. Photochromic Hologram - Instead of the usual photographic emulsion, a material whose index of refraction changes by an amount proportional to its exposure to light is used. Such materials are still in an early stage of development.

The matter of classification is further complicated by the fact that each of the above types of holograms exhibits a striking difference according to whether the object illumination arises from one or more point sources (direct illumination) or an extended source (diffuse illumination). Examples of some of the different holograms and their special characteristics will follow in subsequent sections.

SECTION III
EXPERIMENTAL HOLOGRAPHY

3.1 ELEMENTARY REQUIREMENTS

In addition to the basic requirement of mixing a reference wave with an object wave, a holocamera must meet a number of specific criteria which are important to the formation of high quality holograms (viz, those which reconstruct a bright, accurate image of the object field). This is crucial for the analysis of the information which will be extracted from the hologram. The most basic criteria are:

1. The optical pathlength difference between the object wave and the reference wave (as measured from the laser) must be much less than the temporal coherence length of the laser.
2. Each ray in the reference wavefront must be mixed with a mutually coherent ray in the object wave front. This means that the two rays must be derived from regions in the original laser beam which are separated by no more than the spatial coherence interval.
3. The reference wavefront should exceed the object wave front in intensity by a factor ranging from 2 to 25, depending upon the type of emulsion and upon the type of object illumination.
4. The reference wavefront should be a simple one which can easily be reproduced (e. g., plane or spherical wavefront).
5. The angle between the object and reference beam should not exceed 45 deg; however, if the film resolution is sufficiently high or the image resolution requirement is sufficiently low, the angle can exceed this value.

6. The hologram and the optics must remain stationary to a small fraction of the laser wavelength during the exposure (except for some special cases).
7. The emulsion exposure density should lie in the neighborhood of 0.5.
8. Typically, film resolution should exceed 1000 lines/mm.

These requirements can be relaxed to some extent if individual requirements of the accuracy of the recording are relaxed. Also, special cases exist in which some of the requirements are not necessary. Appendix II contains a description of films and plates which are suitable for holography.

3.2 CONFIGURATION REQUIREMENTS

Configurations required to meet the conditions outlined in Section 3.1 are different according to whether CW lasers or pulsed lasers are used. The requirements could be easily met if the best properties of each laser could be combined. This is gradually happening; but until lasers are further improved, they must be discussed separately.

3.2.1 CW Laser Holography

CW holography is more difficult than pulsed holography; however, it is the easiest way to produce extremely high quality holograms. The problem lies with the exposure times required. Typical exposure times range from a few milliseconds to minutes, depending upon the laser power. Typical exposure times with an inexpensive helium-neon (He-Ne) laser exceed 1 sec. Because of requirement 6, such work must be done in a quiet, still atmosphere on a high stability table. This is, perhaps, the only critical requirement in CW holography. Air currents such as from an air conditioner, a person's walking near the experiment, even breathing, can ruin an otherwise perfect holography experiment. Noise can be tolerated only if the equipment is rigidly mounted. Figure 4 illustrates an experimental apparatus which is designed to produce high quality holograms. The requirements are satisfied by the following experimental conditions. The path lengths are measured such that ABCDE equals AB'C'D'E. With most He-Ne lasers the two can differ by 10 to 20 cm, though some high coherence lasers allow much larger differences. CW lasers can be made spatially coherent over the full beam diameter. This is insured in the above laser by operating it in the TEM_{00} mode and further by passing both beams through pinholes. The pinholes also clear the beam of diffraction noise. The reference wave is made parallel by a diffraction limited lens at D'. Surfaces at A and B' are flat to one-tenth wave. It is important to emphasize that expensive optics are necessary only for refinements and not for ordinary holography.

Requirements 7 and 8 are photographic requirements easily satisfied. Requirement 5 was reserved for last since it requires more discussion. A high stability table was designed and constructed for basic holography studies. The arrangement is shown in Fig. 5.

The table top is steel, weighing 2000 lb, requiring 9.5-psi pressure for lifting. Its natural frequency is 2 Hz. The air-filled legs are separated into two sections by a plastic partition. An orifice in the partition serves to dampen vibrations of the table. The success of the leg design has led to its adoption by several other AEDC groups with similar isolation problems. Simpler, less expensive isolation tables can be constructed, for example, by using inflated inner tubes to support a thick concrete table top. Under most conditions, such tables are suitable even though they are usually characterized by higher natural frequencies and less damping. On the other hand, commercially available tables with highly polished granite surfaces and automatic hydraulic leveling are recommended where cost is not a factor.

3.2.2 Pulsed Laser Holography

Pulsed lasers can provide enough energy to form a hologram in extremely short times. This relaxes the problem posed by requirement 6 since typical mechanical vibrations encountered are characterized by periods much longer than the laser pulse width. Therefore, such experiments can ordinarily be conducted on an ordinary support or table.

Requirements 1 and 2 cause considerably more difficulty in pulsed laser holography; however, techniques have been discovered in the past few years to satisfy them. The direct laser beam from a pulsed laser, for example, from a Q-switched ruby laser, is extremely poor in quality. It is characterized by many off-axis modes, causing poor spatial coherence, and by many axial modes, causing poor temporal coherence. To correct these problems always requires a certain amount of compromise between desired properties. Experience has shown that spatial coherence of a ruby laser can be improved considerably by either (1) lengthening the cavity, or (2) inserting a small aperture in the cavity. Either process does, however, reduce overall laser power. The latter method is usually most convenient. The optimum aperture size for ruby lasers discussed here was found to be approximately 2 mm in diameter. Its axial location in the cavity is seemingly unimportant; however, its radial position should be adjusted until the laser operates at its lowest pumping energy. Such an aperture will typically increase the brightness of a hologram by an order of magnitude. This means simply that, without the aperture, much of the light falling on a hologram in progress fogs the film without forming holographic fringes. Therefore, any pulsed ruby laser which is being used as a source of spatially coherent light should be equipped with an intracavity aperture

(if not some other device for spatial coherence improvement). High spatial coherence can be obtained by focusing the laser beam through an aperture (pinhole) whose diameter is that of the Airy disk of the lens used. For obvious reasons, this technique is not widely beneficial with high-powered lasers. Even if the focused beam does not destroy the pinhole, alignment is extremely difficult.

There are two common methods for improving temporal coherence. The simplest of these is the use of a passive dye "Q" switch. The dye acts as a Q switch for a narrow line of frequencies, often limiting its giant pulsed operation to a single frequency. High quality holograms have been made at AEDC with over a meter's difference in reference and object beam pathlengths indicating high temporal coherence. No effort was made to seek the limit of the criterion.

The second common method for extending spatial coherence is to employ a Fabry-Perot etalon or, better yet, an adjustable Fabry-Perot interferometer either in the cavity or as a part of a cavity reflector. Such an interferometer causes nominally 50-percent power loss. Two of the AEDC systems are equipped with these devices. They act as wavelength selectors, having high transmission or reflection for a single wavelength. They are needed only in the absence of a passive Q switch. When a laser is Q-switched with an active device (such as Pockell's cells, Kerr cells, rotating mirrors) and high temporal coherence is required, Fabry-Perot devices should be employed.

Finally, it should be mentioned that higher coherence is obtained from the Q-switched mode than from the normal lasing mode. It should be emphasized that coherence requirements discussed here are not critical. Indeed, holograms can be made with a poor laser operating in its worst modes. Such holograms, however, are of little practical value.

When coherence of the laser cannot be improved, the holocamera itself must be designed so that it can tolerate poor coherence. Requirements 1 and 2 are thus more difficult to satisfy since a special optical design is imposed on the holocamera. These are discussed in detail in the next section.

3.3 ILLUMINATION ARRANGEMENTS

The optimum choice of illumination and illuminating geometry depends upon the nature of the object field and upon the data desired. The illumination method can employ direct or diffuse illumination, or a combination,

and these can be transmitted through the object field onto the hologram (transillumination) or reflected from the object field onto the hologram or a combination of reflection and transillumination.

3.3.1 Transillumination

Figure 6 is a typical diffuse transillumination holocamera. Removal of the ground glass converts this to direct illumination. The arrangement is shown such that pathlengths are approximately matched for the reference and object beam; but with this arrangement, they cannot be matched exactly. Spatial matching (requirement 2) can be accomplished only without the diffuser. However, spatial matching is not so critical with the diffuser present. Light striking the hologram from a particular portion of the diffuser will interfere with only the portion of the reference beam with which it is coherent. In other areas, it simply fogs the film. Therefore, certain portions of the reconstructed image may appear dark when viewed from certain angles. Also, the overall recording efficiency will be reduced. With direct lighting, this effect can cause portions of the image field to be obliterated entirely since only one angle of view is available.

It is possible to achieve an exact match of spatial and temporal coordinates with diffuse illumination if the diffuser is imaged upon the film (Ref. 17). Such a system is needed when the quality of the laser illumination is poor. This technique has been employed to some extent at AEDC but rarely has been necessary.

3.3.2 Spatial Alignment (Wavefront Matching)

Requirement 2 can be satisfied exactly by ensuring that each object and reference light ray which mixes at the hologram be derived from a single ray at the laser. This can be actively achieved by placing a test pattern (e. g., a graticule) in the laser beam before it is split into object and reference beams. The two shadows of the graticule must then be forced to align at the hologram plane. When a pulsed laser is the illuminating device, this alignment must be carried out by passing a CW laser beam along the same path to be followed by the pulsed illumination. This type of alignment is applicable, of course, only with transillumination.

SECTION IV
APPLIED HOLOGRAPHY

4.1 STUDY OF SMALL PARTICLE FIELDS

The work concerning in-line holography techniques at AEDC has been covered in detail in Refs. 5 through 8. Therefore, this section will deal primarily with more recent developments and applications. Conventional photographic methods for observing small particle fields are insufficient because a high resolution camera system is characterized by small depth of field. Thus, such systems are limited to the observation of planes in the field. Holography does not suffer this limitation and, therefore, provides a new way to freeze a 3-D array for detailed examination.

4.1.1 Application in RTF

A holocamera was designed to examine the particulate matter in rocket exhausts. The ultimate objectives of the instruments are to provide a recording whose analysis will result in the detailed specification of the particle field in a rocket exhaust. The specification should include (1) particle sizes, (2) particle velocities, (3) particle densities, and (4) the three-dimensional distributions of these properties.

The instrument must be capable of:

1. Operating in a high altitude test environment.
2. Recording data from a highly luminous rocket exhaust.
3. Reliably functioning in the presence of a number of severe test conditions including vibration, high temperature, and high contamination.
4. Stopping particles whose velocity exceeds 2000 m/sec.
5. Resolving particles characteristic of a rocket exhaust.

It was not definitely known if any of these requirements could be met. They could only be examined in an actual test of a holocamera.

A portable holocamera which meets the above requirements was designed and constructed. The system is packaged in a sealed container so that it can be operated under a wide variety of environmental conditions. The in-line and sideband transilluminated configurations that have been primarily used in the holocamera are shown in Fig. 7. A

Korad pulsed ruby laser operating in a Q-switched mode is the coherent source of illumination. The pulse lasts approximately 10^{-8} sec and reaches an optical power of approximately 1 MW. The optics are mounted on rigid supports which allow them to be easily aligned and securely fastened. They are aligned with a He-Ne laser by passing its beam through the ruby rod. Through experience it was found that the optical changes caused by the wavelength difference could be neglected. The wedge reflects 4 percent of the light from its front surface and about 3.5 percent from its back surface. The second reflection is passed through a fiber optics probe to a photodetector so that the light pulse may be recorded.

The simplest holographic configuration (in-line) is shown in Fig. 7a. The beam expanding optics in the laser box collimate the laser light before it passes through the object field. Since more light is available than is actually needed, only the light reflected from the wedge is used as the illuminating wavefront. Note that only one beam strikes the film.

The holocamera straddles the rocket exhaust (Fig. 8), and an opening in the support bracket allows the motor to exhaust into the diffuser unperturbed by the camera. The first system tested was a diffuse transillumination image holocamera.

A negative lens diverges the object beam so that it fully illuminates the frosted plate in the porthole of the box. This plate is a quartz window that has been frosted on both sides. The light is, therefore, diffused over the test region, producing a bright background in the reconstructed image. The Fresnel lens collects the diverging light, allowing more of it to illuminate the frosted plate.

The reference beam is deflected by a first surface mirror through the beam protection tube and into the camera box. This tube encloses the narrow beam, shielding it from contaminants from the rocket exhaust, which would impair the image quality of the hologram. A vent to atmospheric pressure was used to protect the camera components and film.

In the camera box the reference beam is deflected by a first surface mirror into a negative lens which diverges the light. A positive lens collimates the light before it reaches the film. Since this beam must be duplicated for accurate reconstruction, the collimated beam was used for its simplicity.

An f/2.5 lens in the object beam magnified the test region and imaged it closer to the film. Consequently, the film sits within the image of the

test region. A 6943-Å line filter is placed between the two sets of lenses which compose the image lens to filter most of the light from the exhaust and allow only the laser light to pass through. Because of the small size of the filter available, the f-number of the lens was increased to f/6. A trade-off between small particle resolution and field-of-view of the exhaust was necessary because of the imaging lens. A compromise sacrificed small particle ($<50\ \mu$) resolution for a larger object field. The distance between the rocket centerline and the imaging lens was dictated by the test cell exhaust diffuser geometry. While this dimension must be as small as possible for high resolution, no attempt was made to move any part of the camera inside the diffuser.

Four 2-sec firings of a Titan II retrorocket were holographed in all. Incorrect sequencing of the laser firing control during the first test caused the laser to fire 1 sec before rocket ignition. The second and third rocket tests were successful from the holography point of view since good holograms were taken when the rocket was firing. However, a slight misalignment in one of the mirrors produced a partially exposed hologram on the third shot.

No particles could be detected in the reconstructions of these holograms. It is believed that the combined effect of the particle's being smaller than the optical system could resolve and/or their moving too fast to be stopped with the laser pulse prevented their detection. For the final firing, the camera was converted to a laser photographic camera by blocking the reference beam and by imaging a plane in the rocket exhaust on the film plate. No particles could be detected above the usual grain and speckle pattern on the film.

Data for the holographic system were taken before and after the rocket tests. A number of tests were run to determine the resolution of the camera. One object used was a standard Air Force resolution chart. Each column number is the power to which two is raised, giving the resolvable lines per millimeter of the first row. These figures indicate resolutions better than 36 lines/mm.

The hologram reconstructed image resolution is shown in Fig. 9. The resolution is poorer without the imaging lens.

From the study, the following was concluded with respect to the tests of a Titan II retrorocket.

1. The holocamera can record through the rocket exhaust at simulated altitude. Every attempt at holographing the field through the exhaust was successful.

2. The rocket exhaust has a high transmissivity of light. The frosted glass was clearly visible through the exhaust.
3. The particle sizes were less than 100 μ in diameter. All available data indicate that particles larger than 100 μ in diameter would be visible in the holographically reconstructed image.
4. The rocket exhaust illumination can be tolerated for either holography or laser photography with narrow bandpass filtering.

Work continued to improve the capacity and reliability of the camera. The camera was tested again after the following improvements were made:

1. A larger diameter narrow bandpass filter to decrease the f/number.
2. Other lens combinations for resolution improvement.
3. Improved Q-switching methods.
4. Improved operating procedures, learned from laboratory testing.

The improved resolution of the holocamera extended its capability to approximately 25 μ. A second series of solid rocket tests in RTF T3 still indicated no appreciable quantity of particles above 25 μ in diameter. Further changes in the camera could increase its resolution to an ultimate limit of approximately 10 μ; however, this would seriously reduce the field of view because of the magnification required. Additional tests will be required if higher resolution is desired.

During the course of these experiments, a closed-circuit TV monitoring system was added to the reconstruction system. This allows an investigator to scan through the reconstructed 3-D field with a high resolution zoom lens and to view the image on the TV monitor. Data for which storage is desired can then be recorded on video tape or photographed directly from the TV screen. Figure 10 is a portion of the reconstructed image of a doubly exposed sideband hologram of a dynamic particle field. The figure was taken from a closed circuit TV monitor while the vidicon scanned the reconstructed image field. The double images of the particles can be easily identified for velocity measurements. For the case shown, the pulse separation was 100 μsec. Respective particle sizes and velocities are designated in the figure. A reference wire shown in the field allowed an easy determination of the system magnification.

The camera is essentially ready for routine use as a research and testing instrument with the limitations stated. However, a number of engineering improvements should be incorporated before it could be considered a versatile operational tool.

1. Automatic film exchange must be incorporated to provide more than one recording during a test.
2. A larger power supply must be acquired to decrease the recording interval from 15 to 1 sec, the maximum pulse frequency of the ruby rod.
3. An automatic alignment device should be incorporated to simplify holocamera alignment.
4. A Pockell's cell Q-switch should replace the passive cell.
5. A traverse should be incorporated to allow accurate variable positioning of the camera.

4.1.2 Velocimetry

A part of the OMD/TS project objective was the study of holographic application to velocity determination of solids and liquids. One obvious approach to holographic velocity determination has already been illustrated in the last section (see Fig. 10). The technique, originally proposed independently by Mycroft of AFFDL and by the authors was studied experimentally and theoretically at AEDC and has been reported in detail (Refs. 5 through 7). The first velocity measurements in the program were made directly from the Fraunhofer diffraction patterns of the particle without reconstruction. This method was, however, shown unsatisfactory except under highly specialized conditions. The method requires (1) small particles of known shape, (2) a low particle density, (3) an extremely clean system, (4) tedious and inaccurate data analysis methods, and (5) a fairly accurate knowledge of the velocity even before the measurement is made. Based upon an experimental and theoretical analysis (Ref. 5), the latter method was discarded in favor of performing the measurement upon the reconstructed image (Refs. 5 through 7). Other attempts to determine flow field velocities by directly analyzing the Fraunhofer diffraction patterns have been reported (Ref. 18); however, because of the reasons already stated, the method is not expected to be widely useful.

Observation of the reconstructed image allows an operator to perform direct interpretations not possible with the diffraction pattern,

i. e., the information is in a form more easily related to experience. This method of velocimetry has been applied with both in-line and off-axis holography in the determination of objects of arbitrary shape, ranging in size from 5 μ to several centimeters and ranging in velocity from a few cm/sec to over 10^5 cm/sec (Ref. 19). Recently, similar results were published by another laboratory (Ref. 19). Generally speaking, the field of view can be as large as 10^4 cm^2 with depths of field of approximately 100 cm for objects above 100 μ. Smaller objects require less field depth. The technique could be used indirectly to determine the 3-D velocity field in a fluid or gas if such a flow has been "seeded" with particles large enough to holograph, small enough and light enough to follow the flow without significantly disturbing it. Finding such a particle is no easy task, and the requirements change with each experiment. Mycroft and Flynn (WPAFB) suggested the possible use of gas-filled bubbles for seeding gaseous flows. If bubbles could be produced with sufficient strength, one might further speculate that an observation of the changing bubble diameters could lead to a determination of the local pressure. The authors' experiences have shown that fibers are much more easily identified in a reconstructed image than circular particles. This suggests the search for a source of fibers of diameter between 10 and 100 μ having a low mass. Silk or woolen fibers have such characteristics as well as the common dust particles found floating in an uncontrolled room.

Although basic techniques for multiple exposure holographic velocity determination are now established, the methods can be improved and extended in hundreds of ways. However, since the most important problems can only be specified by details of a specific type of application, it seems rather pointless to proceed further with the development except as the applications themselves are specified.

4.1.3 Range, Limitations, and Accuracy

To determine the utility of holography for particle field studies, one must consider many factors. Smaller particles scatter less light and are more difficult to record, the difficulty increasing with the distance from the hologram. At higher particle densities, less information can reach the hologram, and the recording quality is reduced. Finally, when the particle moves during the recording, the hologram quality is reduced. The strictness of the requirements depends, of course, upon desired data quality.

A useful parameter in describing the ultimate limits obtainable in a holographic recording is called far-field distance. A particle which is one far-field distance from a hologram is said to have a far-field

number of unity. One far-field distance is defined as the diameter squared of the particle divided by the wavelength of light being diffracted by that particle. For a hologram to contain sufficient information to reconstruct an accurate image of the particle, it must accurately record a minimum number of orders of diffraction of that particle, regardless of the optical system used. As the far-field number increases, the radius of the diffraction pattern containing the minimum required number of orders of diffraction also increases. As the radial position on a certain diffraction pattern increases, signal-to-noise ratio in the recording decreases until finally it reaches a point at which no appreciable signal is contributed to the reconstructed wave. If a lens system is used to re-image the particle to a position closer to the film, that lens system must be capable of collecting and accurately transferring at least the minimum number of diffraction orders required. If it does not meet this requirement, regardless of the magnification of the lens system, the particle resolution will deteriorate; the magnification is then said to be empty. If a lens system is capable of collecting a sufficient number of orders of diffraction for a given particle, one is justified in computing the far-field number in terms of the distance of the image of the particle from the recording. Therefore, if it is desired to make a holographic recording of a small particle which is located at a large distance from any optical element, the problem can be attacked in two ways. A direct recording can be made if the photographic plate is large enough to accept the required number of orders of diffraction. As has been mentioned, signal-to-noise ratio decreases as the radius of the diffraction pattern becomes larger; therefore, a better way to accomplish such a recording is to use a large imaging element such as a lens or mirror which collects the required number of orders of diffraction and converges them back to a small photographic plate. Invariably, such an imaging element introduces aberrations. However, for the purpose of this discussion, such abberations will be neglected. In the following discussion, it will be assumed that the imaging element is not the limiting factor in the recording (that is, imaging elements are sufficiently large and corrected). If one is concerned with an image hologram, he will consider the location and size of the image of the particle as opposed to the actual particle in computing resolution limits. Figure 11 summarizes the required conditions for good quality reconstruction data (see also Refs. 5 and 8). Examples are given to illustrate the use of the chart. Good recording quality can rarely be obtained when conditions place a point in the shaded region to the left of the N = 100 line. To the right of the N = 1 line, in-line holograms must usually be optically filtered to provide good data (see Ref. 7).

Point A - The particle density is 100 per cm^3, 10 cm from the film plate, and the particle radius is 175 μ. Such

particles lie in the Fresnel zone and in-line recording is questionable. Optical filtering or sideband holography must be used.

Point B - In-line or off-axis recording supplies accurate data if the volume depth of particles is less than 20 cm.

Point C - All conditions are satisfied; a lower particle density allows greater volume of particles to be recorded.

Point D - The maximum distance from the hologram that a 20-μ particle can lie and still be accurately recorded is 30 cm.

As the particle speed increases, one must decrease the hologram recording time to maintain quality of the reconstruction. If a particle moves no more than a small fraction of its diameter during the recording, one can expect reasonably accurate recording in either in-line or transillumination sideband holography. Figure 12 gives maximum recording times as a function of particle size and velocity using as a criterion, a one-tenth diameter motion during recording. These illustrate that required recording time varies inversely as the particle diameter and velocity. It should be emphasized that the criterion is quite arbitrary. Figures 13a and b are reconstructed images of particle fields in which appreciable motion occurred during the recording. Streaks can be observed up to several diameters in these figures.

Multiple exposure holography of particle fields has similar requirements to the single exposure case. These are covered in detail in Ref. 7.

Error in determining particle size has been shown by several investigators, including the authors, to be less than 1 percent when a high quality hologram can be made. Extreme accuracy requires diffraction-limited optics, correction for emulsion shrinkage and distortion, and accurate recording parameters. No attempt has been made here to further refine the technique.

Particle location in the plane parallel to the hologram can be located to accuracies similar to those in size determination. Particle location in the plane perpendicular to the recording plane is less accurate. We have found experimentally that particle images (or filaments) can be consistently located in that plane to an accuracy of about ten particle diameters for particles less than 100 μ in diameter. Particles exceeding 100 μ in diameter have consistently been located to less than 1 mm. Ultimately, the location accuracy increases, as with any imaging system, with the ratio of the diameter of the imaging device to the distance of the image from the imaging device. The diameter of the imaging device

in the case of a hologram is the diameter of that portion of the hologram which contributes light to the image. Many factors determine this diameter, including film resolution, linearity, and modulation transfer function.

4.1.4 Other Possible Applications

Application of small particle field holography has been considered in a wide variety of testing applications. It is important to remember that holography is at the present time considerably more complicated and, in most cases, less reliable than photography. Photographic data can be considered a subset of holographic data. The point is that one should usually have a need for data that photography cannot provide before he decides to apply holography to a particular problem. Only problems which cannot be handled more simply by photographic techniques will be discussed here. This includes cases which require (1) high resolution visualization of a 3-D array at a given instant in time, (2) extremely high resolution over a large area, (3) closer proximity to the object than is convenient with photography, and (4) situations in which the exact location of the object is unknown. Also included are cases which require more than simply photography for the visualization. Applications which have been studied include studies of condensation processes, ablation phenomena, impact phenomena, fogs and aerosols, and wake phenomena.

4.2 HOLOGRAPHIC FLOW VISUALIZATION SYSTEMS

In the aerodynamic testing of models in wind tunnels, a method is required to visualize and record the characteristics of the flow which is, unfortunately, in most cases colorless, transparent, and nonluminous. These conditions of the flow make their observation with the unaided eye or by direct photographic techniques impossible. However, the disturbances in the flow of air past an aerodynamic model do effect changes of the refractive index of the air because of variations in density created by nonuniform temperature and pressure regions such as the bow shock, boundary layer, and wake.

Extensive use is made of photo-optical methods to study high-speed airflow since the changes of refractive index that accompany the density gradients across a flow field can readily be observed and recorded photographically. The most commonly used methods of flow visualization are shadowgraph, schlieren, and interferometry (Ref. 20). The shadowgraph method is particularly useful in determining the boundaries of shock waves, turbulence, and boundary-layer characteristics. The

schlieren method, which indicates density gradients, can generally be at least an order of magnitude more sensitive than the shadowgraph method. It is useful in detecting very weak shocks and determining regions of small density gradients in the flow field. The interferometer indicates relative density variations and gives an interpretable picture from which a density distribution may be evaluated.

These methods provide a means to characterize the flow without introducing perturbing instruments into the flow. Since each of these methods characterize the flow field differently, they are complimentary rather than alternative. It would be desirable, in many cases, to record flow visualization data at the same instant in time using each of these conventional methods; however, this is not convenient since each method requires a different optical arrangement.

In conventional schlieren and shadowgraph systems, some operation or transformation is performed upon the radiation emerging from the flow field before observing or recording it. In some cases, this operation places severe restraints upon it, the most common of these restraints being system rigidity. The lack of system rigidity and stability usually makes it impractical to use the interferometry method near the environment of a high-speed wind tunnel.

The basic geometry of a conventional flow visualization system is shown in Fig. 14 and is generally attributed to Toepler (Ref. 21). A well-ordered, collimated beam of light the size of the area of interest is formed by providing a point source of light at the focal point of the first concave primary mirror. After passing through the test region, the collimated beam of light is refocused by the second primary mirror to form a conjugate image of the illuminating light source. A refocusing lens is placed behind this focal point to form an image of the test region for visual observation or recording. Shadowgrams can be recorded of the test region by defocusing the test region, or the schlieren method can be applied by placing a knife edge at the transform plane (focal point of the second primary mirror) as described in Ref. 20.

Since holograms record all of the information contained in the electromagnetic (light) wave that passes through the flow field, the disadvantages of conventional flow visualization methods are circumvented in that the informed light wave is frozen in time and stored, and at a later time, under ideal laboratory conditions, can be reconstructed as a shadowgram, variable knife-edge schlieren, color schlieren, or interferogram. Furthermore, the complete freedom allowed in working with the reconstructed wave opens the way to application of many other optical processing methods. Conventional flow visualization methods employ point or

line source illumination. Holographic flow visualization systems (HFVS) may employ either point source or extended diffuse source radiation. The former appears to be more versatile for flow visualization and will be discussed first. Direct illumination HFV is merely a generalization of conventional flow visualization.

4.2.1 VKF Holographic Flow Visualization System

The basic optical geometry of a direct transillumination HFVS is similar to that of a conventional refocused shadowgraph or schlieren system. Such a system was constructed by VKF/OSG and applied to wind tunnel studies. The primary paraboloidal mirrors of the VKF system have a 488-cm focal length and are 45 cm in diameter. The optical path of the conventional system is shown in dark lines. The additions of the basic optical system that are required for the HFVS are shown by heavy lines in Fig. 15. The coherent light source is provided by a Korad® K1 Q-switched ruby laser which produces a 17-nsec pulse of coherent light. The reference beam proceeds through the beam splitter, is reflected by two flat front-surface mirrors, and is then diverged by a concave lens to cover the photographic film plate. The object wave, a plane wave 45 cm in diameter, is provided by placing a concave lens in the laser beam, after being reflected 90 deg by the beam splitter, to form a point source of light at the focal point of the first primary mirror. The second primary mirror receives the collimated light beam and focuses it off-axis to an astigmatic point image. The film plate is located 50 cm ahead of the focal point of the second primary mirror where the object wave and reference wave are superimposed. After the film plate has been exposed and processed, it is a hologram.

The portable light source unit for the HFVS is shown in Fig. 16, with covers removed, set up for the operation on a Mach number 8 hypersonic wind tunnel.

The holograms are recorded on 4- by 5-in. Agfa-Gevaert Scientia® 8E75 film plates. The emulsion has a peak sensitivity at 6943 Å of 200 e/cm^2 for optimum exposure and has a resolution of 3000 lines/mm.

The film plates were processed in Kodak® D-19 developer for 4 min at 68°F. The density of the holograms was approximately 0.4 with a reference beam to object beam intensity ratio of 4 to 1.

A considerable amount of optical noise was caused initially by interference of light reflected from the second surface of the photographic plates even though the plates were supplied with an antihalation backing.

The emulsion of these plates is extremely thin, allowing a considerable amount of light to pass through to the second surface of the plate. The result is a set of nonlocalized Fabry-Perot fringes existing in the reconstructed wave. The film plate was tilted 10 deg away from perpendicular to the object beam axis which increased the fringe frequency so that the interference effects were not as noticeable. By painting the rear surface of the plates with flat black paint (Ref. 17), the fringes were completely removed.

Figure 17 is a reproduction of a hologram made with the HFVS of a model and flow field in the 50-in.-diam Hypersonic Wind Tunnel (B) operating at Mach number 8. All of the holographic reconstructions shown in this paper were made from this particular hologram.

The geometry used for reconstruction of the hologram is the same as that with which the hologram was made with the reference beam being furnished by a 15-mw continuous-wave He-Ne laser (Fig. 18). Accurate reconstruction requires that the reconstruction beam strike the hologram exactly as the reference beam which was used to form it. It can now be seen that the reconstructed wave that emerges from the hologram will have the same geometry and characteristics as one that would exist with a conventional flow visualization system. In fact, the informed wave is identical in every respect to the original wave, allowing operations to be performed on the light wave as if it were the original.

The portions of the conventional flow visualization system (the knife edge, refocusing lens, and camera) that were omitted from the HFVS can now be employed in the reconstruction setup in order to record flow visualization data. Figure 19 shows the apparatus used to make the holographic reconstructions on 4 by 5 Polaroid® and Kodak Royal Pan film.

4.2.2 Shadowgraph Holographic Reconstruction

It is well known that it is necessary to defocus the image of the flow field when using the shadowgraph method to record flow visualization data. In fact, the sensitivity of the shadowgraph method relative to the magnitude of the density gradient that can be visualized is proportional to the distance from the disturbance to the plane of focus. Therefore, an infinite number of recordings can be made at varying sensitivities which gives the aerodynamicist much flexibility in recording optimum flow data. Figure 20 is a series of shadowgrams of the model and flow field at increasing sensitivities as shown in a through d. If the shadowgraph method does not produce the data that the aerodynamicist desires, reconstruction using other flow visualization methods can be tried until the desired data are obtained.

4.2.3 Schlieren Holographic Reconstruction

In order to make a schlieren reconstruction of the hologram (which is usually an order of magnitude more sensitive than the shadowgraph method), the camera is focused on the virtual image of the model and flow field (Fig. 18). A knife edge is then inserted into the reconstructed light beam at the transform plane and adjusted to any desired position to observe and record the schlieren effects. In aerodynamic testing, one is usually interested in observing the density gradients in the flow field in many different directions. Since the single knife-edge schlieren method detects only the density gradients perpendicular to the knife edge, it is possible to visualize the particular gradients of interest by positioning the knife edge at any angle to the flow field. Figures 21a and b show two schlieren reconstructions made with a vertical knife edge inserted from the left (a) and from the right (b). Figures 20c and d show schlieren reconstructions made using a horizontal knife edge inserted from the top (c) and from the bottom (d).

Another useful facet offered by the complete freedom of knife-edge positioning is that one can vary the sensitivity of the schlieren effect. Many other types of filtering operations, both amplitude and phase, may be performed at the transform plane in order to obtain an infinite number of different flow field characteristics.

4.2.4 Color Schlieren Holographic Reconstruction

In order that the color schlieren holographic reconstruction be understood, it is helpful to know how conventional color schlieren photographs are recorded. A conventional schlieren system can be easily modified to produce a multicolored image of the flow field. One method in which this can be accomplished is to replace the knife edge at the transform plane with a color filter grid consisting of the three primary colors -- red, green, and blue. The width of the center filter, usually green, is made the same width of the undisturbed conjugate image of the light source; therefore, the undisturbed portion of the flow field will be green on the color recording. The density gradients which deflect the light source image its full width will be either red or blue, and those which do not deflect the source image its full width will be represented by a mixture of two colors. The image of the flow field is recorded on color film which presents a particular density gradient in the flow field as a particular color.

Since the He-Ne laser used in the holographic reconstruction set-up is a monochromatic light source, it is evident that a color filter grid

cannot be used to produce color schlieren reconstructions. However, the same results can be obtained by using black and white separation negatives to record three separate plane filtered reconstructions. An opaque filter is used with the same dimensions as those that would be used for each color filter with the conventional method described earlier. Three separation negatives are then made with the opaque filter occupying each of the positions that the three color filters would normally occupy. After the three separation negatives have been exposed and processed, they are registered and punched so that they can be printed in register. Each negative is then printed on the same sheet of Ektacolor® printing paper using the appropriate filter for each negative to provide a color rendition of the flow field. The reader is referred to Ref. 12 for an example of color reconstruction.

4.2.5 Interferogram Holographic Reconstruction

Phase phenomena in the flow field can be observed and recorded through holographic interferometry by a multitude of techniques. In each of these, an unmodulated reference wave is mixed with the object wave (in addition to the holographic reference wave) as in conventional interferometry.

Two of these techniques which are easily applied to the HFVS are sheared wavefront interferometry and stored reference beam holography. The first of these is accomplished by splitting the reconstructed object beam into two beams and subsequently remixing them. The two beams are slightly offset so that the two wavefronts are tilted with respect to each other. The field will now be crossed by a set of fringes because of this tilt. Bright fringes define the locus of points on which two separate components fall after having traveled optical paths differing by an integral number of wavelengths. The frequency and direction of the fringes are easily varied. Figure 22 illustrates this technique. Although this technique is the easiest to accomplish of the two mentioned, it does have a disadvantage in that a double image of the model and flow field is recorded, and useful data can only be obtained in those areas where the flow field of the two images do not interfere.

The second technique is applied by providing a separate holographically reconstructed reference wave to mix with the holographically reconstructed object wave. Two holograms are required: one of the object field with no disturbances and one of the object field with the model and flow field present. The reference wave plate is made by placing a film plate just ahead of the plate location used for making the hologram of the model and the flow field (Fig. 23). After exposure and processing, the

interferogram is reconstructed by placing the reference hologram in the same relative position to the object hologram in which it was made (Fig. 24). The two reconstructed waves are then superimposed, which is equivalent to Mach-Zehnder interferometry. Fine adjustments can be made between the two plates to produce the fringe angle and spacing that is best suited to show the density variations of the regions of interest in the flow field. Figure 25 illustrates this technique.

The method of analyzing this holographic interferogram is identical to that of conventional Mach-Zehnder interferometry; however, the freedom of fringe frequency and orientation selection provides an analysis capability far beyond that of conventional interferometry.

4.3 BASIC STUDIES IN HOLOGRAPHIC FLOW VISUALIZATION

From the wind tunnel studies described in the last section, it was concluded that HFV was practical on a large scale under test conditions. Therefore, it was felt that additional basic studies in HFV were justified to assist in the refinement of wind tunnel HFVS and to provide knowledge for their continued capability improvement through application of additional coherent optical processing methods. Moreover, the extension of even the conventional flow visualization to HFV was not (and still is not) complete. This section describes basic studies in holography which were either continued with a slant toward HFV or which were initiated to support HFV.

4.3.1 Hologram Interferometry

The capability to form an interferogram like Fig. 24 is only the beginning of the flow analysis. The fringe information must be interpreted in order to make it useful. Data reduction for a direct illumination holographic interferogram is the same as for conventional interferograms, with the exception that the former offers versatility in data reduction not offered by the latter. Flow field interferometry provides a method for comparing, quantitatively, the optical path length through a transparent test field with that through a reference test field. In conventional interferometers, the comparison wave, physically separated from the test field, is mixed with a wave which has passed through the test field; and the interference pattern of the two is recorded. For detailed general discussions of interferometry, see Ref. 22. Consider the combination of two waves in two dimensions, one which is plane and one which, originally plane, has a phase distortion caused by the test field. The two

waves can be represented by

$$U_1(y, x) = A_1 e^{-ik\,(x + y \sin \alpha) + i\phi_o} \tag{9}$$

where α is the angle between the wave vector and the x-axis, and ϕ_o is a constant phase factor (Fig. 26).

$$U_2(y, x) = A_2 e^{-ik(x) - i\phi(y)} \tag{10}$$

where $\phi(y)$ is the phase distortion, and the wave vector was assumed originally parallel to the x-axis. It is desired to calculate $\phi(y)$ in terms of fringe information caused by mixing the two waves. The amplitude at x = 0 is

$$U_1 + U_2 = A_1 e^{-iky(\sin \alpha) + i\phi_o} + A_2 e^{-i\phi(y)} \tag{11}$$

The intensity if proportional to

$$I = |U_1 + U_2|^2 = |A_1|^2 + |A_2|^2 + 2A_1A_2 \cos [ky \sin \alpha - \phi(y) - \phi_o] \tag{12}$$

If no phase shift occurs in the test field, then $\phi(y) = 0$ and the resulting intensity pattern appears as a set of equally spaced fringes. The fringe spacing is equal to $\lambda / \sin \alpha$. If, however, a phase object lies in the test field, the nonzero phase shift $\phi(y)$ will cause a disturbance of the fringes which can be used to determine the function $\phi(y)$. If, for example, a fringe is shifted by the test object through a distance $p\,\lambda / \sin \alpha$ where p is called the fractional fringe shift, then $\phi(y)$ is known to equal $2\pi p$ (see Fig. 27). Determining $\phi(y)$ is only part of the data reduction. To make the information useful to the aerodynamicist, one must determine the density of the phase object which caused $\phi(y)$. The phase is given first in terms of index of refraction change $\Delta n(y, x)$ (Fig. 28).

$$\phi(y) = 2\pi p = \frac{2\pi}{\lambda_o} \int_A^B \{n(y,x) - n_o\}\, dx = \frac{2\pi}{\lambda_o} \int_A^B \Delta n dx \tag{13}$$

where n_o is the index of refraction of the reference test field. Gas density, $\rho(y, x)$, can be determined from the equation (Ref. 23):

$$n - 1 = \rho k' (77.6 + 0.584/\lambda_o^2)\, 10^{-9} \tag{14}$$

where ρ is the number of molecules per cm^3, k' is 1.38×10^{-16} e/°K,

and λ_o is the wavelength in microns. For dry air at optical frequencies, the above equation is approximately

$$n - 1 = 1.07 \times 10^{-23} \rho \text{ cm}^{-3} \tag{15}$$

Equation (13) can be solved exactly, only if n = n(y) (two-dimensional object) or if $n = n(x^2 + y^2)^{1/2}$ (axisymmetric test object). The two-dimensional case is simplest (the second dimension, z, is omitted for simplicity). Equation (13) becomes

$$\phi(y) = (2\pi \Delta n(y)\, \Delta x)/\lambda_o \tag{16}$$

where Δx is the thickness of the test object. Combining Eqs. (13) and (16), the index of refraction is found.

$$\Delta n(y) = \lambda_o p/\Delta x \quad \text{(two-dimensional case)}$$

The remaining case (axisymmetric) is widely applicable in wind tunnel studies. A computer solution of Eq. (13) was developed by Kneile (OMD/CCO) for use in data reduction of holographic data. A brief description of the problem and its solution, including the program, are included as Appendix III. Briefly, the fringe shift is measured as a function of z and y. For each complete function p(y) which is provided by measurement solution of the equation provides the function n(r) where $r = (x^2 + y2)^{1/2}$.

The holographic interferogram reconstruction in Fig. 25 was partially analyzed using this method to provide $n(y) - n_o$ for three values of z (Fig. 25 defines y, z, and r_n). The gas density change can be computed with Eq. (15) since the fluid was dry air. The tunnel conditions were given in Section 4. 2. 1. To check the accuracy of the experimental data, the measured values of $n(y) - n_o$ were compared with values predicted by the solution of the inviscid Navier-Stokes equation (data supplied by E. Marchand, VKF, using Ref. 24). These are plotted for comparison in Fig. 29. Theoretical data were not available for the case $z/r_n = 1$. Exact agreement between the experimental and theoretical curves cannot be expected since the model was supplied with boundary-layer trips at the junction of the sphere and cone. The theory is for a simple sphere-cone model. Furthermore, the boundary-layer trips render the model nonaxisymmetric, so the experimental data are correct only to within the assumption of axial symmetry. The theory is not valid in the boundary layer of the model. Close agreement was found between the experimental and theoretical values at the axial position $z/r_n = 3$. Reasonable agreement also occurred at $z/r_n = 2$.

The hand techniques used to reduce these data were cumbersome and inaccurate, and the data are presented strictly to illustrate the validity of the method. If the method is to be used at length, data reduction methods should be automated to some extent. A device is needed which can be used to trace over the fringes while electronically providing a digital output of the x-y coordinates. An automatic film reader could be adapted to this part of the data reduction.

4.3.2 Other Types of Hologram Interferometry

The type of interferometry discussed in the last section is Mach-Zehnder interferometry. Every other type of conventional interferometry can be performed holographically by storing either the reference beam, object beam, or both. It is possible to store the interferometer reference wave and the test field wave on the same photographic plate, if the plate can be forced to remain stationary between the two recordings. The multiple exposure techniques developed in this program were used to produce such interferograms (Ref. 13). These are primarily of interest when the field of view is dynamic. Moreover, a number of types of hologram interferometry have no conventional analogues. Among them are opaque object interferometry, diffuse illumination interferometry, time averaged interferometry, and sheared wave front interferometry.

Hologram interferometry eliminates the usual requirement of extremely high quality optics. The principal difference between conventional and hologram interferometry is perhaps the most important from the practical standpoint. Unlike conventional interferometry, wherein a comparison wave passes through a field separated from the test field, hologram interferometry can compare waves which pass at different times through the same field. Therefore, only those changes which occurred between the two recordings are seen in the comparison. Effects of aberrated lenses, poor mirrors, and poor glass windows are not revealed by interference fringes as they would be conventionally because these effects have been imposed upon both the test wave and the comparison wave. The requirement is that everything in the system except for the test field remain unchanged between the two recordings. If the two recordings are made on two separate plates, slight motions can be tolerated between the exposures in some cases.

All of the mentioned types of hologram interferometry have been performed in these studies. Most of them have been covered in detail in the references; and since they are all similar, they will not be discussed in detail here.

4.3.3 Research Holographic Flow Visualization System

Many basic questions arose during the operation of the full-scale HFVS that could be examined more efficiently and more accurately in a small-scale experiment where conditions are more easily controlled. Moreover, advanced optical processing methods could more easily be attempted first in a smaller system. To provide more design data for larger systems and to prepare for advanced work in the area which seemed most promising, a small laboratory HFVS was assembled. The system is similar to that shown in Fig. 12 except that its small size allowed it to be completely isolated. Figure 30 is a sketch of the system. The entire structure is mounted on inner tubes and is enclosed by curtains to reduce air currents, extraneous lights, and other contaminants. The experiment is located in a temperature and contaminant controlled room. Diffraction limited optics were incorporated throughout the system. The primary mirrors are 75-cm radius spherical surfaces to within one-quarter wavelength. The system can be operated as (1) a conventional flow visualization system, (2) laser flow visualization system, or (3) a generalized holographic flow visualization system. For increased accuracy, holographic reconstruction capability was built into the system. The system became operational in early 1969 and, therefore, much of the data still under analysis must be presented in later papers.

Sample holographic reconstruction data from this system are shown in Figs. 31a through c. The object scene was composed of a 0.5-deg wedge, a 0.030-in.-diam wire, and a microscope slide coated with small particles. These were located halfway between the two primary mirrors. Figure 31b shows an enlargement of a section of the microscope slide in which particles as small as 20-μ diameter can clearly be seen. Figure 31c is a reconstructed image taken from a hologram in which the recording area has been reduced to less than 1 cm^2. Resolution in this image is still high. This means that such recording can be made with less total optical energy and with smaller recording areas, which opens the way to motion-picture holography recordings.

4.4 OTHER POSSIBLE APPLICATIONS

A wide variety of applications exist for the techniques described in facilities other than those mentioned. Any test facility which is optically accessible can be equipped with holographic instruments. With instruments used to date, window quality is important only to visualization techniques such as knife-edge schlieren. With more development, this

limitation on schlieren photography may be eliminated by holography. In principle, the quality of all optics in the visualization system can be relaxed by holography. This has already been accomplished on a small research scale; however, its practicality on a large scale is still undetermined.

The holocamera discussed in Section 4.1.1 is also usable in flow visualization. The camera has been used for holographic diffuse illumination interferometry to observe gas turbulence density gradients and shock waves (Ref. 13). Figure 32 shows typical reconstructed images of impact events. In two of the figures, a transmitted and reflected shock can be seen. Analysis of fringes inside these shocks leads to the density field.

For some applications, a wider angle of view will be required than that provided by an image holocamera like the ones described here. Such cameras have been constructed and applied successfully in a number of aerodynamic experiments.

SECTION V
FUTURE WORK

The work described in this report is merely the beginning of the exploitation of holography in solving aerodynamic instrumentation problems. Many laboratories are presently concentrating work in the field of holography. The field is presently advancing at a rate so fast that it is impossible to predict the future of holographic instrumentation. With reference to the systems and techniques discussed herein, however, the course of required work in the immediate future is clear. Even so, a continuing flexibility should be maintained for capitalizing upon developments which will unquestionably take place in other laboratories.

A considerable amount of work must now be devoted to applications of the techniques. This includes both feasibility studies and solutions of engineering problems encountered in the integration of the techniques with test facilities. Secondly, more basic experimental and theoretical work is required to establish critical parameters to extend the techniques and to explore new possibilities. The two categories of studies will be complementary and hopefully will involve a number of groups at AEDC.

5.1 PARTICLE FIELD HOLOGRAPHY

Within the limits specified in Section IV, the basic data and design criteria for particle field holography are complete. A number of important applications, however, lie beyond those limits. Therefore, a portion of the program should be directed to the study of techniques and materials required to further extend those limits. Apparently, little can be done to relax natural diffraction limits involved in the problem. However, a number of optical data processing methods, advanced film processing methods, and other refined techniques are available to extend limits imposed by presently required signal-to-noise ratio.

Since particle field holography is at an advanced state of development, a considerable amount of attention should be paid to applications feasibility studies. A number of application areas are under consideration. These are listed in Section IV.

5.2 HOLOGRAPHIC FLOW VISUALIZATION

Holographic flow visualization techniques are still in an early stage of development; however, some of the systems described can at present be used reliably to perform tasks which could not otherwise be performed. Limited applications of these systems can now be considered, keeping in mind that, in their present stage of development, they will not possess the versatility of a conventional flow visualization system. It is apparent, however, that the more powerful holographic flow visualization techniques will eventually supersede conventional visualization techniques in applications where the conventional methods are not entirely sufficient. The drawbacks which are presently apparent are the following:

1. The time between successive recordings is too great in our present systems. At this time it is approximately 15 sec and could be decreased readily with present techniques to no less than 1 sec. There are two exceptions to this. One of these involves the application of multiple exposure holography techniques discussed in Section IV, in which a limited number of holograms can be superimposed in a period of approximately 700 μsec. The other exception is the application of real time holographic interferometry in which a hologram provides the comparison reference wave for the interferometry while a

CW laser passing through the object field provides the continuously changing object wave which is recorded by conventional photographic techniques. Alignment problems involved in this technique have limited its applications so far to small systems. Methods for increasing the rate at which holographic recordings can be made are now under study.

2. Holographically reconstructed images are inherently noisier than conventional images because of the high coherence of light involved. Methods will be studied to remove or to compensate for such noise on both research levels and on application levels. Since the beginning of these studies, signal-to-noise ratios have been increased by more than a factor of 100. It is believed that continuing studies can result in reconstructed images of quality at least as high as those obtained from conventional imagery.

3. Data presentation and reduction procedures are complicated. Holographic data reduction methods are completely different from those of conventional systems and, therefore, require special designs and mounts, viewing instruments, and recording instruments. Many of these have been developed already in the course of these studies. It is apparent that, with continued development, holographic reduction systems and recording systems can be made even more versatile than those used in conventional techniques.

A number of other studies have been initiated to extend the holographic capability and to take advantage of other possibilities offered by holography. Most of these are associated with the general field of holographic optical data processing. These include optical systems aberration removal, optical processing methods which have greater sensitivity or more versatility than knife-edge schlieren and shadowgraph techniques, data enhancement and retrieval methods, and automatic data reduction procedures.

Additional work is needed in holographic interferometry to simplify the applications of data recording and data reduction. Additional work is planned in computer methods for data reduction which includes a study of error analysis in the overall technique. Three-dimensional holographic interferometry has not yet been attempted on a large scale. Additional basic experimental and theoretical work is required before such an application can be useful.

Work can now be justified in the research, development, and application of the holographic interferometry of opaque objects. These methods can offer an extremely sensitive nondestructive testing instrument which can monitor extremely small changes in the consistency of the stress and strain characteristics or of the thermal coefficient of expansion characteristics of an object. Feasibility studies along these lines have been initiated.

It is obvious that the limited effort in holographic instrumentation technology at AEDC cannot completely span the number of problems listed in this section during the next year. It is also obvious that during these studies more problems will become apparent which have not been mentioned and which will require considerable effort. The present plan is to attack these problems on a priority basis, the priority being established by the necessity of the problem solution for the most important applications.

SECTION VI
SUMMARY AND CONCLUSIONS

Some of the most important results of the programs in holography at AEDC have been presented. Working systems have been described which range from small laboratory research apparatus to full-scale systems which were applied on large operating wind tunnels. These systems have been shown to provide needed data which apparently could not be otherwise obtained. In some areas, systems have approached an operational status, and in some areas they have not. It can be concluded that particle field holography can now provide a capability within certain limits which should be considered as a tool available for certain test requirements. Additional refinement is needed in those applications which do not lie within the specified limits. Additional work is justified in establishing how far these limits can be pushed to extend the range of applications for the technique.

Flow field holography is ready for limited application where the advantages of the technique are highly desirable. Additional work is needed to specify the areas in which holographic data are more accurate and more sensitive than conventional data. Such a specification will better point out application areas in which holography should be used in the place of conventional methods. Techniques which are made possible through holography should be more closely studied to determine if and how they can extend the AEDC instrumentation capabilities.

A number of holographic camera configurations were designed and tested. These have provided design data for future applications which can now be made available to other facilities. From the progress made in holographic instrumentation here and in other laboratories, it can be concluded that such instrumentation should play an important role in extending capability of test facilities at AEDC.

REFERENCES

1. Gabor, D. "A New Microscopic Principle." Nature, Vol. 161, May 15, 1948, pp. 777-778.
2. Leith, E. N. and Upatnieks, J. "Reconstructed Wavefronts and Communication Theory." Journal of the Optical Society of America, Vol. 52, No. 10, October 1962, pp. 1123-1130.
3. Brooks, R. E., Heflinger, L. O., Wuerker, R. F., and Briones, R. A. "Holographic Photography of High-Speed Phenomena with Conventional and Q-Switched Ruby Lasers." Applied Physics Letters, Vol. 7, No. 4, August 15, 1965, pp. 92-94.
4. Thompson, B. J. "Fraunhofer Diffraction Patterns of Opaque Objects with Coherent Background." (Abstract) Journal of the Optical Society of America, Vol. 53, No. 11, November 1963, p. 1350.
5. Belz, R. A. "Analysis of the Techniques for Measuring Particle Size and Distribution from Fraunhofer Diffraction Patterns." AEDC-TR-68-125 (AD674741), September 1968.
6. Trolinger, J. D., Farmer, W. M., and Belz, R. A. "Multiple Exposure Holography of Time Varying Three-Dimensional Fields." Applied Optics, Vol. 7, No. 8, August 1968, pp. 1640-1641.
7. Trolinger, J. D., Belz, R. A., and Farmer, W. M. "Holographic Techniques for the Study of Dynamic Particle Fields." Applied Optics, Vol. 8, No. 5, May 1969, pp. 957-961.
8. Farmer, W. M. "Dynamic Holography of Small Particle Fields Using a Q-Spoiled Laser." Masters Thesis, The University of Tennessee Space Institute, June 1968.
9. Trolinger, J. D., O'Hare, J. E., Farmer, W. M., and Belz, R. A. "Holographic Flow Visualization." Applied Measuring Techniques (F. Shahrokhi, Editor). AIAA Tennessee Section Weekend Workshop Manual, February 8 and 9, 1969, pp. 290-322.

10. Trolinger, J. D., Farmer, W. M., and Belz, R. A. "Conversion of Large Schlieren Systems to Holographic Visualization Systems." Fundamentals of Aerospace Instrumentation, Vol. II. (B. Washburn, Editor). Instrument Society of America, 1969.

11. O'Hare, J. E. "A Holographic Flow Visualization System." Symposium Proceedings, SPIE 14th Annual Technical Symposium, San Francisco, California, August 11-14, 1969.

12. O'Hare, J. E. and Trolinger, J. D. "Holographic Color Schlieren." Applied Optics, Vol. 8, No. 10, October 1969, pp. 2047-2050.

13. Trolinger, J. D., Farmer, W. M., and Belz, R. A. "Applications of Holography in Environmental Science." Journal of Environmental Sciences, Vol. XII, No. 5, October 1969, pp. 10-13.

14. Farmer, W. M. and Gee, T. H. "Holographic Optical Data Processing and Its Application at AEDC." AEDC-TR-70-56, July 1970.

15. Goodman, J. W. Introduction to Fourier Optics, McGraw-Hill Book Company, San Francisco, 1968.

16. Wyant, J. C. and Givens, M. P. "Effect of the Photographic Gamma on the Luminance of Hologram Reconstructions." Journal of the Optical Society of America, Vol. 58, No. 3, March 1968, pp. 357-361.

17. Matthews, B. J., Wuerker, R. F., and Harrje, D. T. "Small Droplet Measuring Technique." AFRPL-TR-68-156, July 1968.

18. Menzel, R., Russell, T. G., and Shofner, F. M. "Recording Fluid Velocity Fields Holographically." Holography; SPIE Seminar Proceedings. Vol. 15, 1968, pp. 167-170.

19. Fourney, M. E., Matkin, J. H., and Waggoner, A. P. "Aerosol Size and Velocity Determination via Holography." Review of Scientific Instruments, Vol. 40, No. 2, February 1969, pp. 205-213.

20. O'Hare, J. E. "Flow Visualization Techniques." Applied Measuring Techniques (F. Shahrokhi, Editor). AIAA Tennessee Section Weekend Workshop Manual, February 8 and 9, 1969, pp. 256-289.

21. Toepler, A. "Beobachtungen Nach Einer Neven Optishen Methods." Annalen der Physik, Vol. 127, 1886, p. 556.

22. Born, M. and Wolf, E. Principles of Optics, Third (Revised) Edition. Pergamon Press, Oxford, 1965.

23. U. S. Air Force Cambridge Research Center. Handbook of Geophysics. Macmillan Company, New York, 1960.

24. Inouye, M., Rakich, J., and Lomax, H. "A Description of Numerical Methods and Computer Program for Two-Dimensional and Axisymmetric Supersonic Flow over Blunt-Nosed and Flared Bodies." NASA-TND-2970, August 1965.

APPENDIXES

I. ILLUSTRATIONS
II. FILMS AND SENSITIZED GLASS PLATES FOR HOLOGRAPHIC RECORDING
III. NUMERICAL METHOD FOR RADIAL INVERSION

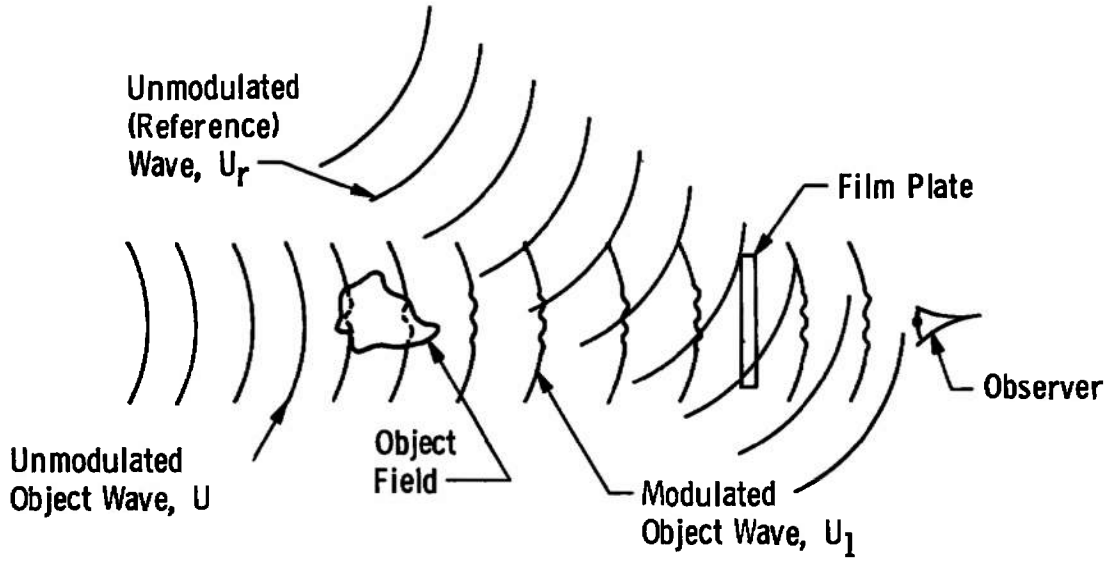

a. Formation of a Hologram of a Modulated Wave

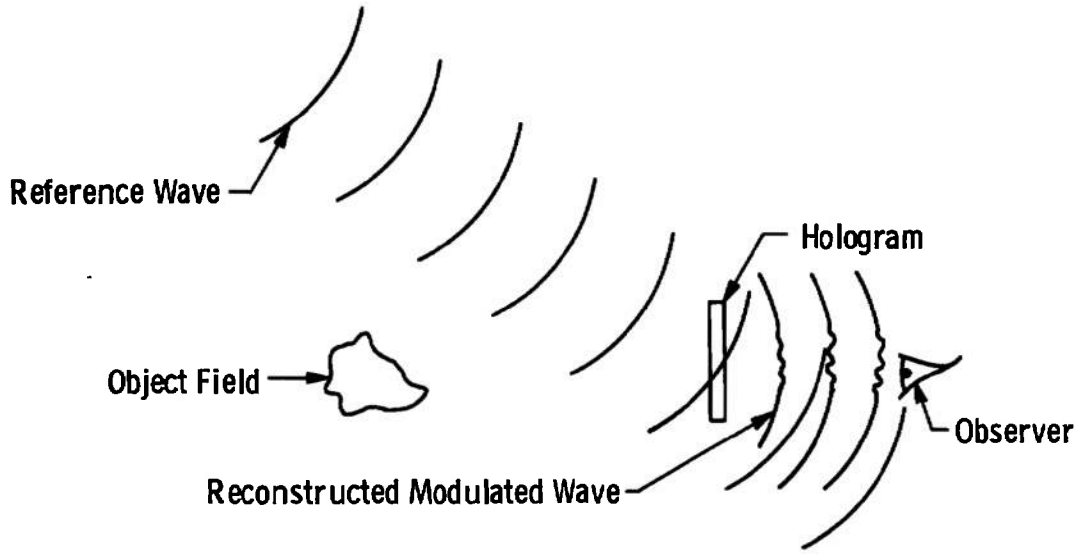

b. Reconstruction of the Modulated Wave

Fig. 1 Holography Process

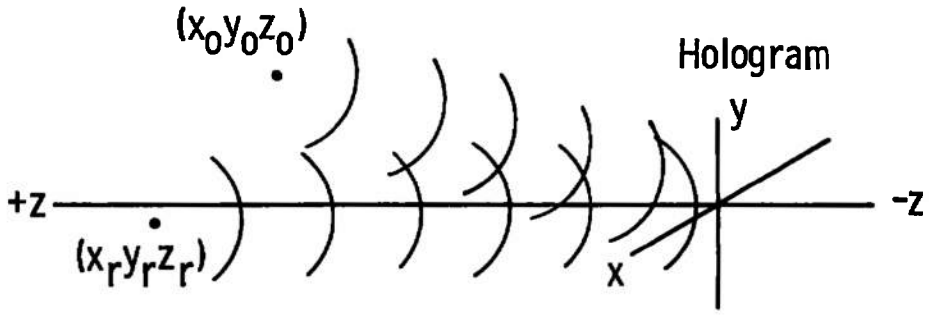

a. Hologram Formation with Wavelength, λ_1

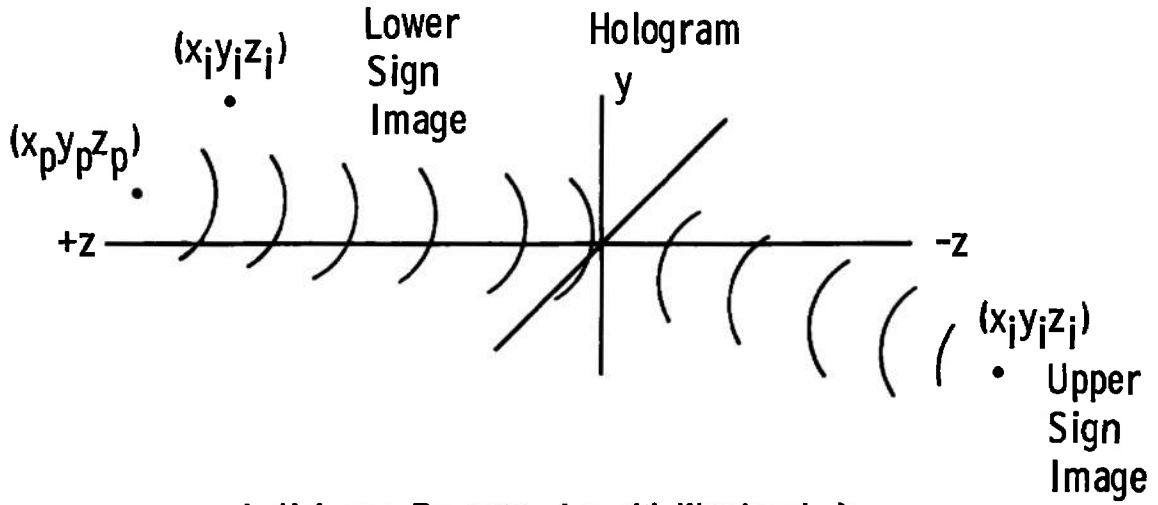

b. Hologram Reconstruction with Wavelength, λ_2

Fig. 2 Hologram Reconstruction

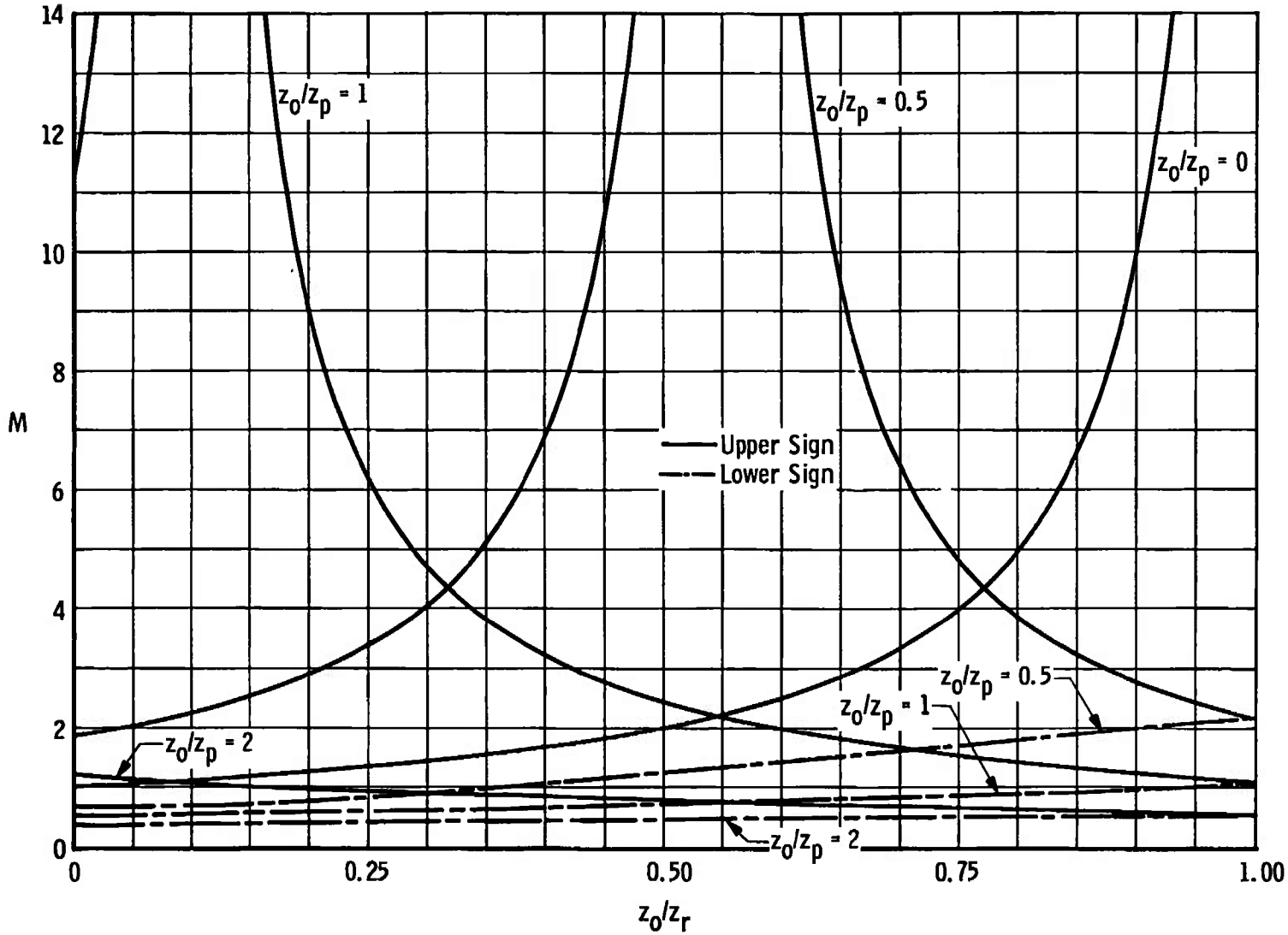

Fig. 3 Holographic Magnification

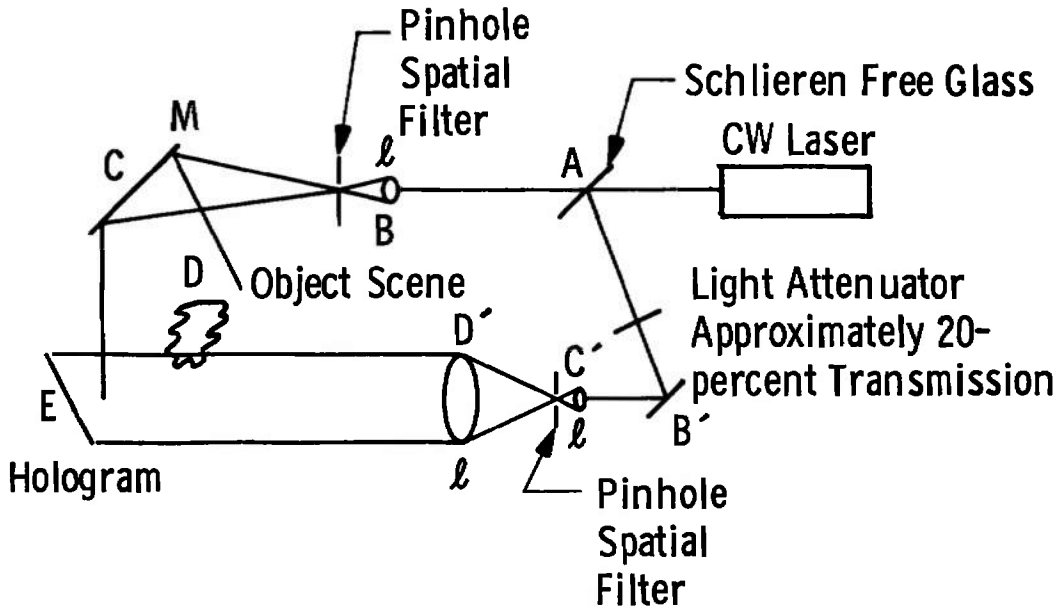

Fig. 4 Typical CW Laser Holography Configuration

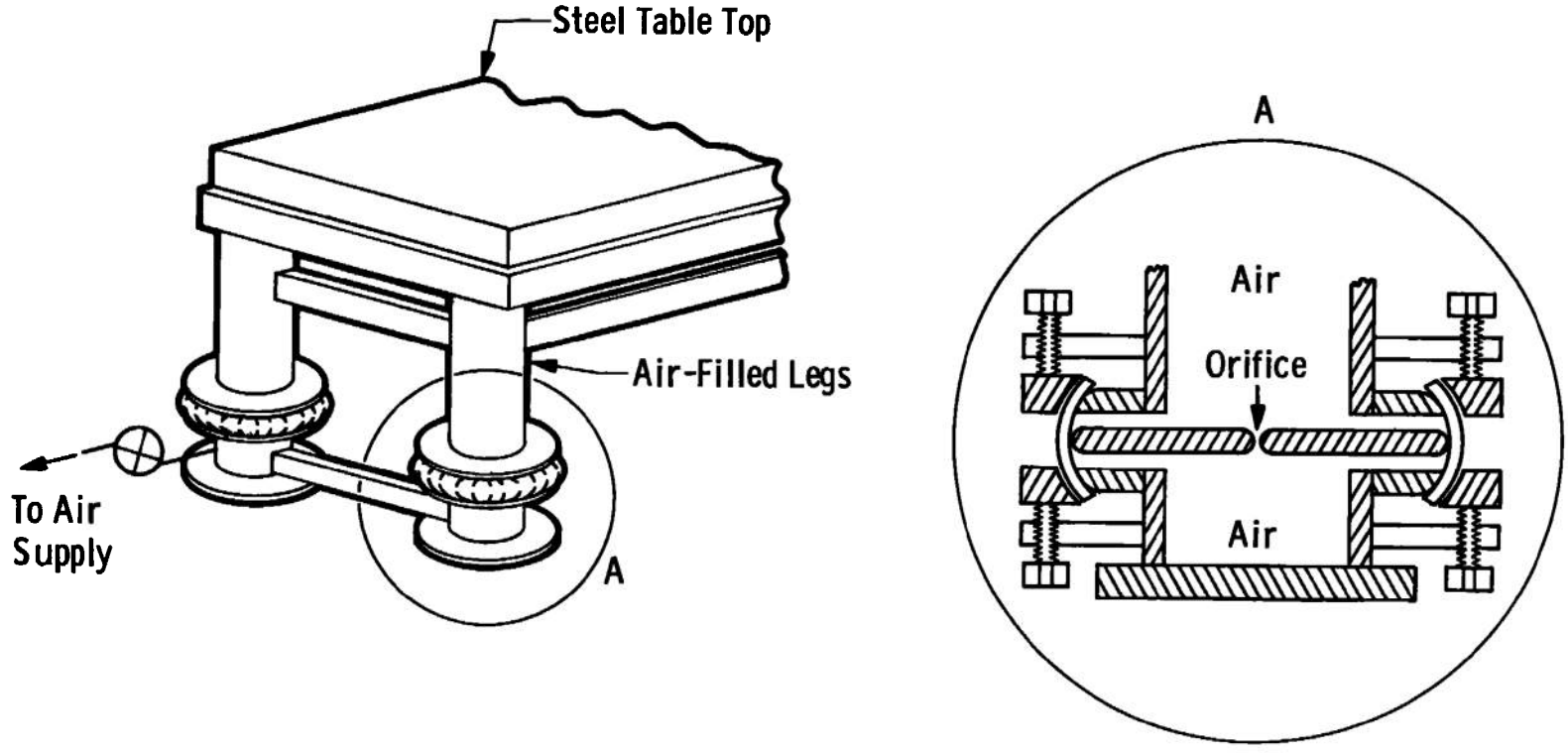

Fig. 5 High Stability Table Design

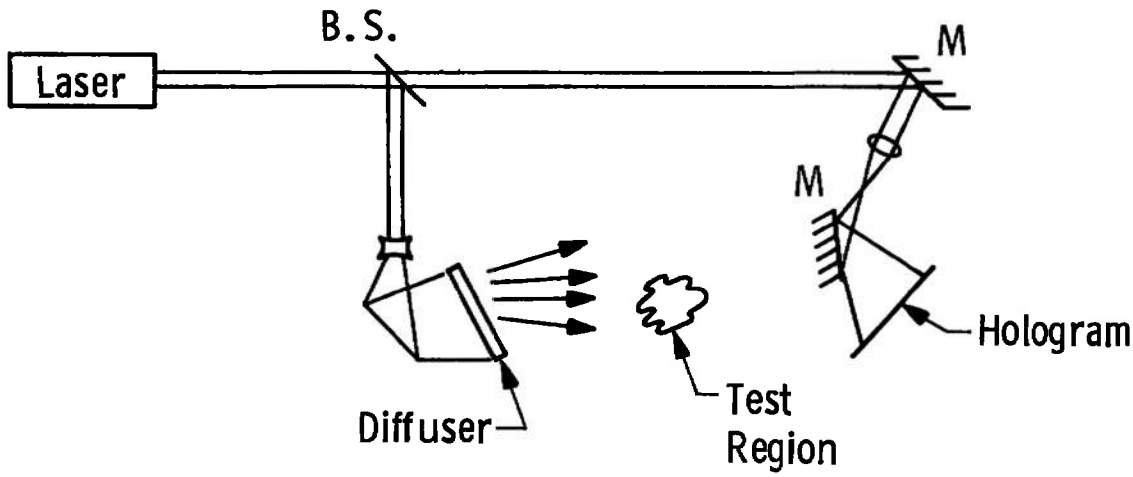

Fig. 6 Diffuse Transillumination Holocamera

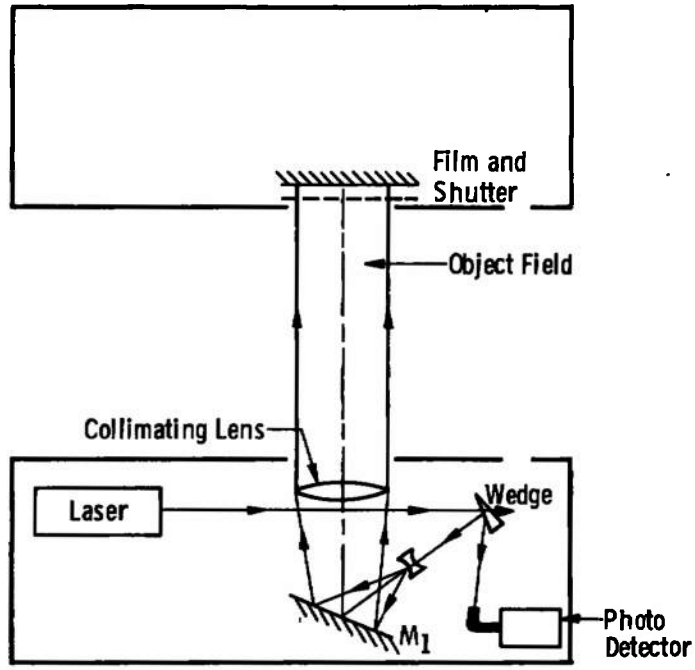

a. In-Line

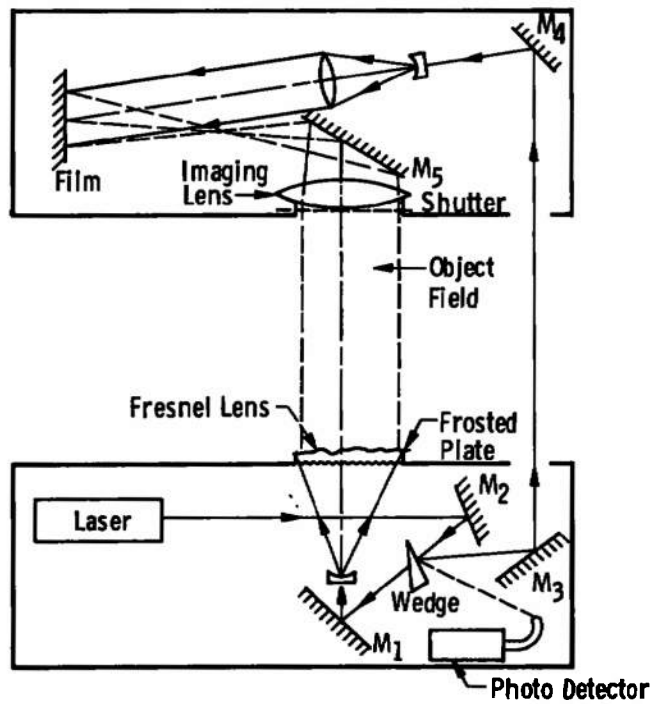

b. Sideband Transillumination

Fig. 7 Holography Configurations

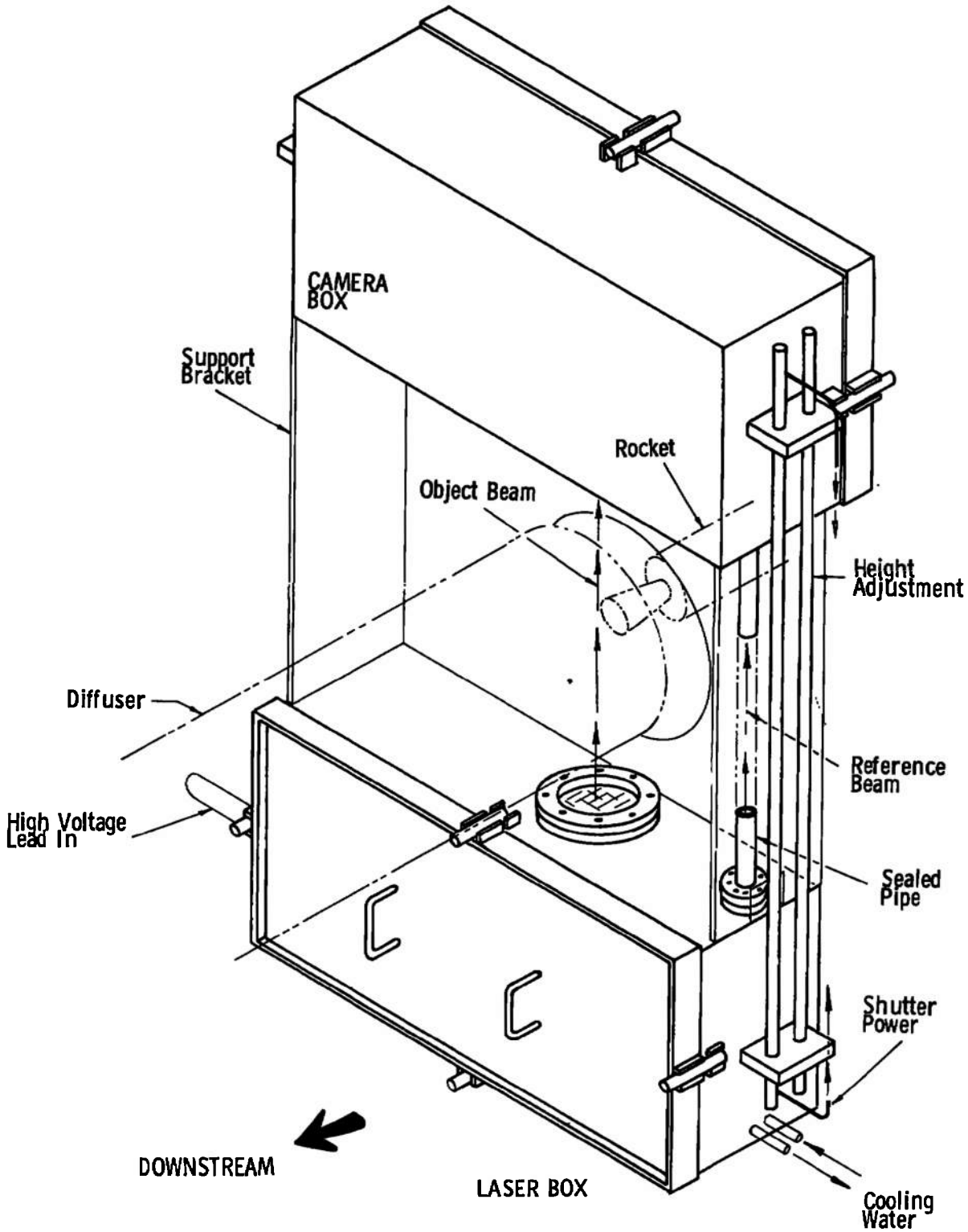

Fig. 8 Rocket Exhaust Holocamera Pictorial View

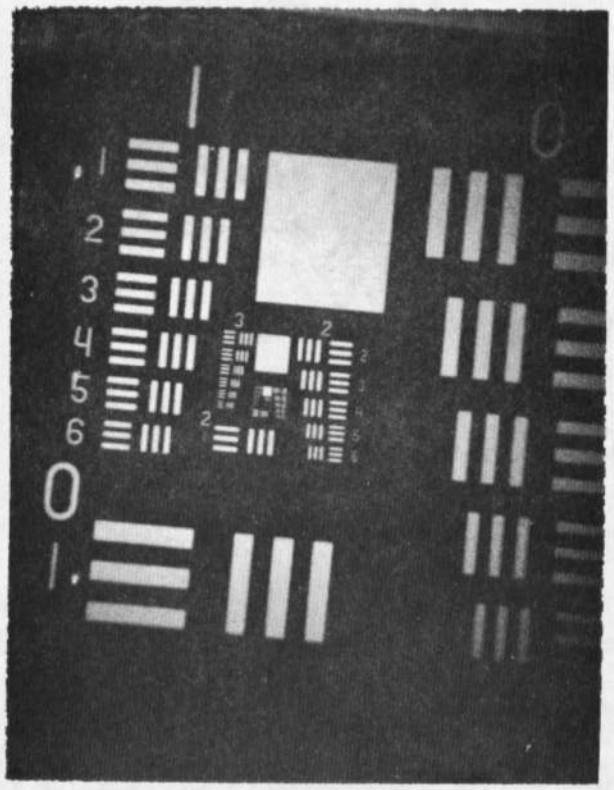

Fig. 9 Reconstruction from a Hologram of a Standard Air Force Resolution Chart Taken in Configuration Shown in Fig. 4

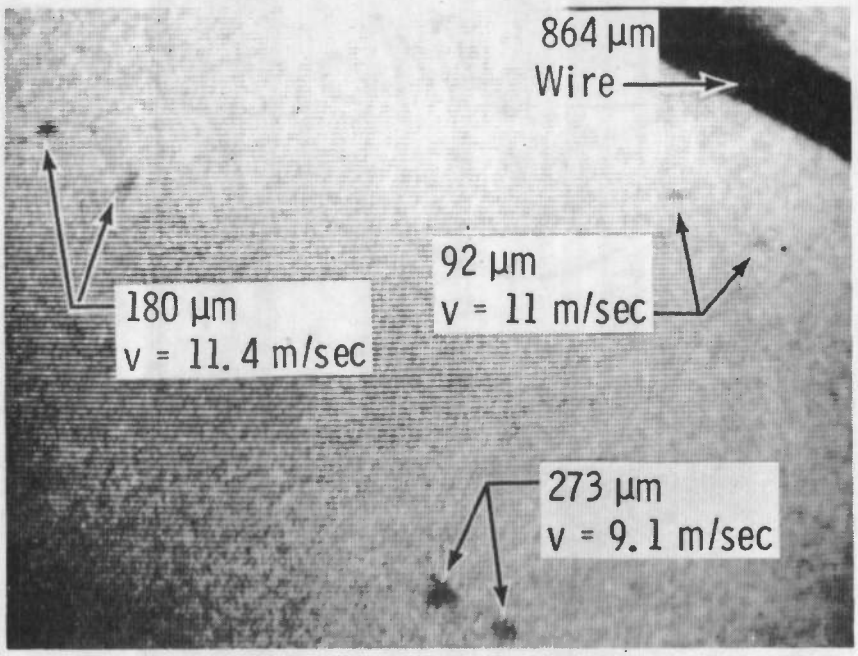

Fig. 10 Reconstructed Images from a Double-Pulsed (100-µsec Pulse Separation) Sideband Hologram (Photograph Taken from a Closed-Circuit Television Monitor)

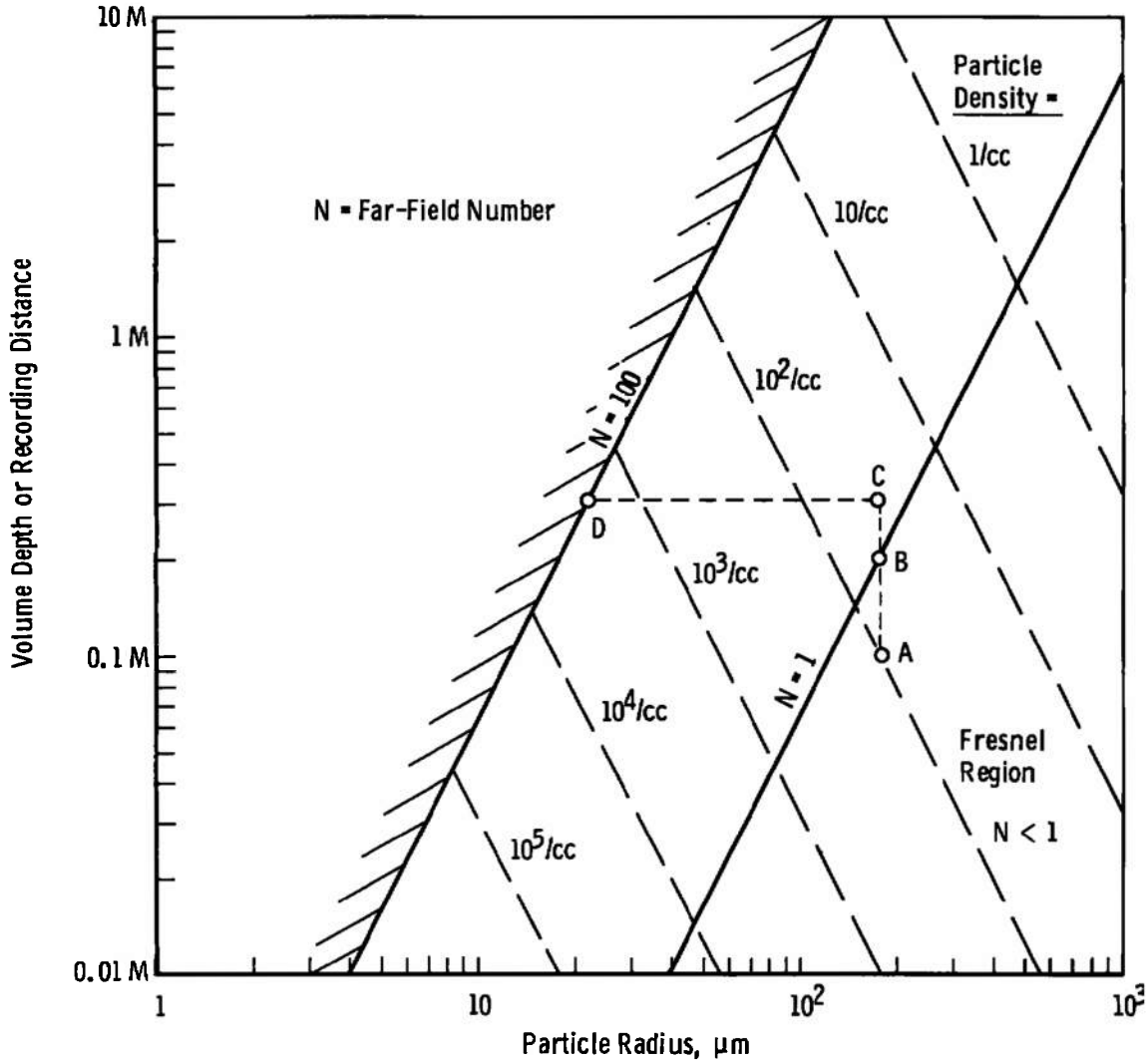

Fig. 11 Dependence of Recording Distance and Volume Depth on Particle Size and Density for Clean Reconstructions from Fraunhofer Holograms

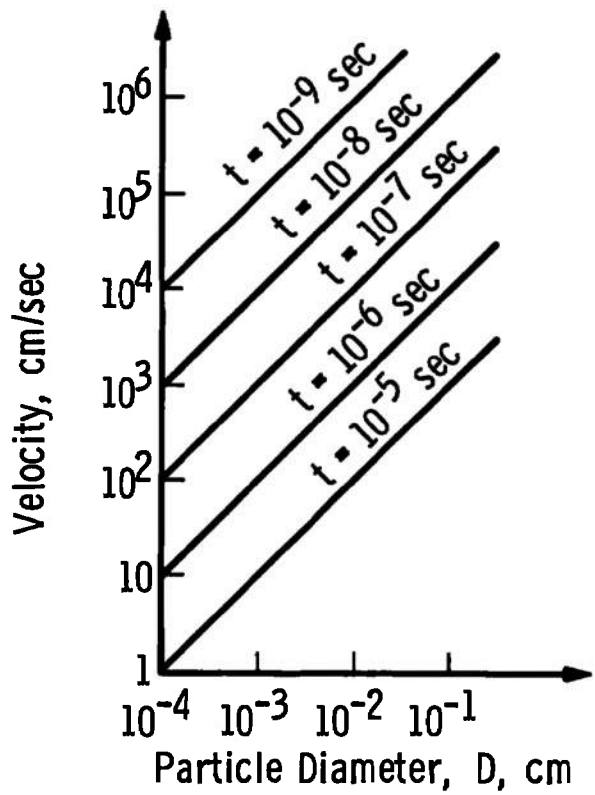

Fig. 12 Velocity versus Particle Diameter for Specific Exposure Times

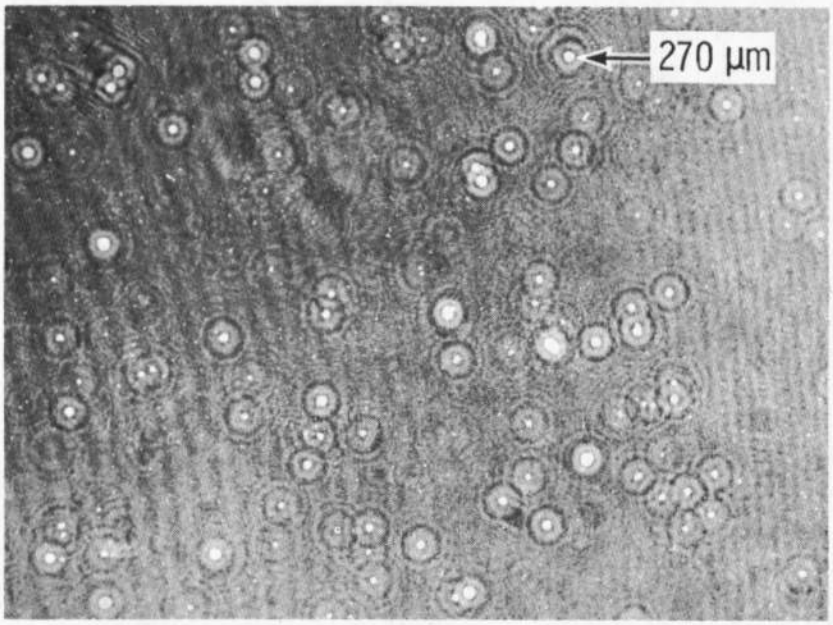

a. Slight Motion

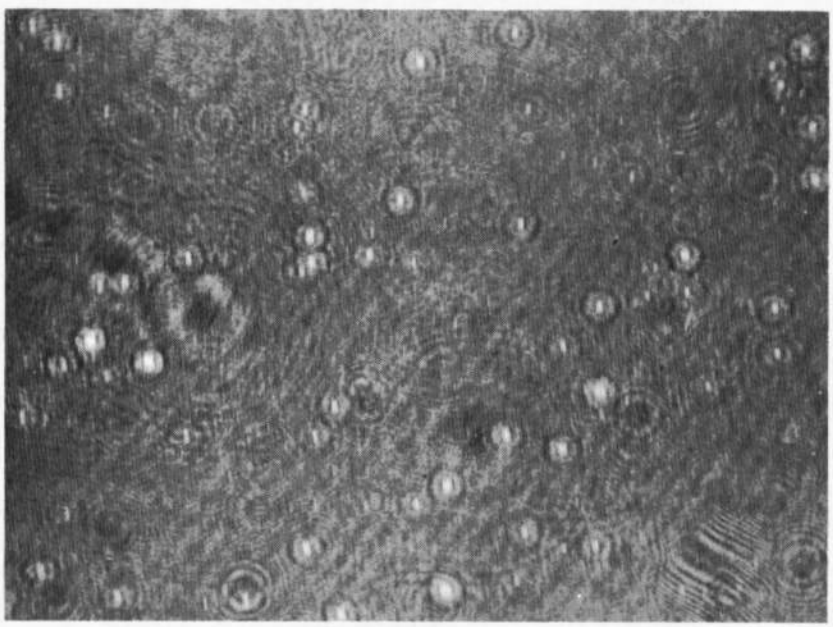

b. Appreciable Motion

Fig. 13 Effect of Motion of the Scene on the Reconstructed Image

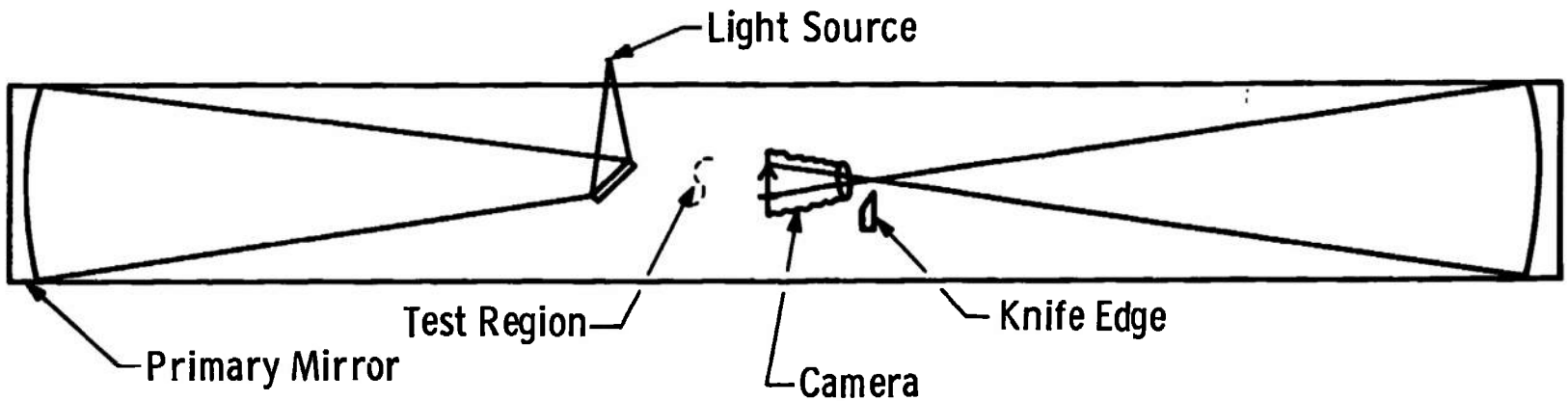

Fig. 14 Conventional Flow Visualization System

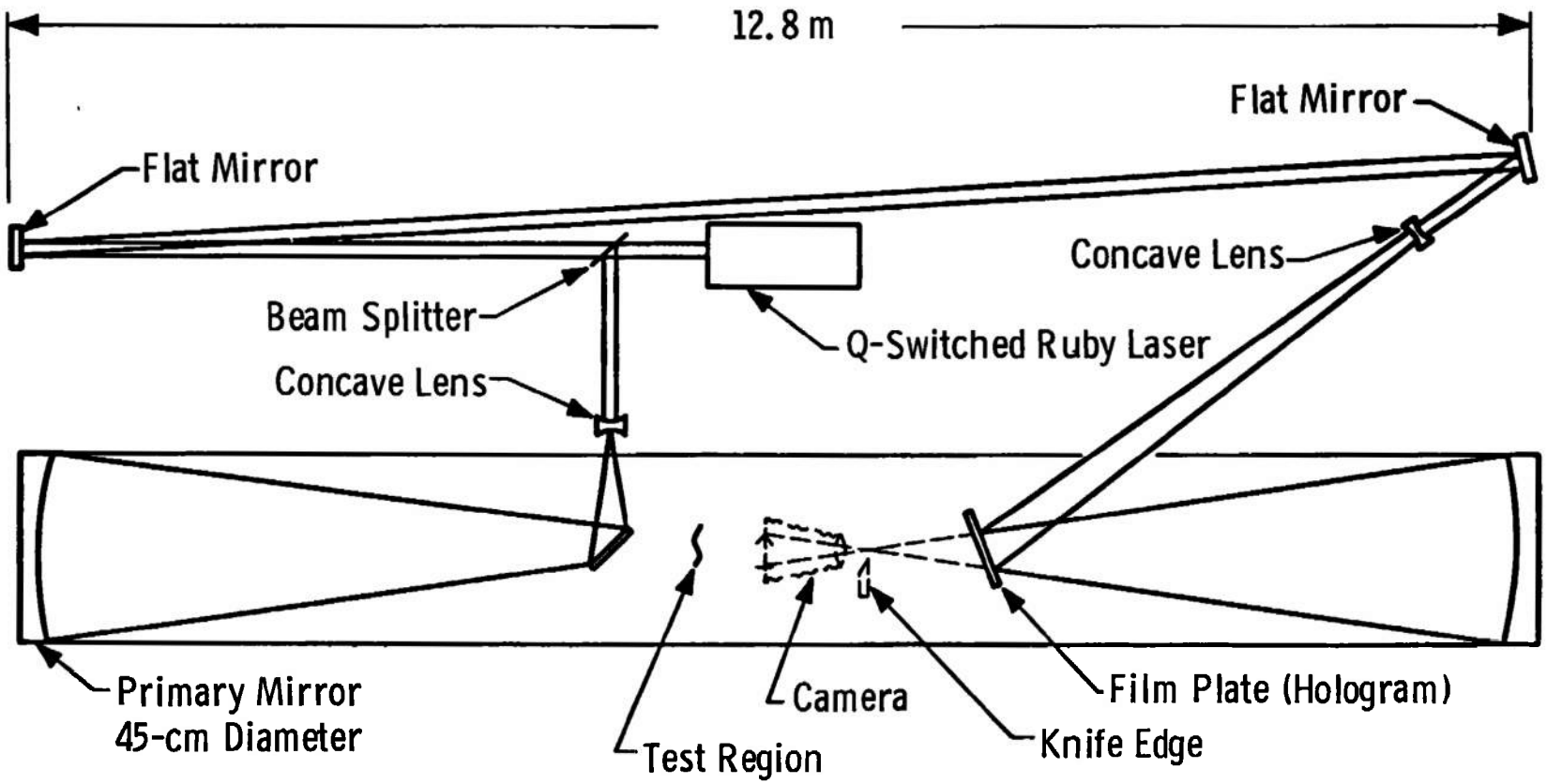

Fig. 15 Holographic Flow Visualization System (Heavy Lines)

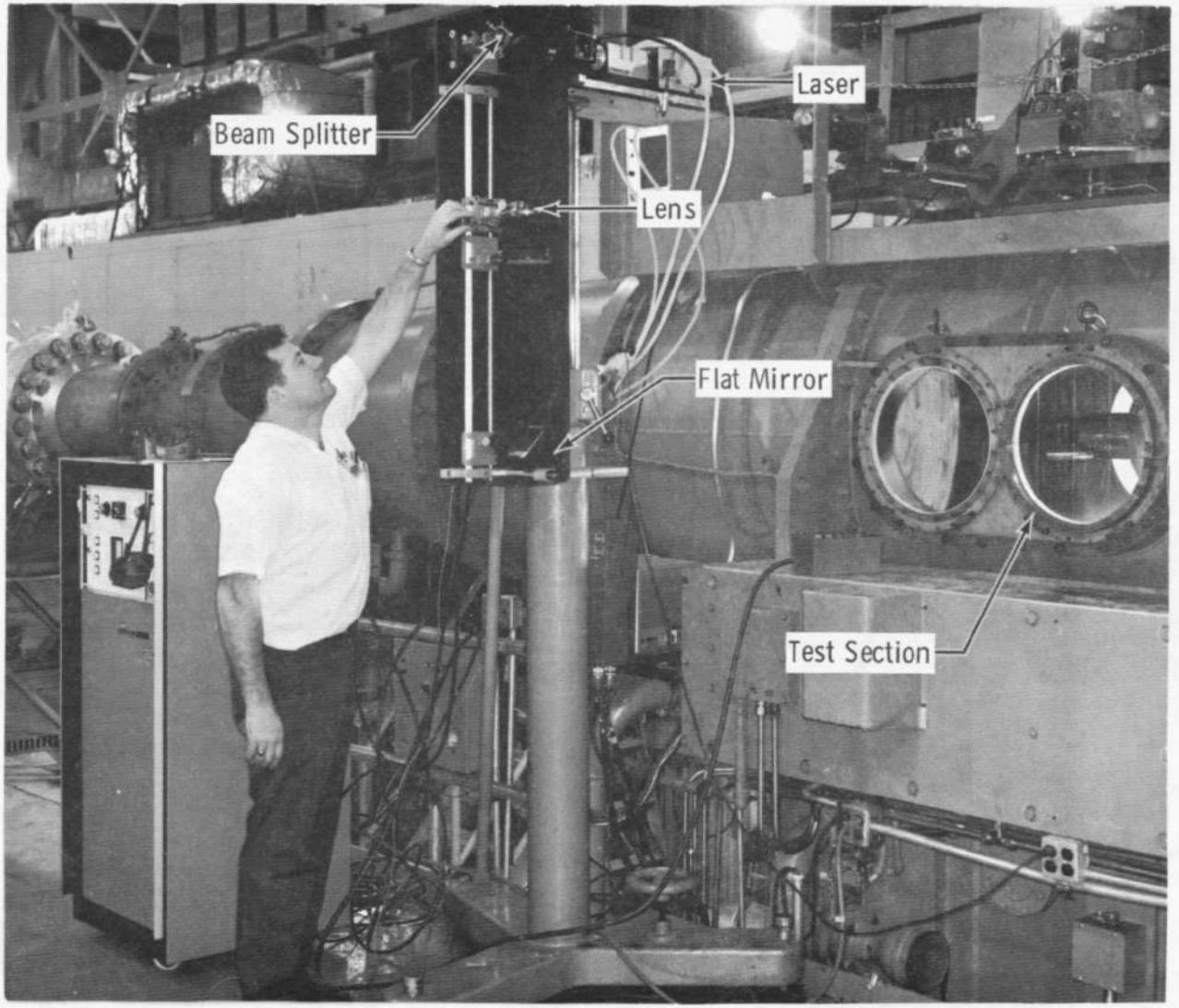

Fig. 16 Light Source Unit for Holographic Flow Visualization Systems

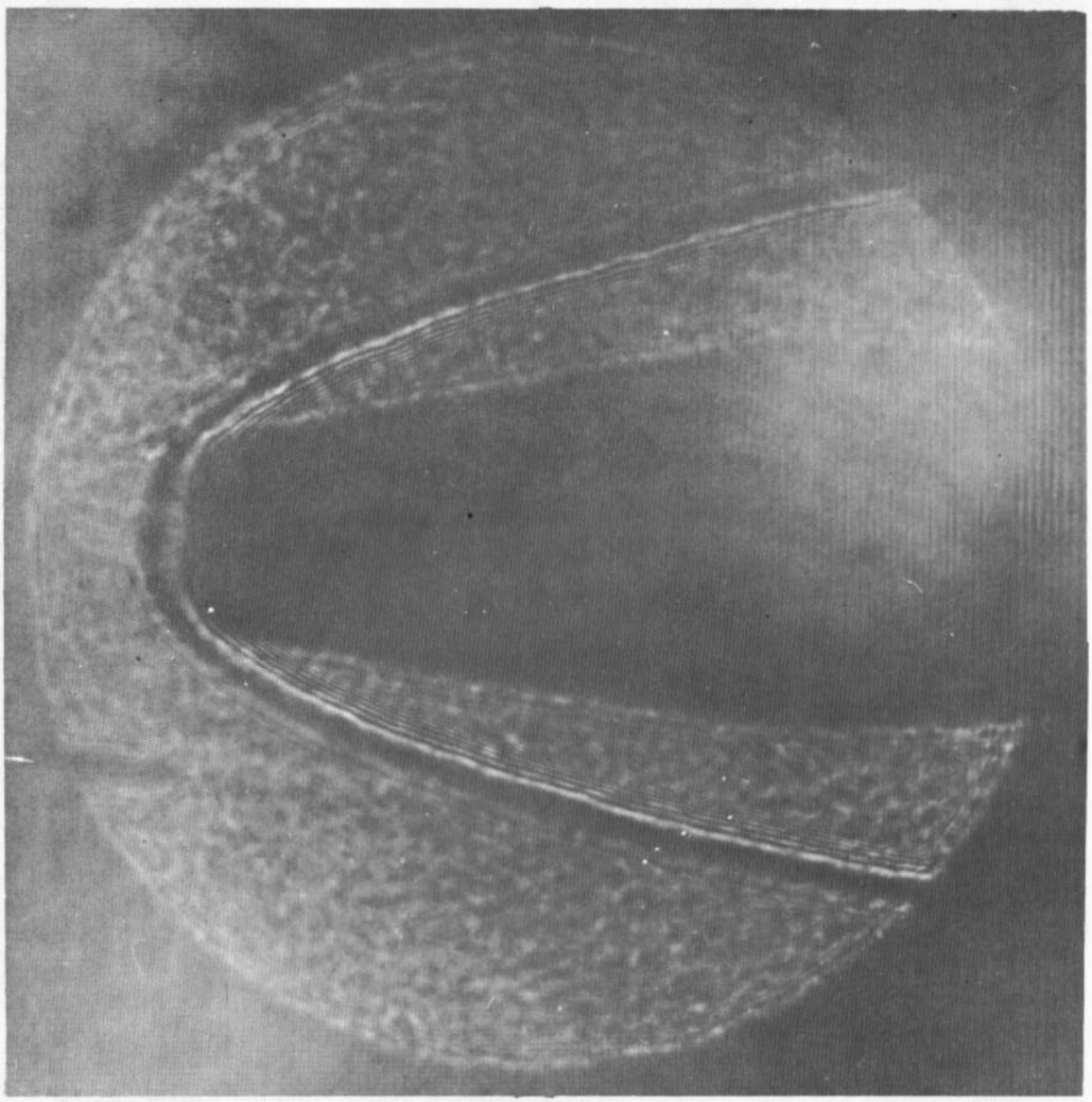

Fig. 17 Photograph of a Hologram Made with the Holographic Flow Visualization System

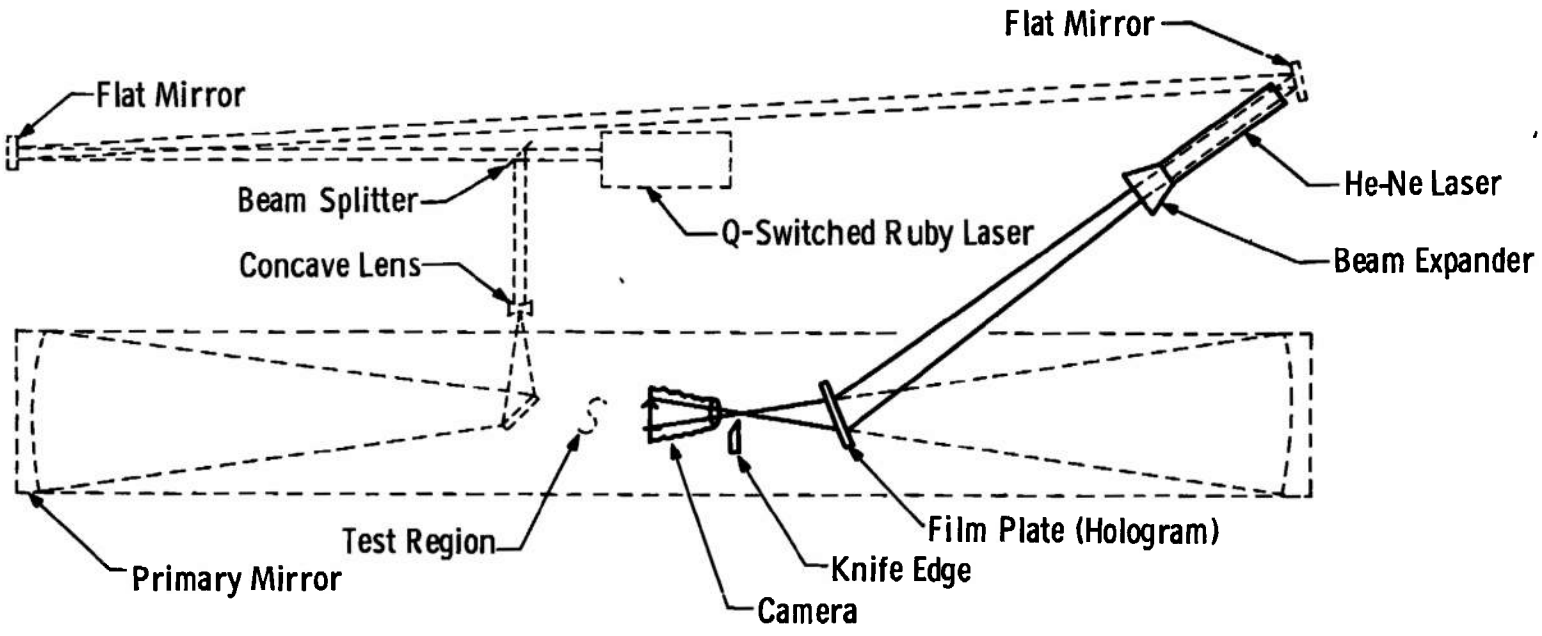

Fig. 18 Schlieren and Shadowgraph Reconstruction (Heavy Lines)

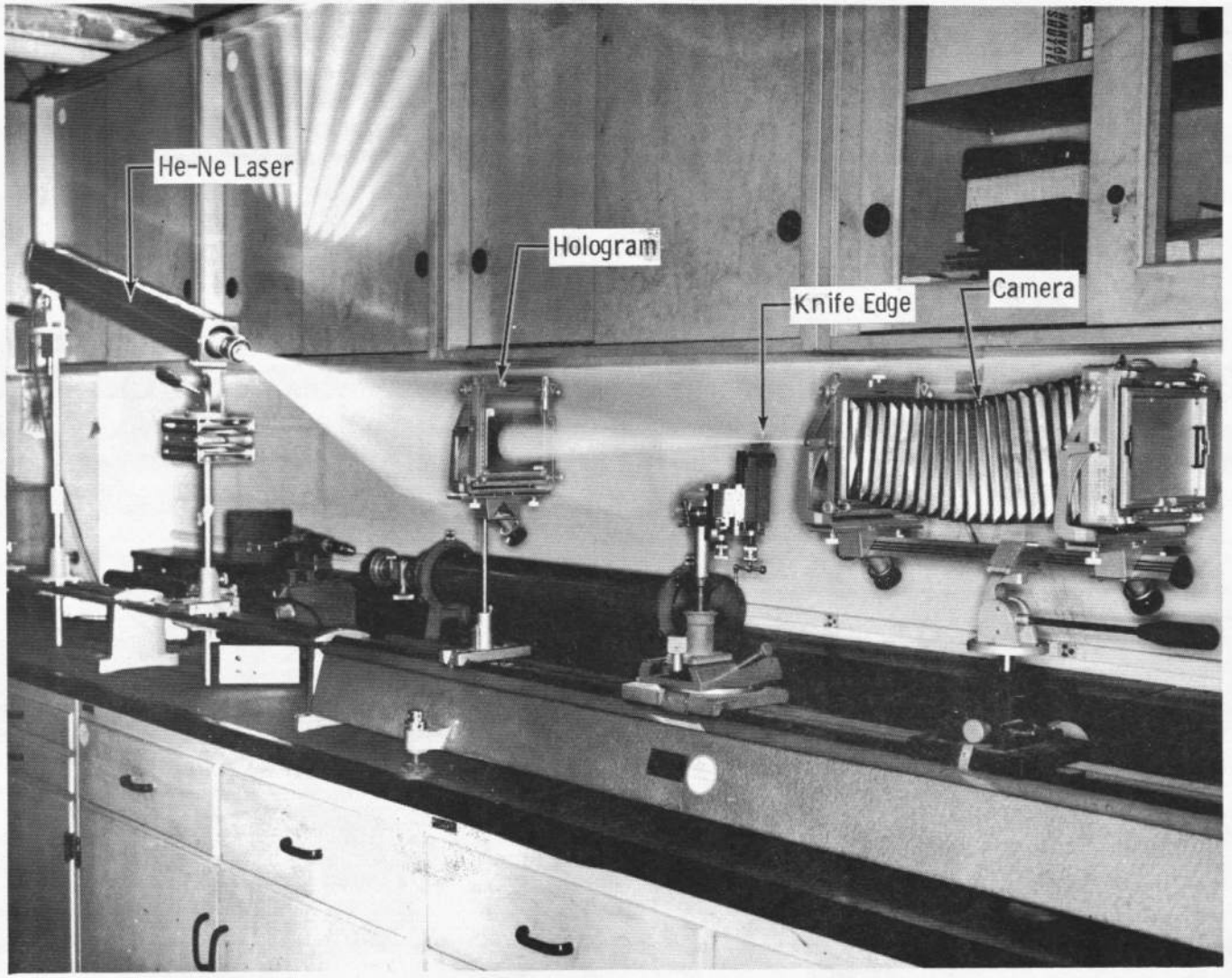

Fig. 19 Reconstruction Apparatus

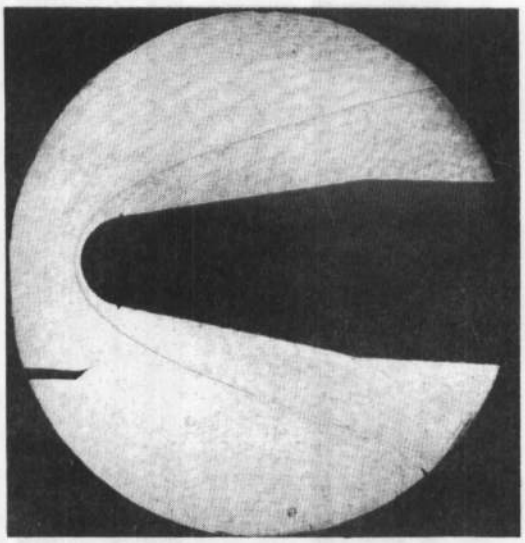

a. Vertical Knife Edge, Left Side

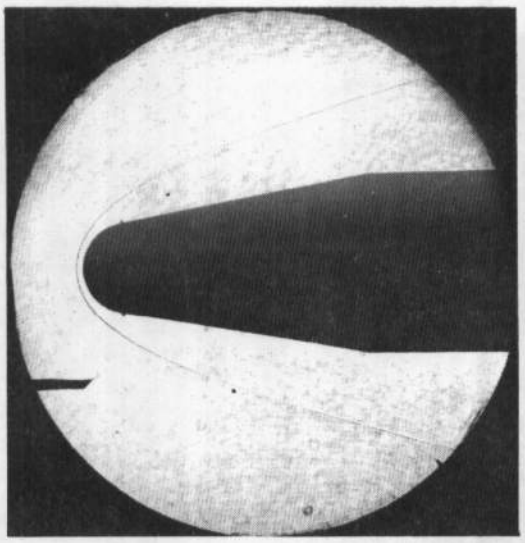

b. Vertical Knife Edge, Right Side

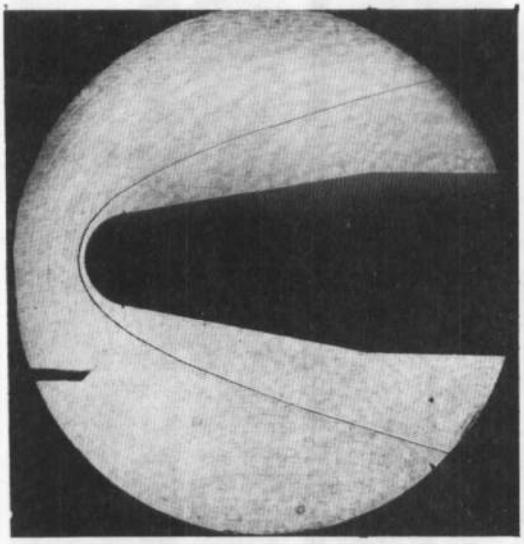

c. Horizontal Knife Edge, Top

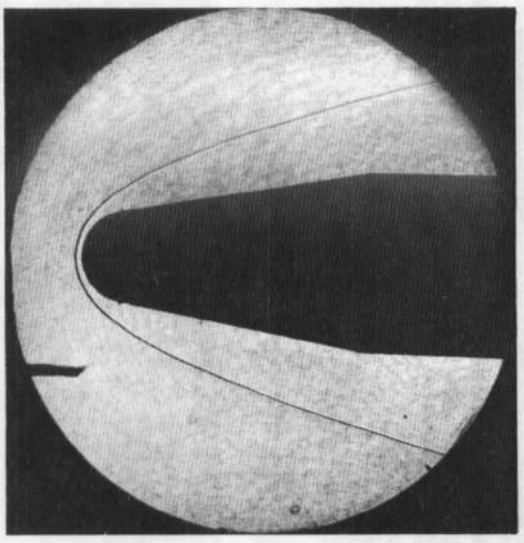

d. Horizontal Knife Edge, Bottom

Fig. 20 Shadowgraph Reconstructions

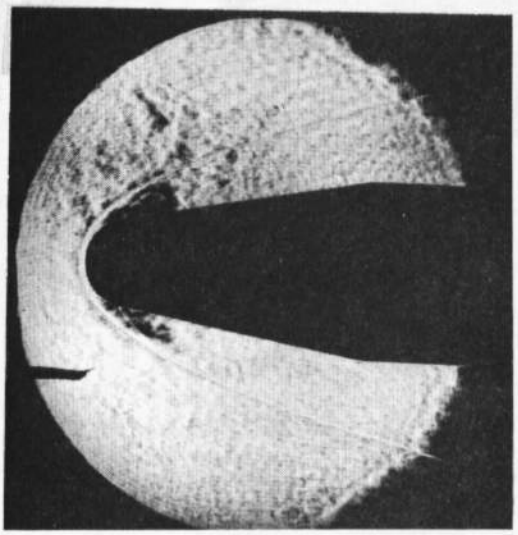

a. Vertical Knife Edge, Left Side

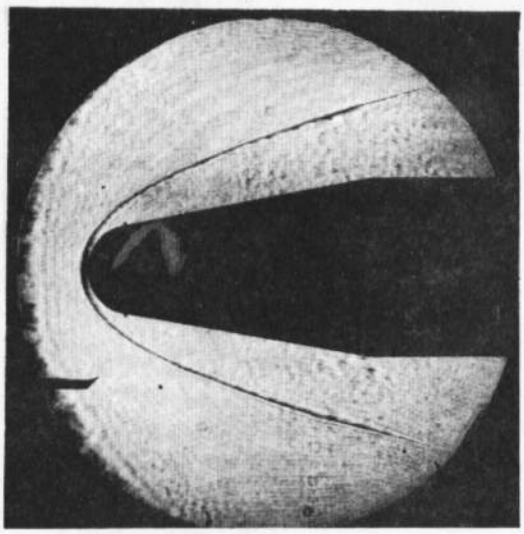

b. Vertical Knife Edge, Right Side

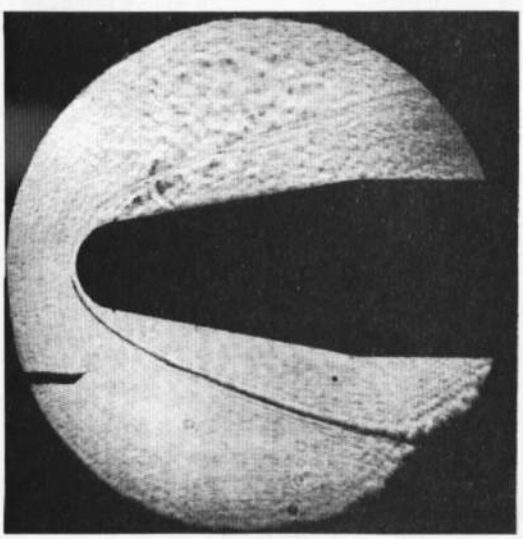

c. Horizontal Knife Edge, Top

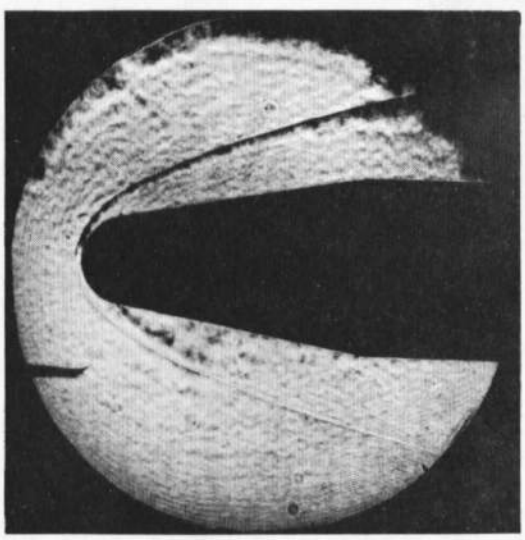

d. Horizontal Knife Edge, Bottom

Fig. 21 Schlieren Reconstructions

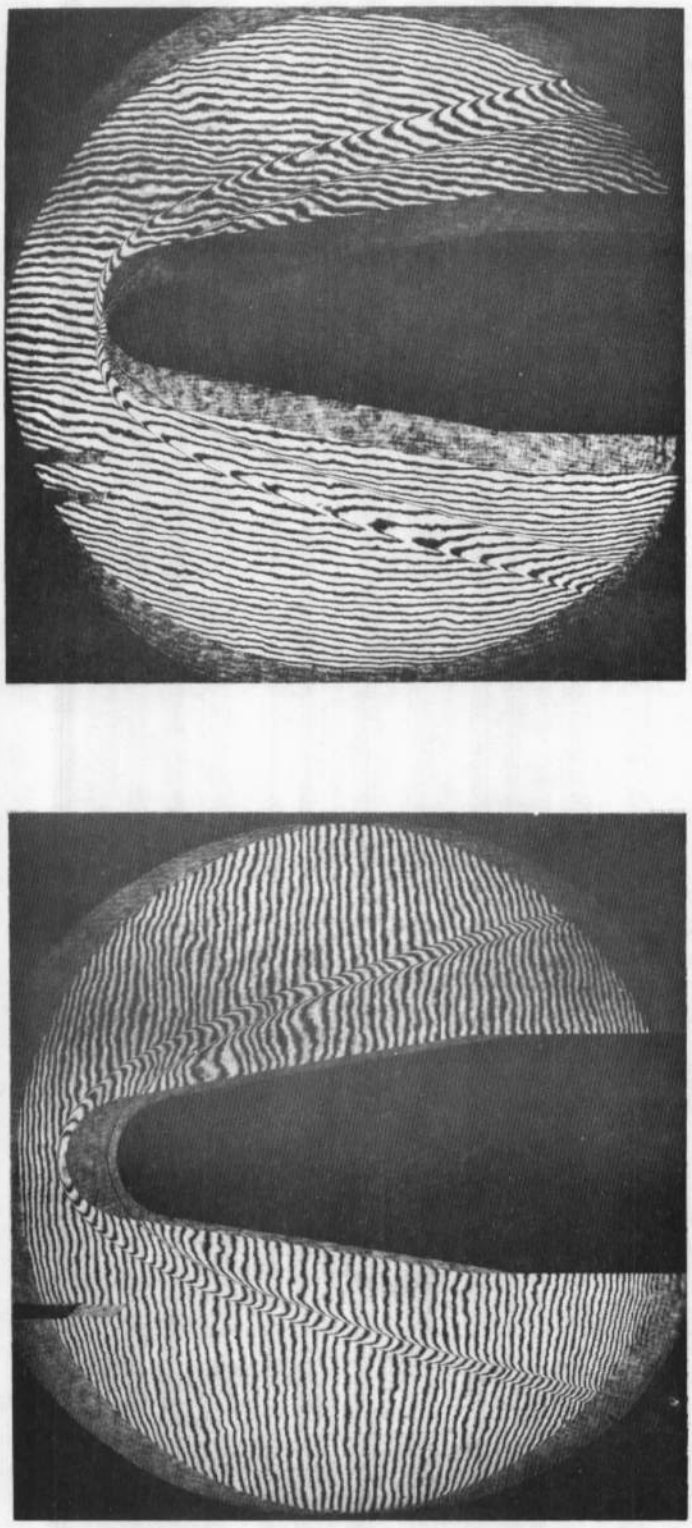

Fig. 22 Sheared Wavefront Interferograms

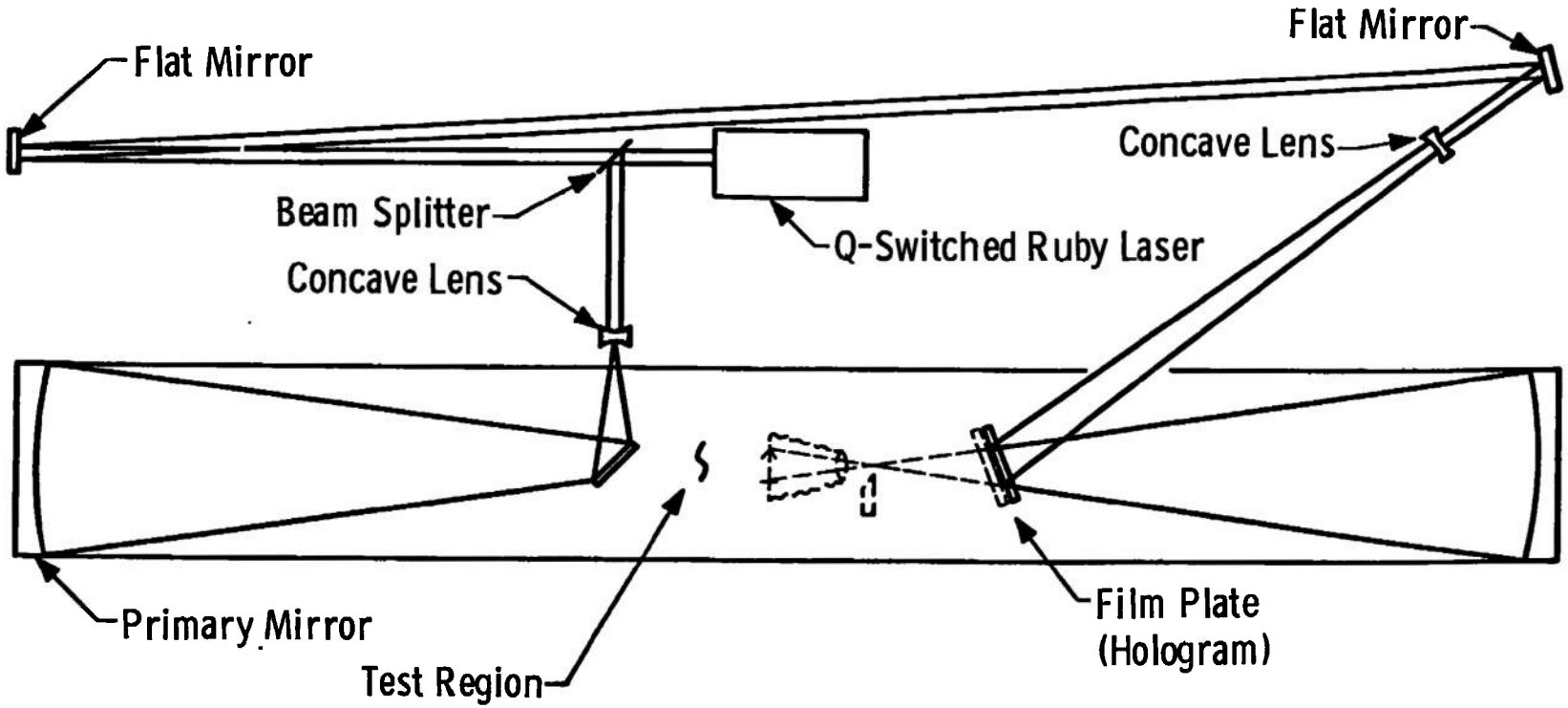

Fig. 23 Film Plate Position for Interferogram Reference Hologram (Heavy Lines)

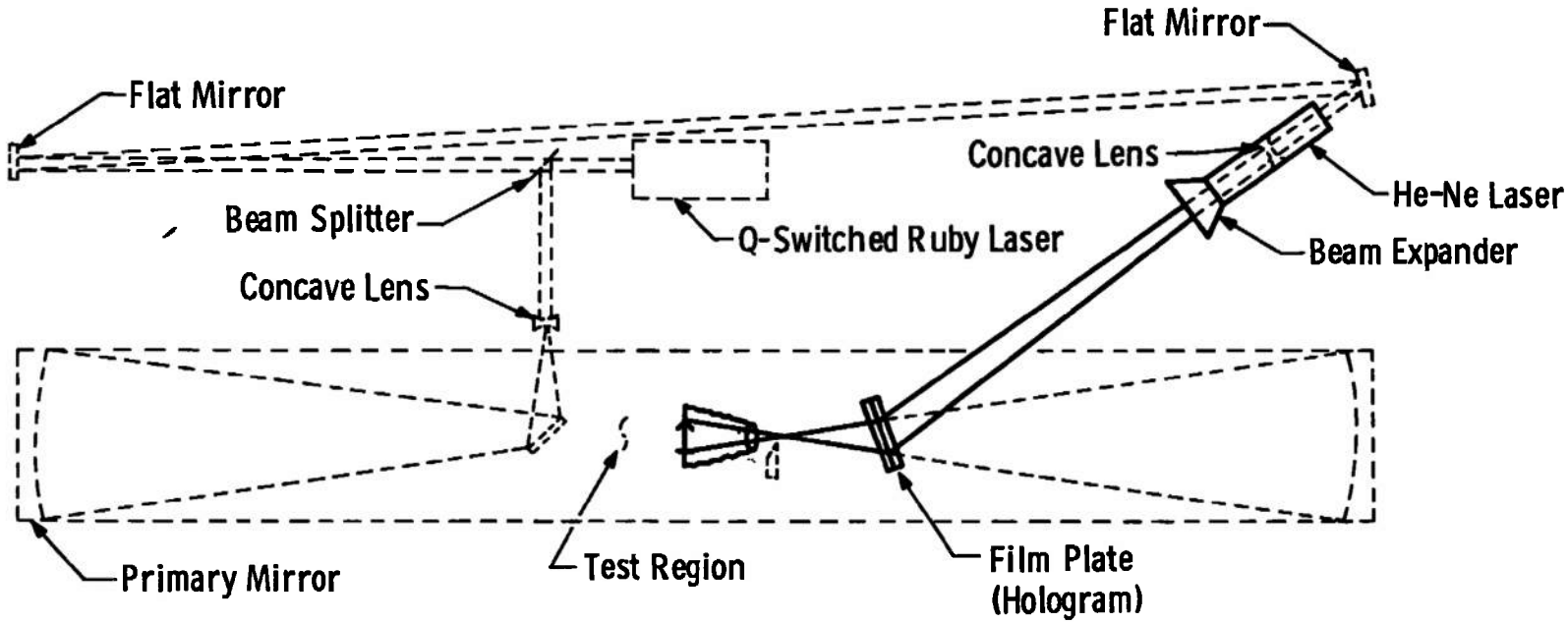

Fig. 24 Reconstruction of Holographic Interferogram (Heavy Lines)

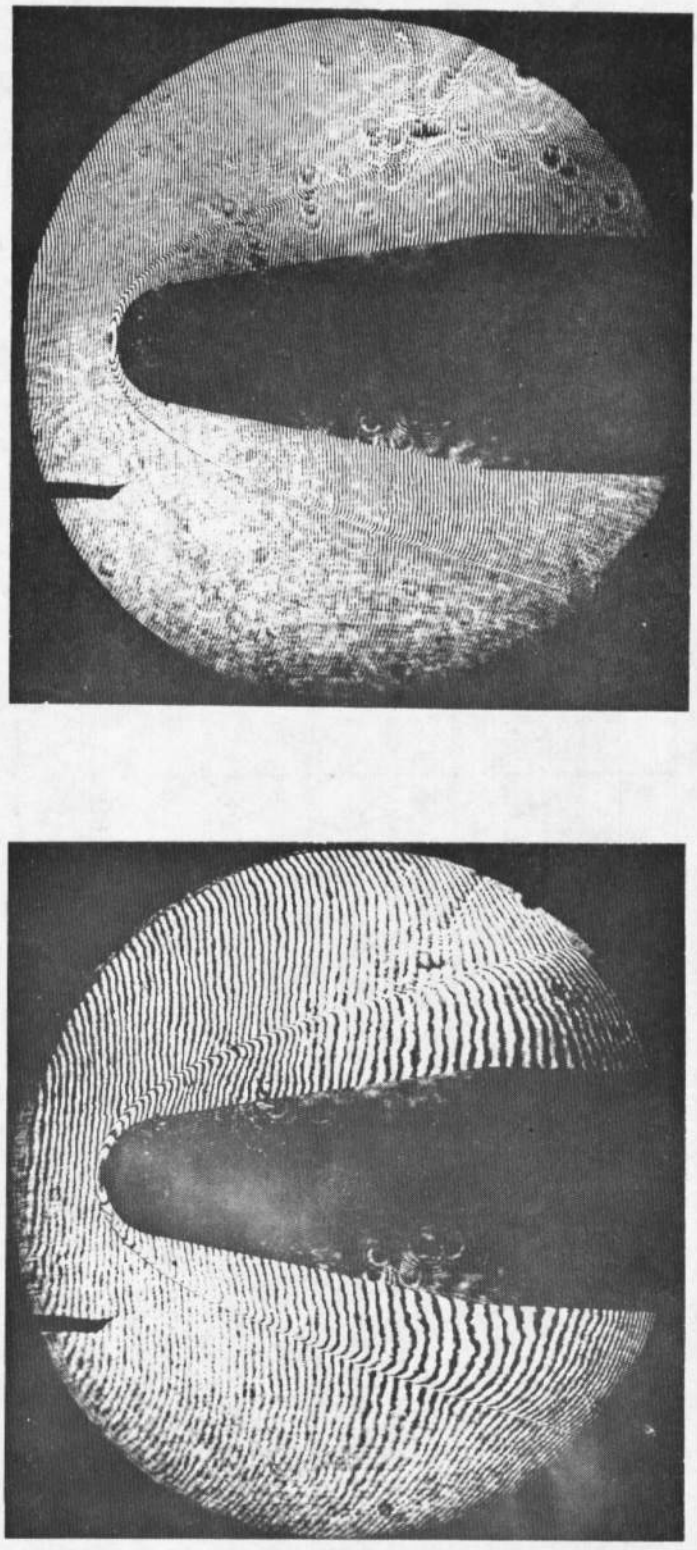

Fig. 25 Interferogram Reconstructions

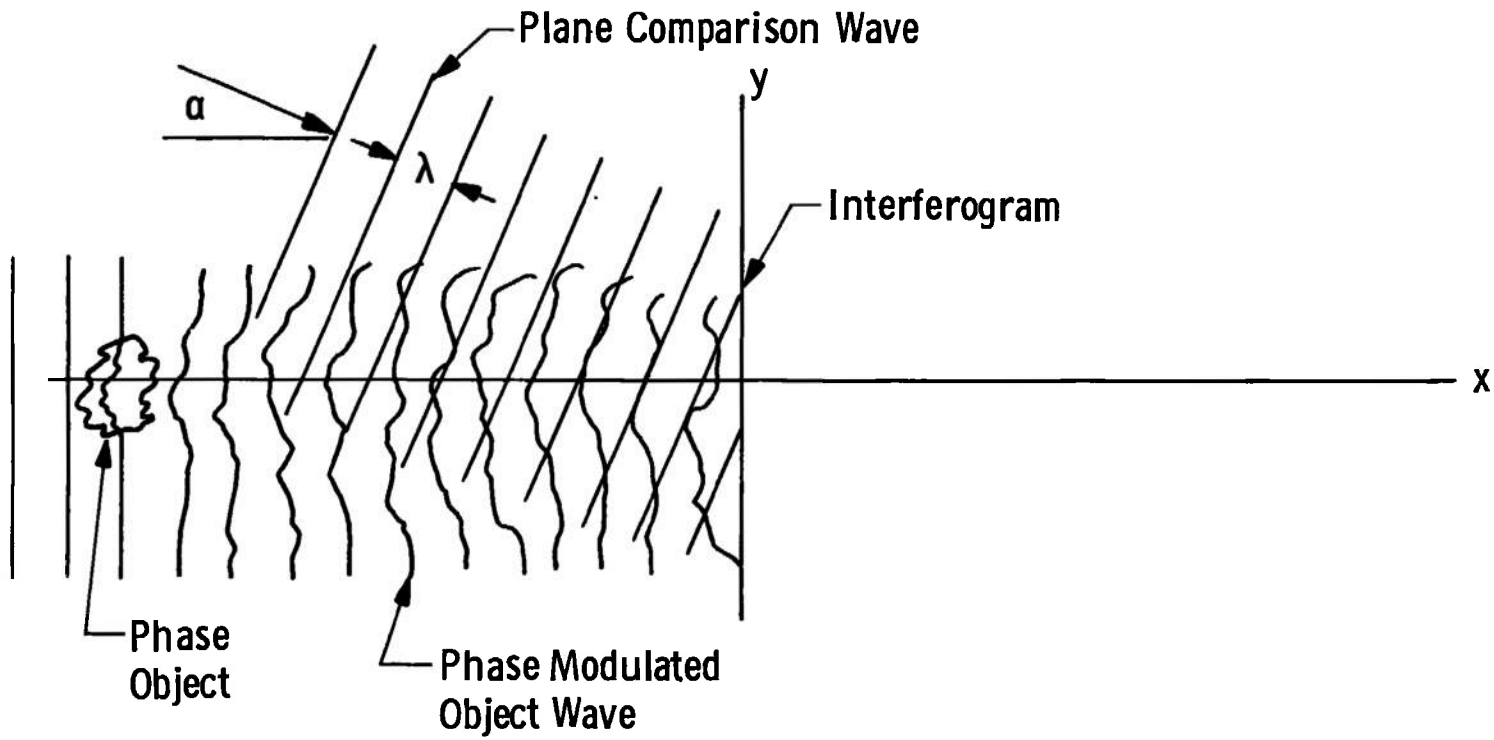

Fig. 26 Geometry for Eqs. (9) and (10)

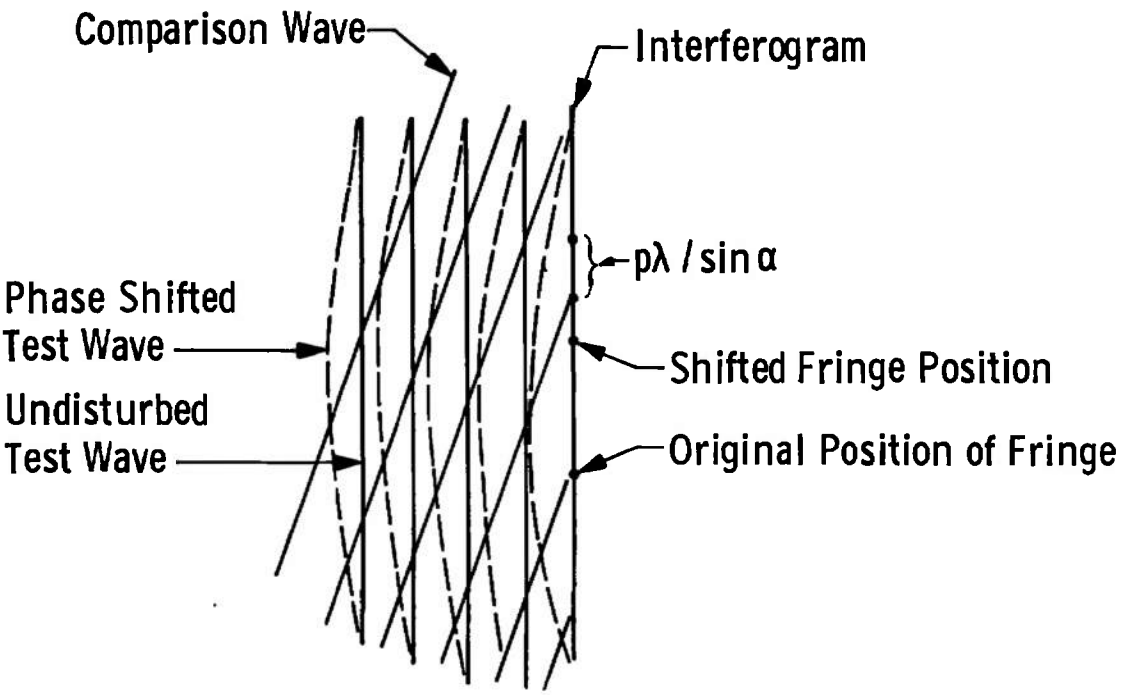

Fig. 27 Fractional Fringe Shift Definition

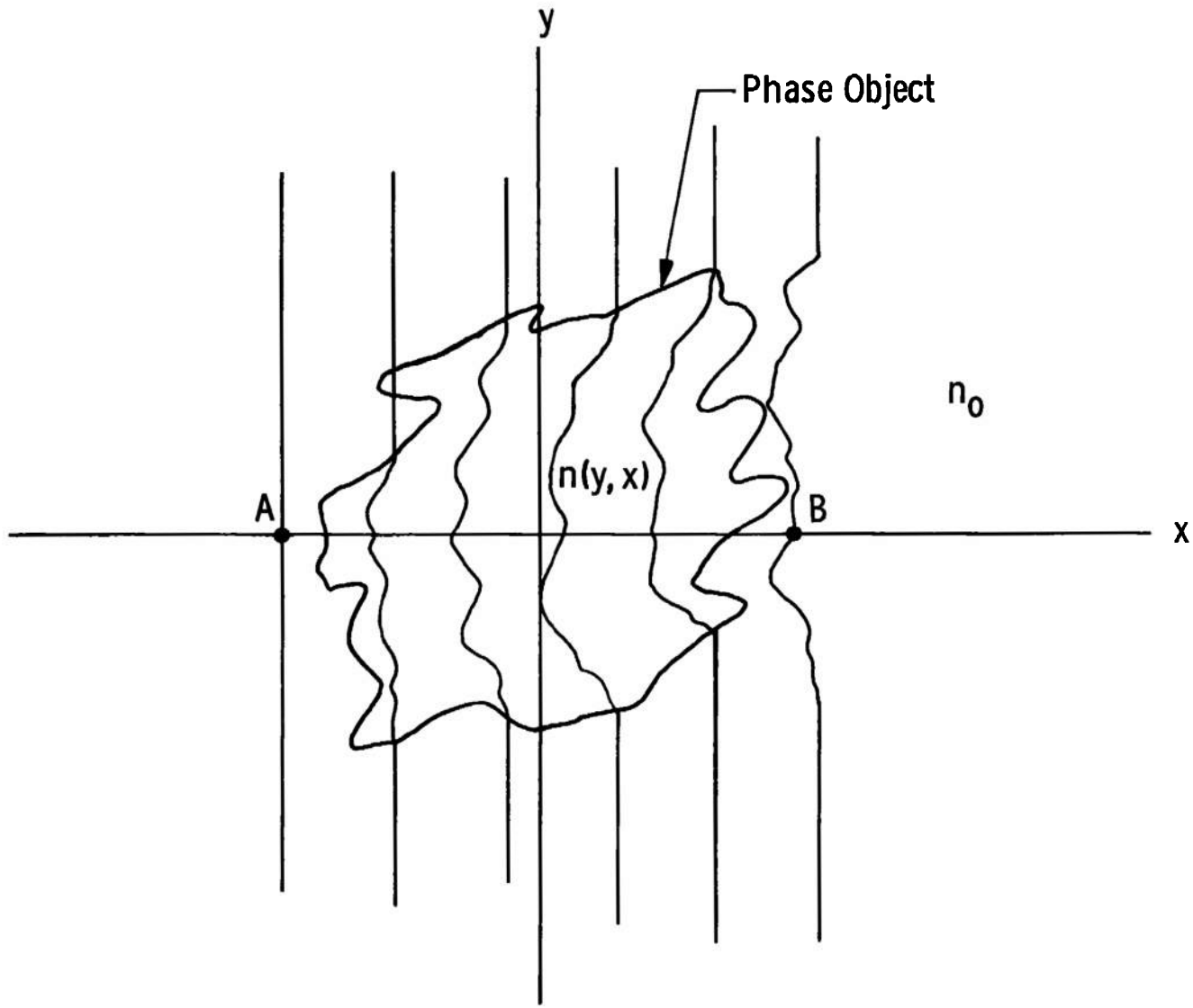

Fig. 28 Geometry for Eq. (13)

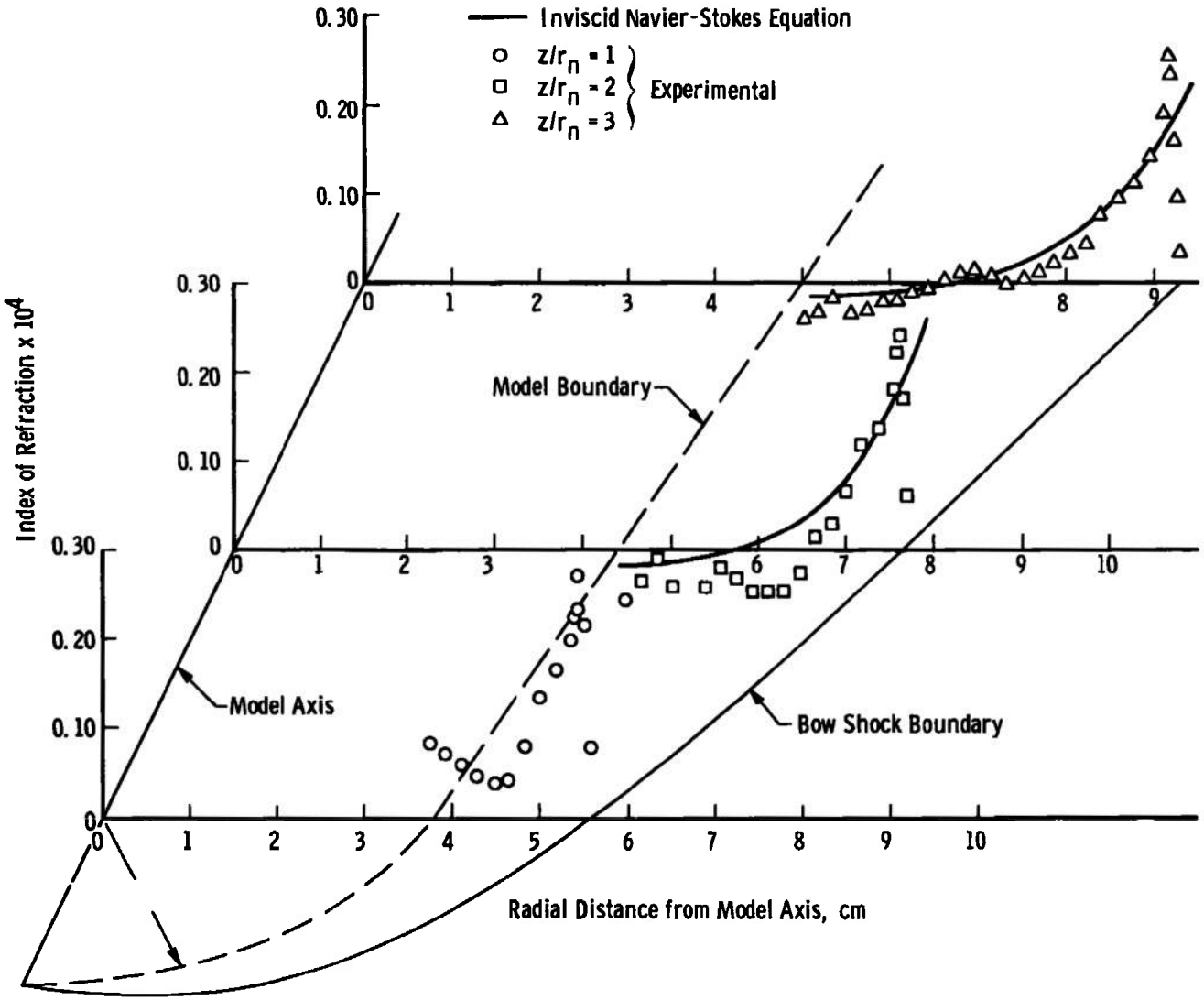

Fig. 29 Comparison of Holographic Interferometry Data with Theory

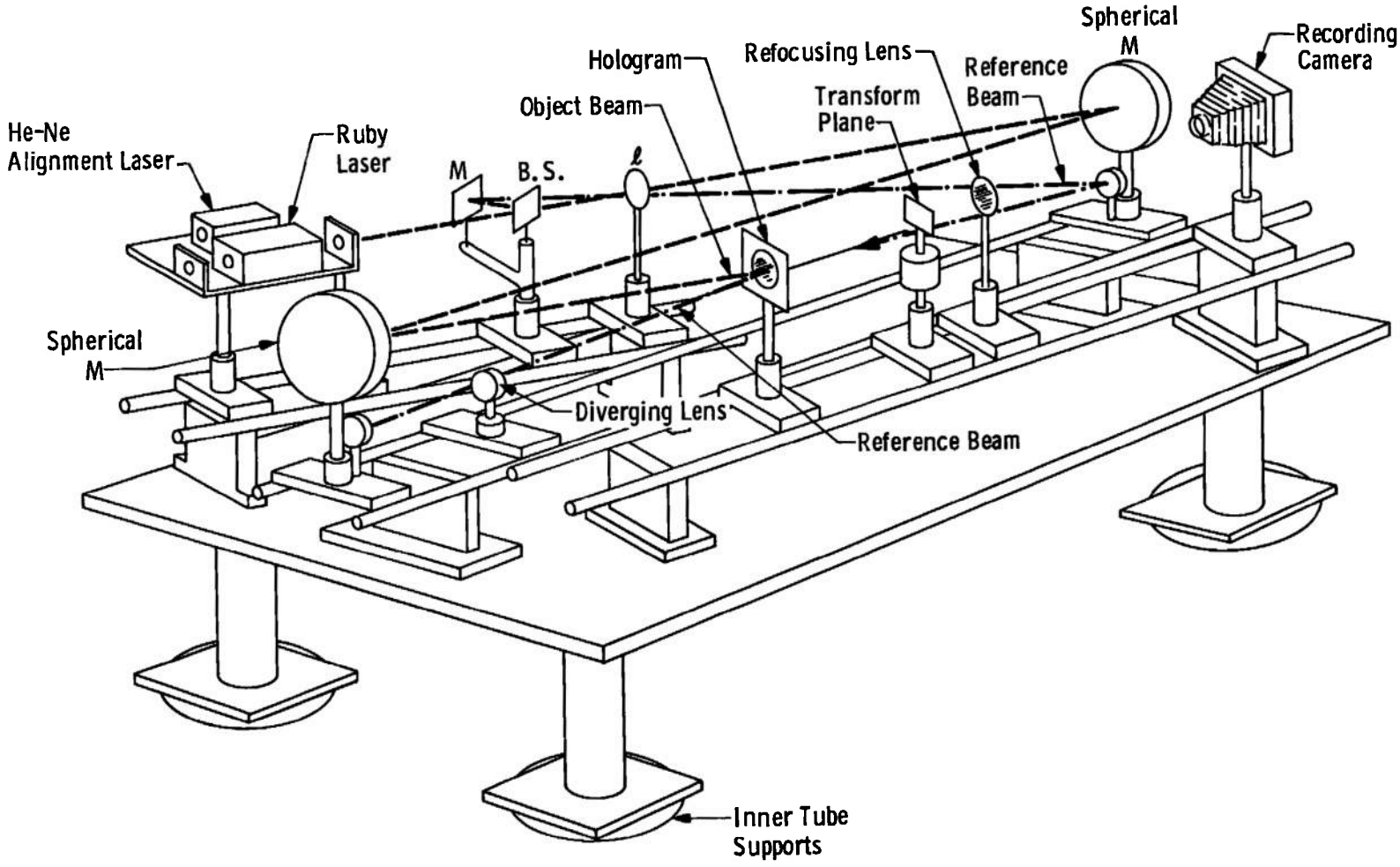

Fig. 30 Research Holographic Recorder-Processor

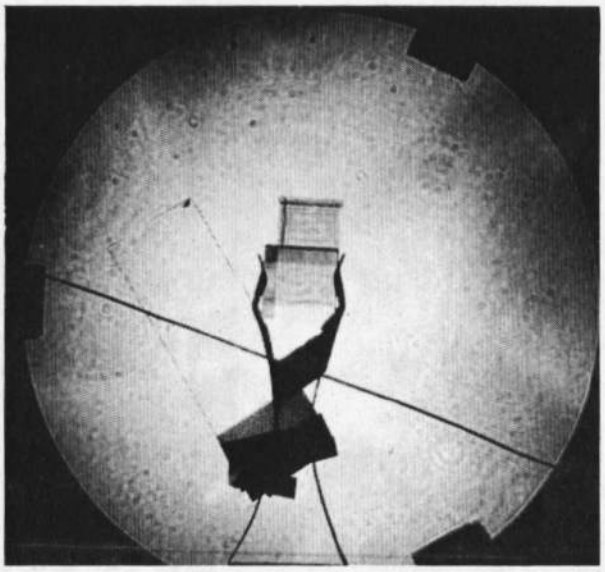

a. Hologram Diameter—4 in.

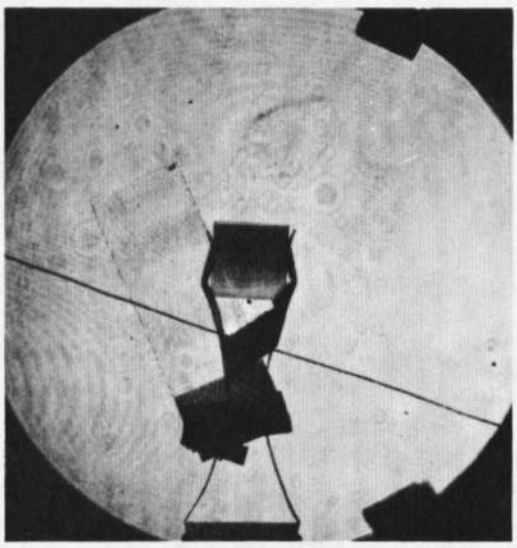

b. Hologram Diameter—1 cm

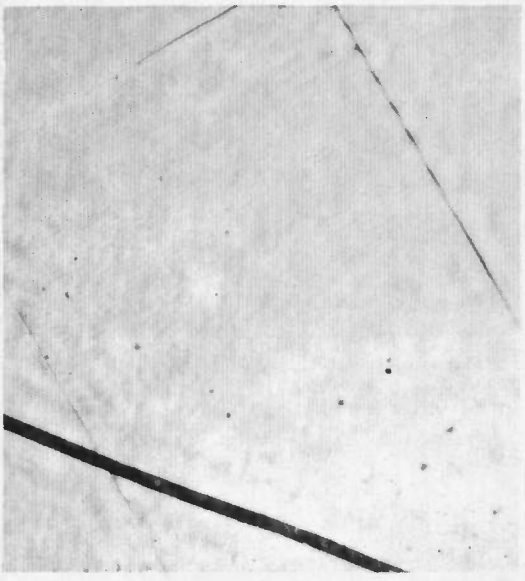

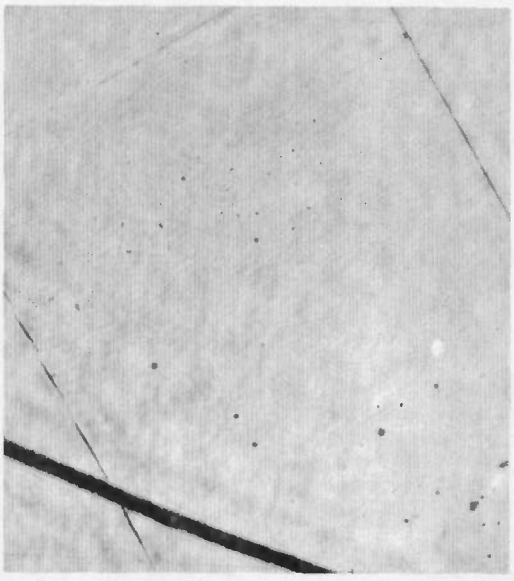

c. 5X Holographic Magnification of Above Field

Fig. 31 Effect of Hologram Size on Reconstruction

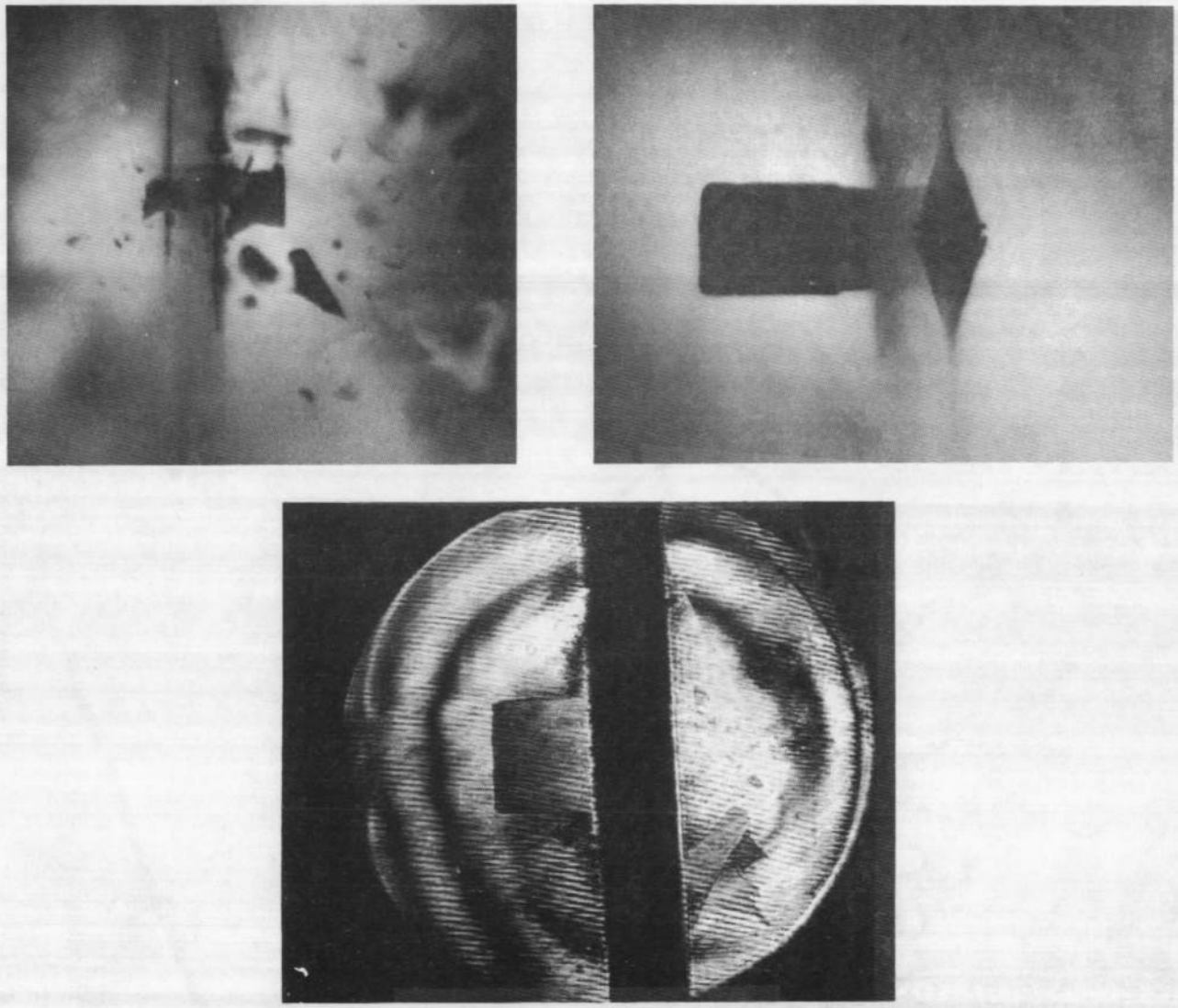

Fig. 32 Reconstructed Images of the Impacts of 0.22-cal Projectiles with a Plexiglass Plate

APPENDIX II
FILMS AND SENSITIZED GLASS PLATES FOR HOLOGRAPHIC RECORDING

There are a number of photographic emulsions available on triacetate film bases and glass plates that are suitable for holographic recording. The emulsions made by Eastman Kodak Co. were originally marketed for aerial reconnaisance and spectroscopy recordings. The Agfa-Gevaert Scientia emulsions are made specifically for use with lasers and are laser-frequency sensitized.

The rigidity and dimensional stability of glass plates are important considerations for most holographic applications and are not significantly more costly than their companion film products. Except for those situations requiring the flexibility of film supports, glass plates are generally used.

The general requirements for a photographic emulsion as the recording medium for holography are as follow:

1. The resolution of the emulsion must be a minimum of 500 line pairs/mm.
2. The film should be free of defects such as air bubbles and inclusions.
3. The film should not contain special purpose layers such as anticurl coatings and antistatic layers which may affect the phase characteristics of the film.
4. The emulsion should have a high sensitivity at the frequency in the spectrum that is being used for the recording.
5. The film should have a minimum gamma of 2 after processing and have a large linear dynamic range.
6. The film should have an effective antihalation backing.

Photographic emulsions that are presently available and meet the general requirements that have been outlined are listed in Table II-1. The relative sensitivities of the emulsions were determined by exposing sheets of each emulsion side by side with a 649F glass plate with a step tablet over the adjoining edges. Both He-Ne gas laser and ruby laser wavelengths were used to test the Eastman Kodak emulsions. The Agfa-Gevaert Scientia emulsions are sensitized for one specific wavelength;

therefore, only the appropriate laser wavelength was used for each emulsion. All of the emulsions tested were developed in Kodak D19 developer 6 min at 68°F. The density of the steps exposed through the calibrated step wedge were then read on a densitometer. Each emulsion sensitivity was referenced to Kodak 649F glass plates which were assigned an arbitrary speed of unity (1). The sensitivities given refer to a density of approximately 0.2. The sensitivity of an emulsion measured in photograph stops doubles with each additional unit (an emulsion with the relative sensitivity of 3 requires two stops less than Kodak 649F plates for the same exposure density, or one-fourth the total energy for a given exposure density). An exposure of 649F plates required 169 times as much energy as is required for Agfa 14C70 plates.

APPENDIX III
NUMERICAL METHOD FOR RADIAL INVERSION

The relationship between the refractive index change Δn and the fractional fringe shift $F(x)$ is

$$F(x) = \frac{1}{\lambda_o} \int \Delta n(x,y)\, dy \qquad \text{(III-1)}$$

or letting $\Delta n = \lambda_o I$

$$F(x) = \int I(x,y)\, dy \qquad \text{(III-2)}$$

In the axisymmetric case (see Fig. III-1), I is a function of radial distance r. Also, I is assumed zero outside of the shock line, a circle of radius R. Transforming the variable of integration in Eq. (III-2) from y to r, one gets the following integral equation:

$$F(x) = 2 \int_x^R \frac{I(r)\, r dr}{(r^2 - x^2)^{1/2}} \qquad \text{(III-3)}$$

The problem now is to solve Eq. (III-3) for I(r) given F(x). In practice F(x) is known only at discrete points x_o, x_1, x_2, ..., x_{n-1} where x_o is on the body or at the centerline (see Fig. III-2). Letting $x_n = R$, assume that I(r) can be represented by (see Fig. III-3)

$$I(r) = c_i \qquad x_{i-1} < r < x_i \qquad i = 1, 2, \ldots n \qquad \text{(III-4)}$$

Substituting Eq. (III-4) into Eq. (III-3) the following is obtained:

$$F(x_{i-1}) = 2 \sum_{j=i}^{n} c_j \int_{x_{j-1}}^{x_j} \frac{r dr}{(r^2 - x_{i-1}^2)^{1/2}}$$

or (III-5)

$$F(x_{i-1}) = 2 \sum_{j=1}^{n} c_j \left[(x_j^2 - x_{i-1}^2)^{1/2} - (x_{j-1}^2 - x_{i-1}^2)^{1/2}\right] \quad i = 1,2, \ldots$$

The above is a system of n linear equations in the n unknown c's. Because of the triangular structure of the system, it can be solved very easily by solving for the c's in reverse order. After the c's are obtained, the Δn's for the corresponding intervals may be calculated from

$$\Delta n_i = k \lambda_o c_i \tag{A6}$$

where k is a conversion factor to account for the fact that x and F(x) were not measured in physical units.

A value for Δn at the points $r = x_i$, $i = 1, 2, \ldots, n - 1$ may be obtained from the following weighted average

$$\Delta n(x_i) = \frac{(x_{i+1} - x_i)\,\Delta n_{i-1} - (x_i - x_{i-1})\,\Delta n_i}{x_{i+1} - x_{i-1}} \tag{A7}$$

$\Delta n(x_o)$ and $\Delta n(x_n)$ may then be calculated by using an extrapolation method. The one used in this report is finding the quadratic $\Delta n = a + br^2$ passing through the two neighboring points and calculating the extrapolated value from the quadratic.

A program using this technique has been written in FORTRAN IV for an IBM 360/50. Results are plotted using a CalComp plotter. A listing of the program is given at the end of this appendix. The subroutines PLOTS, PLOT, GRAPH, SETGR, THEOR, INV, and STEP are used for obtaining plots.

A few results of the technique are shown in Figs. III-4 through III-7. Figure III-4 is a plot of the input values

$$F(x) = (2 + 4x^2)(1 - x^2)^{1/2}/3 \qquad o \leq x \leq 1$$

with a $\Delta x = 0.05$. In Fig. III-5 the smooth line is the theoretical solution.

$$I(r) = r^2 \quad o \leq r \leq 1$$

The step function is the calculated function defined by Eq. (III-4), and the diamond shaped points are the values given by Eq. (III-7) and quadratic extrapolation on the end points. Figure III-6 shows actual test data. The results of the inversion are shown in Fig. III-7.

TABLE II-1
EMULSIONS FOR HOLOGRAPHY

a. Sensitivity Using Helium-Neon Laser Light (6328 Å)

Emulsion	Bases Available	Sizes Available	Relative Sensitivity	Manufacturers Quoted Resolution Lines/mm
Eastman 649 F Film	Film	3 1/4 by 4 1/4 in.; 4 by 5 in.	0.35	2000
Eastman 649 F Film	Glass Plates	3 1/4 by 4 1/4 in.; 4 by 5 in.	1	2000
Agfa 8E70 Plates	Film and Glass Plates	70- to 105-mm by 250-ft roll 3 1/4 by 4 1/4; 4 by 5, 8 by 10 in.	4	3000
Eastman SO386 Film	Film	4 by 5 in.	3	1000
Agfa 10E70 Film	Film and Glass Plates	70- to 105-mm by 250-ft roll 3 1/4 by 4 1/4; 4 by 5, 8 by 10 in.	7	2800
Agfa 14C70 Film	Film	35 mm by 100 ft 70 mm by 250 ft 105 mm by 250 ft	13	1500
Eastman 243 Film	Film	4 by 5 in.	13.5	500

b. Sensitivity Using Ruby Laser Light (6943 Å)

Emulsion	Bases Available	Sizes Available	Relative Sensitivity	Manufacturers Quoted Resolution Lines/mm
Eastman 649F Film	Film		0.9	2000
Eastman 649F Plates	Glass Plates		1	2000
Eastman SO382 Film	Film		7.5	1000
Agfa 8E75 Plates	Glass Plates	3 1/4 by 4 1/4, 4 by 5, 8 by 10 in.	8	3000
Agfa 10E75 Plates	Glass Plates	3 1/4 by 4 1/4, 4 by 5, 8 by 10 in.	11	2800
Eastman 243 Film	Film		18	500

PROGRAM LISTING

```
      COMMON F(103),C(103),Z(103),X(103),N,TH
      DIMENSION S(103)
      DIMENSION BUFF(2000)
      EQUIVALENCE (Z,S)
      REAL*4 LAMBDA
      LOGICAL TH
      TH=.FALSE.
      CALL PLOTS(BUFF,8000,10)
   91 READ (5,100,END=90) LAMBDA,DELXL
  100 FORMAT(2E20.0)
      READ (5,100) RN,DELXRN
      READ (5,101) N
  101 FORMAT(I3)
      READ (5,103) (X(J),F(J),J=1,N)
  103 FORMAT(6E12.0)
      N1=N-1
      WRITE (6,200)
  200 FORMAT(1H1,30X,'RADIAL INVERSION'///)
      WRITE (6,201) LAMBDA,DELXL,RN,DELXRN
  201 FORMAT(10X,'LAMBDA =',E16.7,5X,'MEASUREO VALUE',E16.7,' UNITS'/
     *   5X,'NOSE RADIUS =',E16.7,5X,'MEASURED VALUE',E16.7,' UNITS'//)
      WRITE (6,202)
  202 FORMAT(7X,'PT.',9X,'POSITION',14X,'SHIFT'/)
      WRITE (6,203) (J,X(J),F(J),J=1,N1),N,X(N)
  203 FORMAT(I10,2E20.8)
      CALL GRAPH
      C(N)=0.0
      DO 2 JJ=1,N1
      J=N1-JJ+1
      C(J)=0.5*F(J)/SQRT(X(J+1)*X(J+1)-X(J)*X(J))
      DO 3 K=1,J
    3 F(K)=F(K)-2.0*C(J)*SQRT(X(J+1)*X(J+1)-X(K)*X(K))
    2 C(J)=C(J)+C(J+1)
      DO 4 J=1,N1
      X(J)=RN*X(J)/DELXRN
    4 C(J)=LAMBDA*DELXRN*C(J)/(DELXL*RN)
      DO 7 J=1,3
    7 X(N1+J)=RN*X(N1+J)/DELXRN
      WRITE (6,200)
      WRITE (6,204)
      WRITE (6,205) (J,X(J),X(J+1),C(J),J=1,N1)
  205 FORMAT(I10,3E20.8)
  204 FORMAT(5X,'INTERVAL',4X,'LOWER LIMIT',9X,'UPPER LIMIT',11X,
     *       'DELTA N'/)
      CALL SETGR
      IF (TH) CALL THEOR
      TH=.FALSE.
      DO 5 J=2,N1
    5 S(J)=((X(J)-X(J-1))*C(J)+(X(J+1)-X(J))*C(J-1))/(X(J+1)-X(J-1))
      S(1)=S(2)+(S(3)-S(2))*(X(1)*X(1)-X(2)*X(2))/(X(3)*X(3)-X(2)*X(2))
      S(N)=S(N-1)+(S(N-2)-S(N-1))*(X(N)*X(N)-X(N-1)*X(N-1))/
     *     (X(N-2)*X(N-2)-X(N-1)*X(N-1))
      WRITE (6,200)
      WRITE (6,206)
  206 FORMAT(7X,'PT',9X,'POSITION',13X,'DELTA N'/)
      WRITE (6,203) (J,X(J),S(J),J=1,N)
      CALL INV
      CALL STEP
      GO TO 91
   90 CALL PLOT(17.25,0.0,999)
      STOP
      END
```

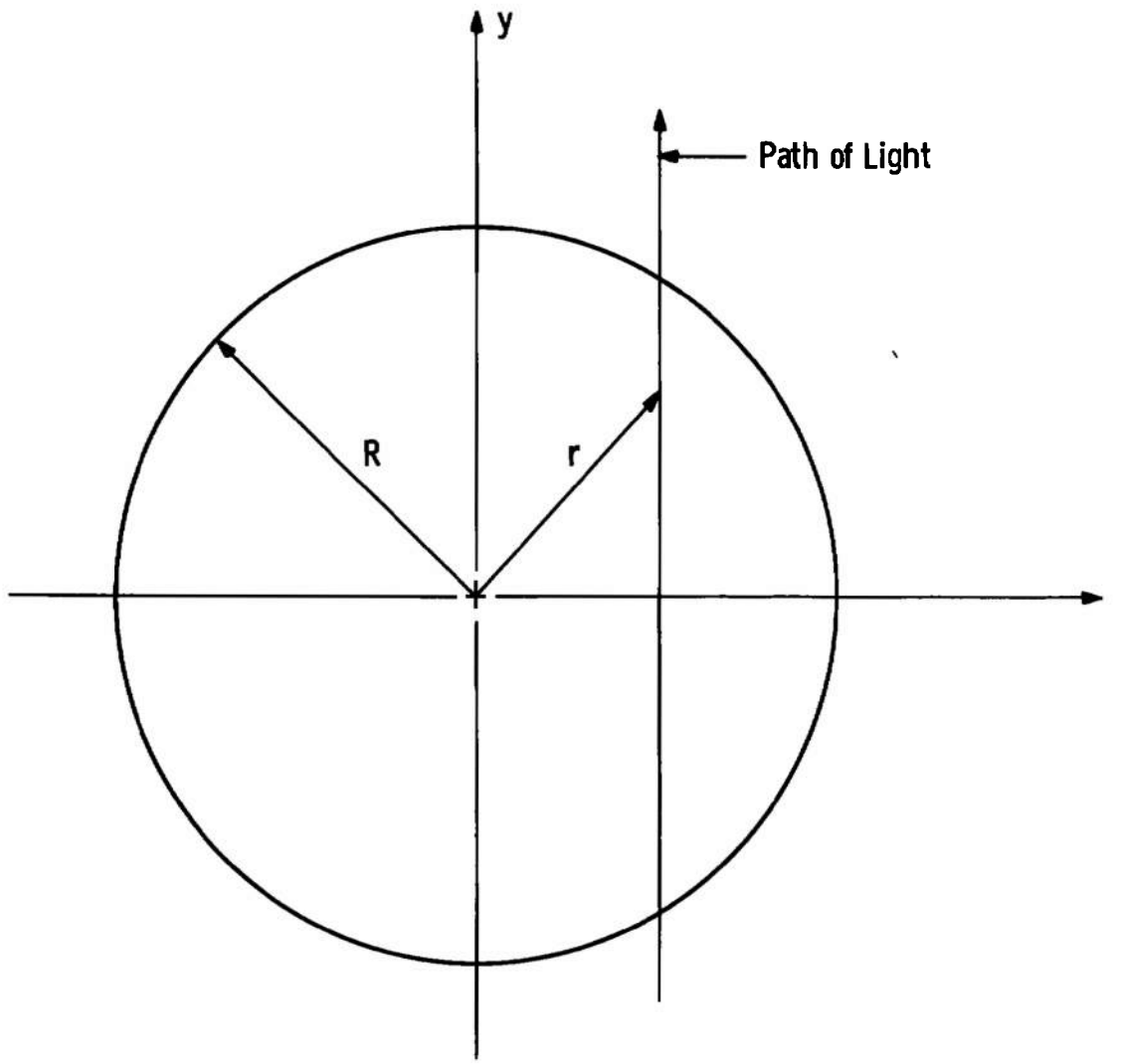

Fig. III-1 Axisymmetric Case

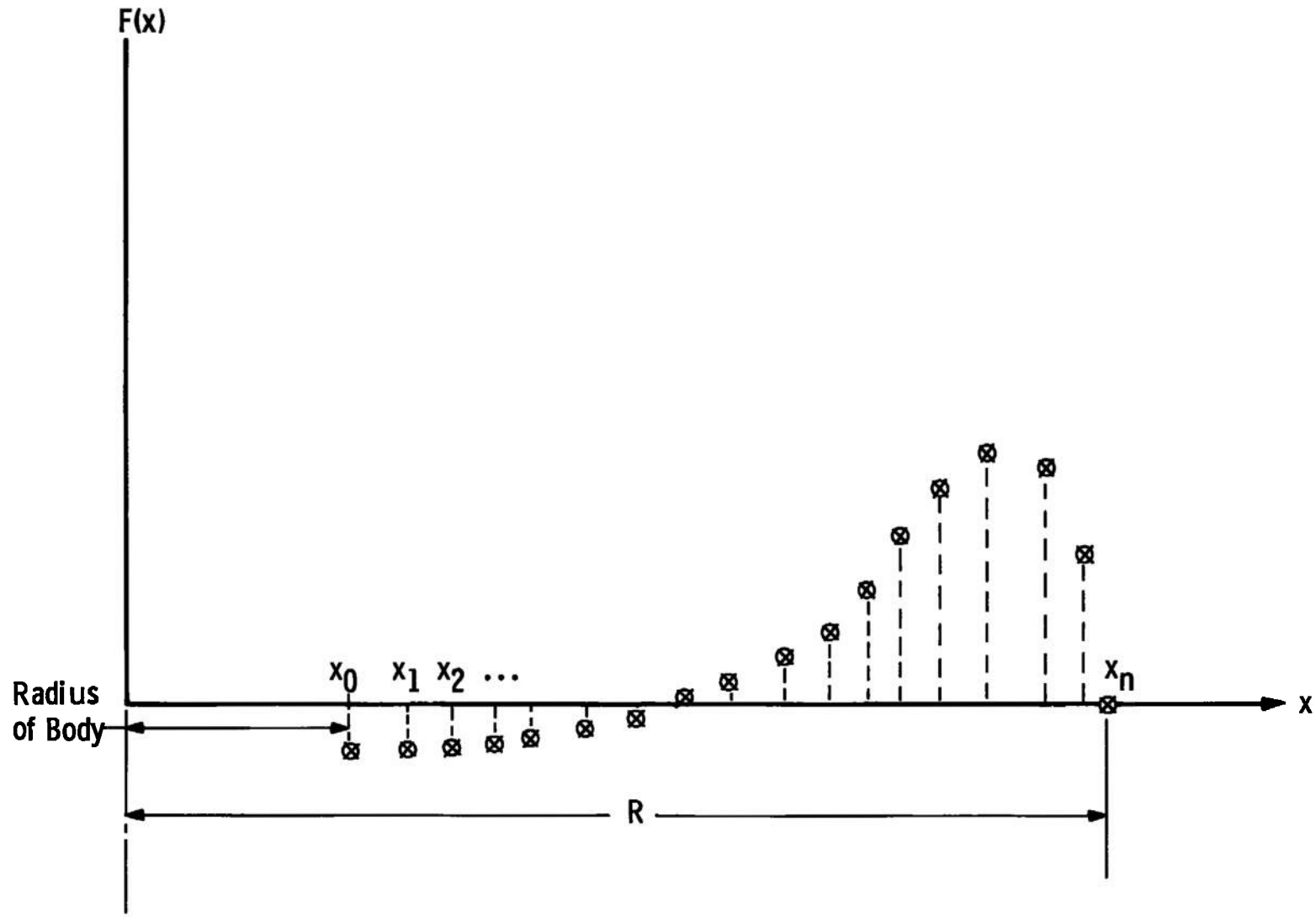

Fig. III-2 Typical Fringe Shift Data

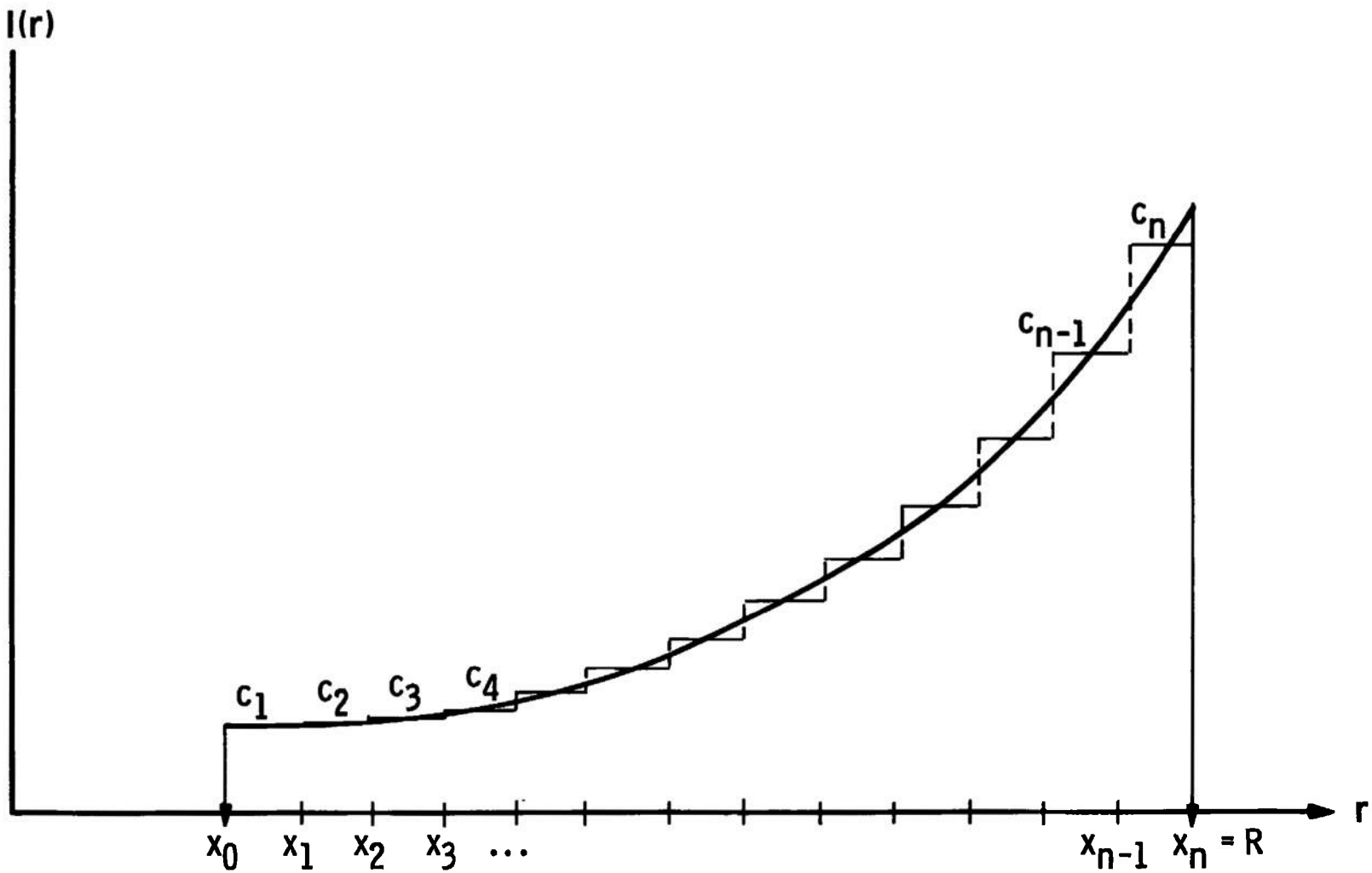

Fig. III-3 Step Function Representation of I(r)

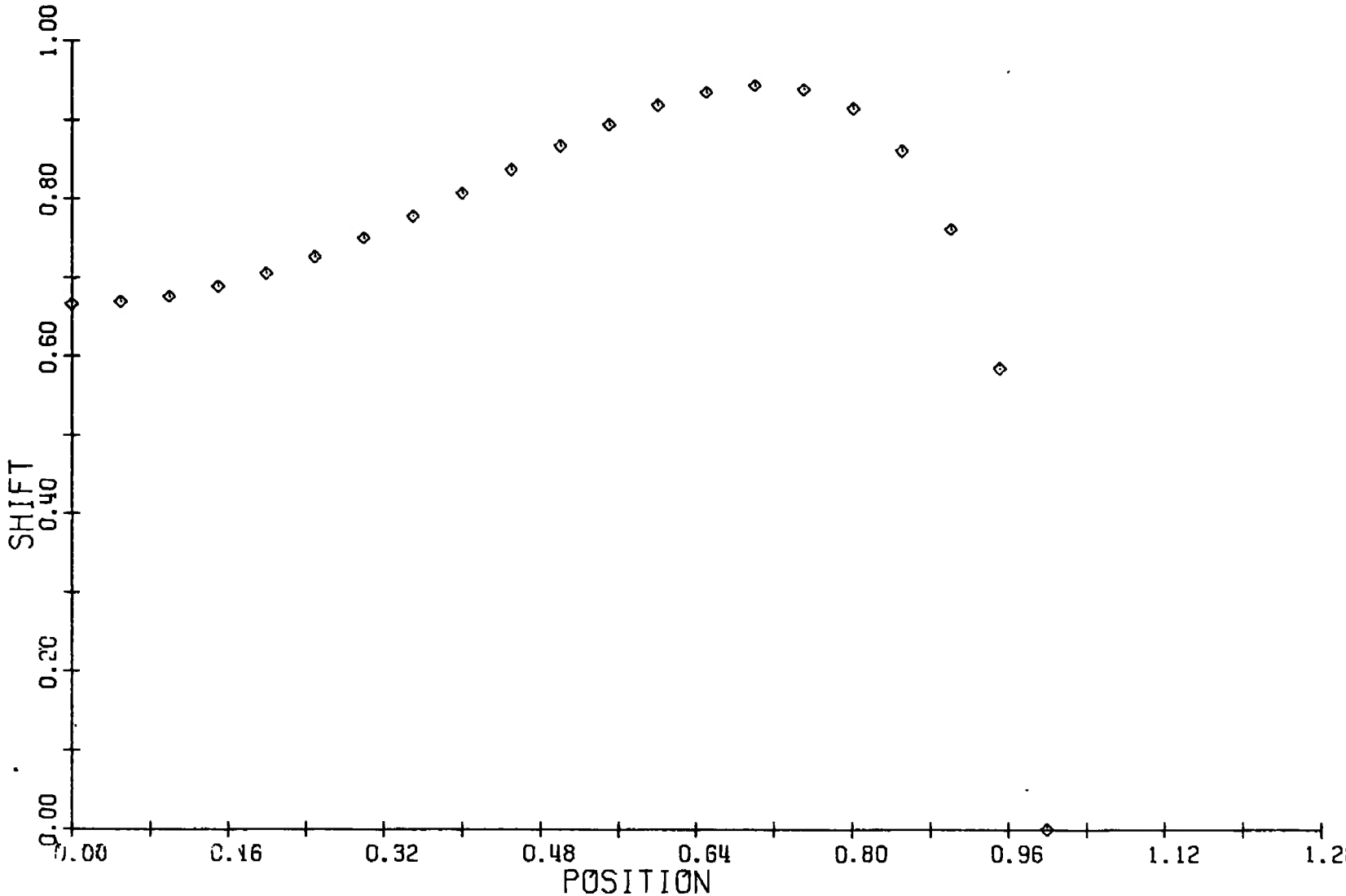

Fig. III-4 Theoretical Fringe Shift

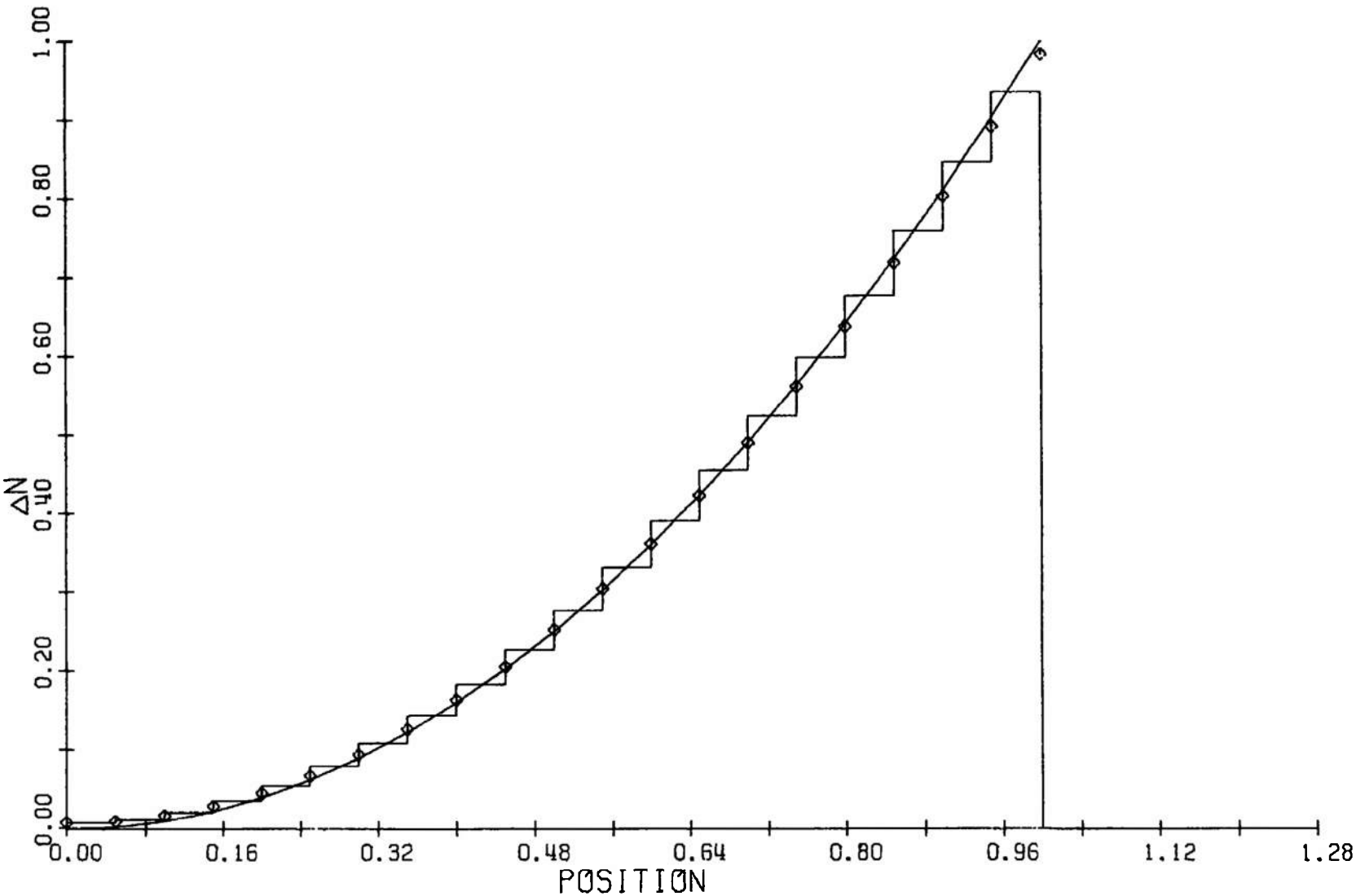

Fig. III-5 Theoretical Refractive Index Change

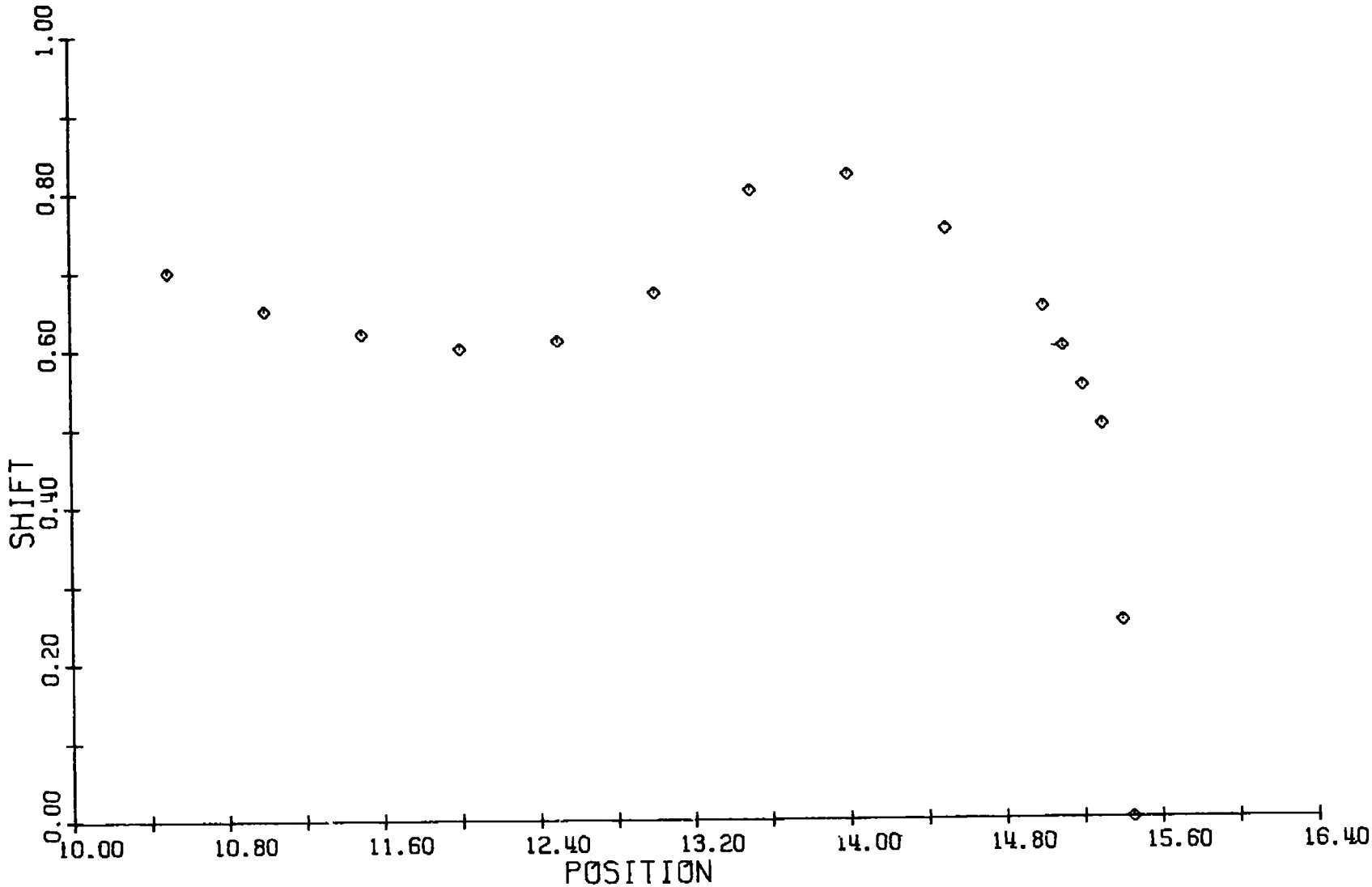

Fig. III-6 Typical Fringe Shift Data

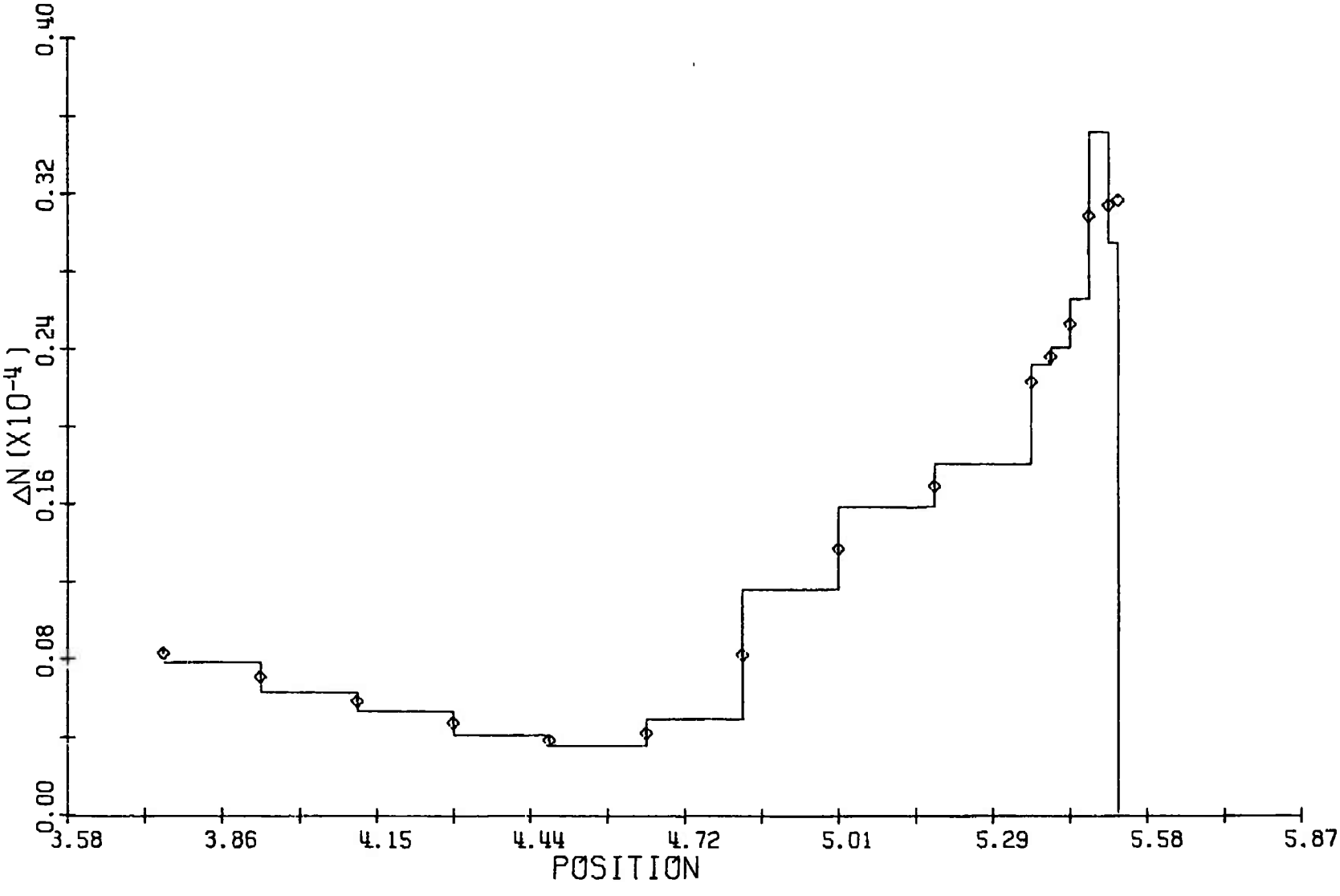

Fig. III-7 Typical Refractive Index Solution

UNCLASSIFIED
Security Classification

DOCUMENT CONTROL DATA - R & D

(Security classification of title, body of abstract and indexing annotation must be entered when the overall report is classified)

1. ORIGINATING ACTIVITY (Corporate author)	2a. REPORT SECURITY CLASSIFICATION
Arnold Engineering Development Center ARO, Inc., Operating Contractor Arnold Air Force Station, Tennessee	UNCLASSIFIED
	2b. GROUP N/A

3. REPORT TITLE

AERODYNAMIC HOLOGRAPHY

4. DESCRIPTIVE NOTES (Type of report and inclusive dates)

July 1967 to July 1969 - Final Report

5. AUTHOR(S) (First name, middle initial, last name)

J. D. Trolinger and J. E. O'Hare, ARO, Inc.

6. REPORT DATE	7a. TOTAL NO. OF PAGES	7b. NO. OF REFS
August 1970	98	24

8a. CONTRACT OR GRANT NO.	9a. ORIGINATOR'S REPORT NUMBER(S)
F40600-71-C-0002 b. PROJECT NO. 4344 c. Program Elements 64719F and 62201F d.	AEDC-TR-70-44
	9b. OTHER REPORT NO(S) (Any other numbers that may be assigned this report) ARO-OMD-TR-70-44

10. DISTRIBUTION STATEMENT

This document has been approved for public release and sale; its distribution is unlimited.

11. SUPPLEMENTARY NOTES	12. SPONSORING MILITARY ACTIVITY
Available in DDC	Arnold Engineering Development Center, Air Force Systems Command Arnold AF Station, Tennessee 37389

13. ABSTRACT

A summary of the work in holography at AEDC is presented. The work includes basic and applied research with emphasis on the applications of holography to aerodynamic testing.

DD FORM 1 NOV 65 1473

UNCLASSIFIED
Security Classification

14. KEY WORDS	LINK A		LINK B		LINK C	
	ROLE	WT	ROLE	WT	ROLE	WT
holography						
data storage						
lasers						
aerodynamics						
flow visualization						
optical equipment						

AFSC
Arnold AFS Tenn